การวิเคราะห์ทางเคมีไฟฟ้าของยาโดยใช้ขั้วไฟฟ้าฟิล์มบางของเพชรซึ่งโดปด้วยโบรอนในระบบโฟลอินเจคชัน

นางสาว ณัฐกานต์ หวังเฟื่องคณากุล

สถาบันวิทยบริการ
จุฬาลงกรณ์มหาวิทยาลัย

วิทยานิพนธ์นี้เป็นส่วนหนึ่งของการศึกษาตามหลักสูตรปริญญาวิทยาศาสตรมหาบัณฑิต
สาขาวิชาเคมี ภาควิชาเคมี
คณะวิทยาศาสตร์ จุฬาลงกรณ์มหาวิทยาลัย
ปีการศึกษา 2544

ISBN 974-03-1100-8

ลิขสิทธิ์ของจุฬาลงกรณ์มหาวิทยาลัย

ELECTROCHEMICAL ANALYSIS OF DRUGS USING BORON-DOPED DIAMOND THIN FILM ELECTRODE IN FLOW INJECTION SYSTEM

Miss Nattakarn Wangfuengkanagul

สถาบันวิทยบริการ
จุฬาลงกรณ์มหาวิทยาลัย

A Thesis Submitted in Partial Fulfillment of the Requirements
for the Degree of Master of Science in Chemistry

Department of Chemistry
Faculty of Science
Chulalongkorn University

Academic Year 2001

ISBN 974-03-1100-8

Thesis Title	Electrochemical analysis of drugs using boron-doped diamond thin film electrode in flow injection system
By	Miss Nattakarn Wangfuengkanagul
Field of Study	Chemistry
Thesis Advisor	Assistant Professor Orawon Chailapakul, Ph.D

Accepted by the Faculty of Science, Chulalongkorn University in Partial Fulfillment of the Requirements for the Master 's Degree

..... Deputy Dean for Administrative Affairs
(Associate Professor Pipat Karntiang, Ph.D.) Acting Dean, Faculty of Science

THESIS COMMITTEE

..... Chairman
(Associate Professor Sophon Roengsumran, Ph.D.)

..... Thesis Advisor
(Assistant Professor Orawon Chailapakul, Ph.D.)

..... Member
(Associate Professor Umaporn Titapiwatanakun, Ph.D.)

..... Member
(Nongnuj Jaiboon, Ph.D.)

สถาบันวิทยบริการ
จุฬาลงกรณ์มหาวิทยาลัย

ณัฐกานต์ หวังเฟื่องคณากุล : การวิเคราะห์ทางเคมีของยาโดยใช้ขั้วไฟฟ้าฟิล์มบางของเพชรซึ่งโดปด้วยโบรอนในระบบโฟลอินเจคชัน (ELECTROCHEMICAL ANAYSIS OF DRUGS USING BORON-DOPED DIAMOND THIN FILM ELECTRODE IN FLOW INJECTION SYSTEM) อาจารย์ที่ปรึกษา : ผศ.ดร. อรวรรณ ชัยลภากุล 122 หน้า. ISBN 974-03-1100-8

ในงานวิจัยนี้ได้ทำการศึกษาการวิเคราะห์ทางเคมีไฟฟ้าของยาโดยใช้ขั้วไฟฟ้าฟิล์มบางของเพชรซึ่งโดปด้วยโบรอน ยาที่ใช้ตรวจสอบในงานวิจัยนี้คือ acetaminophen D-penicillamine barbituric acid ทำการศึกษาเคมีไฟฟ้าของยาโดยใช้ไซคลิกโวลแทมเมทรี เปรียบเทียบการทดลองกับขั้วไฟฟ้ากลาสสิคาร์บอน ขั้วไฟฟ้าเพชรจะให้ผลของไซคลิกโวลแทมโมแกรมที่ชัดเจนและมีอัตราส่วนของสัญญาณกระแสต่อกระแสพื้นหลังที่สูงกว่าที่ได้รับจากขั้วไฟฟ้ากลาสสิคาร์บอน ค่าขีดจำกัดต่ำสุดของการวัดของขั้วไฟฟ้า สำหรับ acetaminophen เท่ากับ 10 ไมโครโมลาร์ D-penicillamine เท่ากับ 25 ไมโครโมลาร์ และ barbituric acid เท่ากับ 50 ไมโครโมลาร์ นอกจากนั้นยังนำระบบโฟลอินเจคชันและแอมเปอโรเมตรีที่มีขั้วไฟฟ้าเพชรเป็นอุปกรณ์ตรวจวัดมาใช้ในการวิเคราะห์ วิธีการนี้จะให้ค่าขีดจำกัดต่ำสุดได้ต่ำถึง 10 นาโนโมลาร์ซึ่งให้ค่าสัญญาณกระแสต่อสัญญาณรบกวนมากกว่า 3 และให้ค่าความเข้มข้นที่เป็นเส้นตรง 2-3 ออร์เดอร์ของแมกนีจูด

วิธีการที่ใช้ในงานวิจัยนี้ยังนำไปประยุกต์ใช้การตัวอย่างจริงของยาเตรียม คือ พาราเซตตามอลแบบน้ำเชื่อม และเพนนิซิลามีนแบบแคปซูล โดยได้ผลการทดลองที่ทำซ้ำได้ มีค่าใกล้เคียงกับที่ระบุไว้ในฉลาก

สถาบันวิทยบริการ
จุฬาลงกรณ์มหาวิทยาลัย

ภาควิชา.....เคมี.....ลายมือชื่อนิสิต.....
สาขาวิชา.....เคมี.....ลายมือชื่ออาจารย์ที่ปรึกษา.....
ปีการศึกษา.....2544.....

4272273123 : MAJOR ANALYTICAL CHEMISTRY
KEYWORDS : BORON-DOPED DIAMOND THIN FILM ELECTRODE/ FLOW INJECTION SYSTEM/DRUGS

NATTAKARN WANGFUENGKANAGUL : ELECTROCHEMICAL ANALYSIS OF DRUGS USING BORON-DOPED DIAMOND THIN FILM ELECTRODE IN FLOW INJECTION SYSTEM. THESIS ADVISOR : ASSISTANT PROFESSOR ORAWON CHAILAPAKUL, Ph.D., 122 pp., ISBN 974-03-1100-8

In this research, electrochemical analysis of drugs using a boron-doped diamond thin film electrode has been studied. Drugs, including acetaminophen, D-penicillamine and barbituric acid were investigated. The electrochemistry of drugs was studied by cyclic voltammetry. Comparison experiments were carried out using a polished glassy carbon (GC) electrode. At the diamond electrode, well-resolved cyclic voltammograms were obtained with current signal to background ratios higher than that obtained from the glassy carbon electrode. Detection limits of 10, 25 and 50 μM for acetaminophen, D-penicillamine and barbituric acid, respectively were obtained at the diamond electrode. Flow injection with amperometric detection using the diamond electrode was also studied. A significant low detection limit at 10 nM with signal to noise ratios higher than 3 and a linear range over 2-3 orders of magnitude were obtained.

The purposed method was further applied to real drug samples in pharmaceutical preparations. These were paracetamol syrup and penicillamine capsule. The results obtained were satisfactory.

สถาบันวิทยบริการ
จุฬาลงกรณ์มหาวิทยาลัย

Department ..Chemistry..... Student's signature.....
Field of study ..Chemistry..... Advisor's signature.....
Academic Year ..2001.....

ACKNOWLEDGEMENTS

This research could not have been successfully completed without the assistance and contribution from several people as well as my university, Chulalongkorn University.

First of all, let me express my sincere appreciation to my advisor, Assistant Professor Dr. Orawon Chailapakul for her invaluable guidance, support, and tolerance throughout the proofreading process as well as Dr. R. Bates (CRI) and the Thesis Committee for their valuable input, which has clearly endorsed the completion of this thesis.

Special thank are also extended to Prof. Akira Fujishima (The University of Tokyo) for the boron-doped diamond thin film electrodes that used in this thesis.

I feel very much grateful to the Ratchadaphisek Somphot Endowment Grant and the Thailand Research Fund for their financial support.

Thank you to all staffs in the department of chemistry who have rendered their endless assistance throughout my time in the laboratory. Special thanks go to my friends as well as the others on the 4th floor of the Chemistry III Building.

Above of else, I am deeply thankful to my parent for their support, encouragement and kindness.

CONTENTS

PAGE

CONTENTS (cont.)

PAGE

CONTENTS (cont.)

PAGE

CONTENTS (cont.)

PAGE

CONTENTS (cont.)

PAGE

LIST OF TABLES

TABLE **PAGE**

LIST OF TABLES (cont.)

TABLE **PAGE**

LIST OF TABLES (cont.)

TABLE **PAGE**

สถาบันวิทยบริการ
จุฬาลงกรณ์มหาวิทยาลัย

LIST OF FIGURES

FIGURE **PAGE**

LIST OF FIGURES (Cont.)

FIGURE **PAGE**

LIST OF FIGURES (Cont.)

FIGURE **PAGE**

LIST OF FIGURES (Cont.)

FIGURE **PAGE**

LIST OF FIGURES (Cont.)

FIGURE **PAGE**

LIST OF FIGURES (Cont.)

FIGURE **PAGE**

LIST OF FIGURES (Cont.)

FIGURE **PAGE**

LIST OF FIGURES (Cont.)

FIGURE **PAGE**

LIST OF FIGURES (Cont.)

FIGURE **PAGE**

LIST OF FIGURES (Cont.)

FIGURE **PAGE**

LIST OF FIGURES (Cont.)

FIGURE **PAGE**

LIST OF FIGURES (Cont.)

FIGURE **PAGE**

ABBREVIATIONS

i	-	current (A)
i_p	-	peak current (A)
i_{pc}	-	cathodic peak current (A)
i_{pa}	-	anodic peak current (A)
E_p	-	peak potential (V)
E_{pc}	-	cathadic peak current (V)
E_{pa}	-	anodic peak current (V)
n	-	electron per molecule oxidized; faradays mole of substance electrolyzed
F	-	the faraday; charge on one mole of electrons
A	-	area (cm^2)
k_f	-	heterogeneous rate constant for "forward' reaction
α	-	transfer coefficient
n_a	-	number of electrons involved in the rate-determining step
C_0^*	-	bulk concentration of species O
D_0	-	diffusion coefficient of species O (cm^2/sec)
ν	-	scan rate (V/sec)
$C_0(x,t)$	-	concentration of species O at the distance *x* at the time *t* (M)
$C_0(0,t)$	-	concentration of species O at the electrode surface (M)
$C_R(0,t)$	-	concentration of species R at the electrode surface (M)
$E^{0'}$	-	formal potential of an electrode (V)

ABBREVIATIONS (cont.)

f - F/RT (V^{-1})

K - equilibrium constant

Λ - equivalent conductivity of a solution ($cm^2\Omega^{-1}equiv^{-1}$)

สถาบันวิทยบริการ
จุฬาลงกรณ์มหาวิทยาลัย

CHAPTER I
INTRODUCTION

1.1 Introduction

Electrochemical techniques are well established and are used relatively inexpensively to produce unique characterization information for molecules and chemical systems such as qualitative and quantitative analytical data, thermodynamic data, and kinetic data. They are also sensitive techniques, which are able to detect submicromolar concentrations and subpicomole amounts of electroactive material. The heart of these techniques is the working electrode. The working electrodes that are extensively used are mercury or mercury amalgam, gold, platinum, carbon and chemical modified electrodes. However, these electrodes have some limitations such as the toxicity of mercury, narrow working window potentials, limited stability of electrode responses and large background currents. In recent years, boron-doped diamond thin films have emerged as electrode materials in many electrochemical application especially in electroanalysis [1-4]. They can overcome these limitations due to their superior properties [5], such as very low and stable voltammetric background currents, wide potential windows in aqueous solution, high resistance to deactivation via fouling, insensitivity to dissolved oxygen [6], and negligible adsorption of polar organic molecules. There have been several reports in the past few years describing the outstanding performance of diamond electrodes and the application of this material as the detection unit in flow injection systems for the

electroanalysis of some organic molecules such as polyamine [7], histamine and serotonin [8]. The results obtained were excellent.

Drugs are one type of chemical that are important for human life because they are used for the treatment of many diseases. Although they are useful, they have toxicity due to their side effects or improper use. For instance, hepatotoxic effects occur due to acetaminophen overdose. In this work, drugs that have different functional groups including hydroxyl group, thiol group and keto - enol group were investigated. They are acetaminophen, D-penicillamine and barbituric acid. Acetaminophen is a common drug that is used as an analgesic and antipyretic drug. D-penicillamine is a common thiol drug that used as a therapeutic agent for diseases such as Wilson's disease. Barbituric acid analogs are useful for the treatment of benign or malignant tumors. A variety of techniques have been used for determination of these compounds. High performance liquid chromatography with spectroscopy such as fluorescence [9,10], chemiluminescene [10-12] or UV-visible spectroscopy [13-15] was extensively used. One of the important limitations of liquid chromatgraphy techniques is the fact that many drug compounds are inactive species for direct detection with spectroscopic detectors. Therefore, a pre or post-column derivatization procedure is normally required. Electrochemical techniques are alternatives, which can be cheap, fast and sensitive. The working electrodes that are extensively used include mercury or mercury amalgam electrode [16-19] and chemically modified electrodes [20-25]. These electrodes have some problems such as the large background current and the stability of the electrodes [26]. Boron-doped diamond thin film electrodes, with their unique electrochemical properties, are expected to be more suitable for drug determination. Therefore, the boron-doped

diamond thin film electrode was used and was applied to the amperometric detection of drugs.

1.2 Objective and scopes of the research.

The main objective of the research is to investigate the application of the boron-doped diamond thin film electrode in an electrochemical system using cyclic voltammetry and amperometry with flow injection for the determination of drugs. The work was divided into three parts. First part, electrochemical properties of analytes were investigated at the diamond electrode by cyclic voltammetry. The analytical performance including linear range and detection limit for the diamond electrode were studied by cyclic voltammetry. Moreover, the results were compared to that of the glassy carbon electrode. Secondly, the optimum potential for amperometric detection using the diamond electrode with a flow injection system was examined by hydrodynamic voltammetry. Analytical parameters such as sensitivity, linear range, detection limit, repeatability and stability of the electrode were also determined. Finally, flow injection with amperometric detection using the diamond electrode was applied to the determination of drug formulations including drug syrup and drug capsule.

สถาบันวิทยบริการ
จุฬาลงกรณ์มหาวิทยาลัย

CHAPTER II

THEORY AND LITERATURE SURVEY

2.1 Electrochemical techniques [27,28]

Electrochemistry is the science of electron transfer across a solution-electron interface. At the cathode, ions or molecules are transformed within the interface via reaction with electrons (from the electrode) to produce reduced molecules or ions. At the anode, molecules or ions (from the solution) are transformed within the interface to produce electrons (at the electrode surface) and oxidized ions and molecules. The resulting electrons move from the anode though the wires of the external circuit to the cathode as electronic current. There are two types of electrochemical techniques, namely potentiometry and amperometry

The potentiometric technique determines the potential of electrochemical cells usually at zero current. The potential of the electrode of interest responds (with respect to a standard reference electrode) to changes in the concentration of the species under study. The most commonly potentiometric methods used by the analyte employ voltmeters, potentiometers or pH meters. Such measurements are generally relatively cheap to perform, however they can be slow and tedious unless automated.

The amperometric technique relies on the current passing through a polarizable electrode. The magnitude of the current is direct proportional to the concentration of the electroanalyte, with the most common amperometric techniques being polarography and voltammetry. The apparatus needed for amperometric measurements tends to be more expensive than those used for amperometric

measurements alone. It should also be noted that amperometric measurement can be overly sensitive to impurities such as gaseous oxygen dissolved in the solution, and capacitance effects at the electrode. Nevertheless, amperometry is a much more versatile tool than potentiometry because the amperometric measurements are generally more precise and more versatile that those made by using potentiometry.

2.1.1 Cyclic voltammetry [28-30]

In cyclic voltammetry, the current response of a small stationary electrode in an unstirred solution is excited by a triangular wave form (Figure 1a). While the amount of Ox at the electrode becomes depleted by the reduction, it is of course replaced by R, which diffuses away into the solution. Hence if we reverse the potential sweep from the positive side of the peak we shall observe the reverse effect. As the potential sweeps back towards the redox potential, the R species will start to be reoxidized to Ox. The current will now increase in the negative (oxidizing) direction until an oxidation peak is reached. The overall cyclic voltammogram is shown in Figure 2.1b. Depending upon the composition of the sample the direction of the initial scan may be either negative or positive.

สถาบันวิทยบริการ
จุฬาลงกรณ์มหาวิทยาลัย

(a)

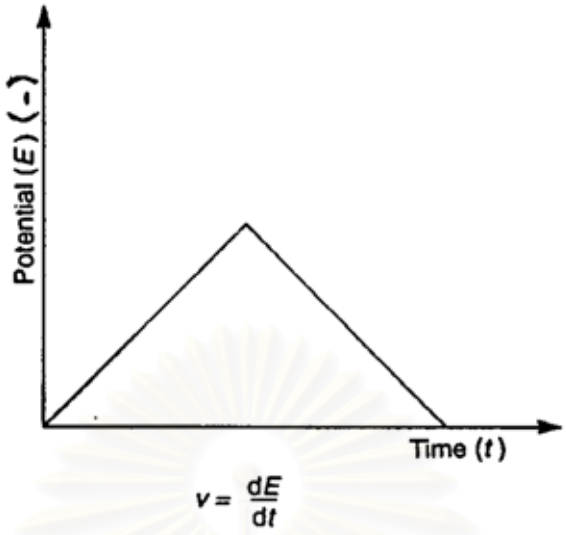

(b)

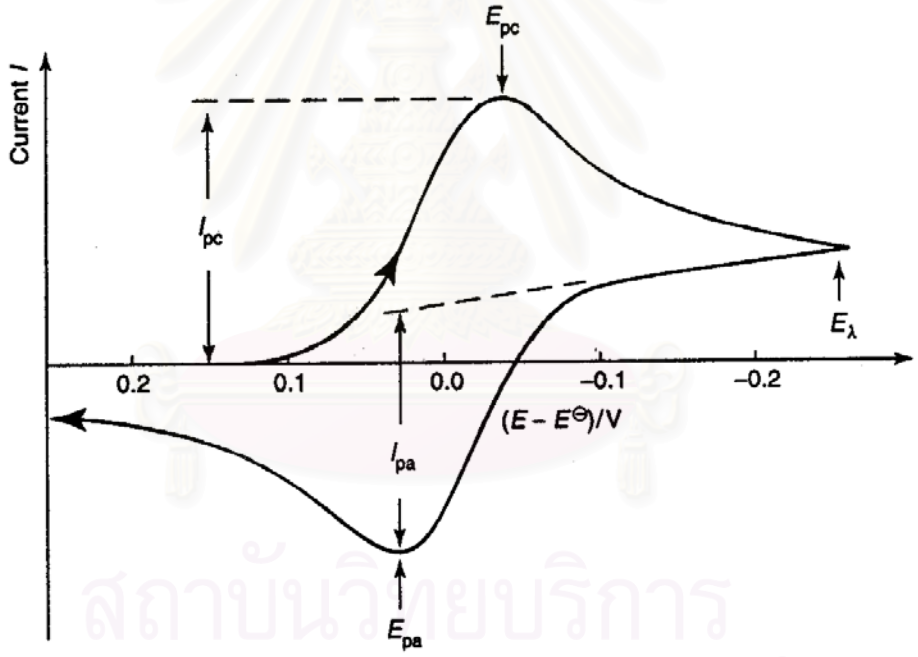

Figure 2.1 Schematic (a) Potential wave form (b) cyclic voltammogram

Important parameters in cyclic voltammetry are the cathodic peak potential E_{pc}, the anodic peak potential E_{pa}, the cathodic peak current i_{pc} and the anodic peak current i_{pa}..

The shape of the cyclic voltammogram in Figure 2.1b is typical for a couple that is wholly reversible in the thermodynamic sense; other simple diagnostic tests for electro-reversibility are listed in Table 2.1

Table 2.1 Diagnostic tests for the electrochemical reversibility of a redox couple, carried out by cyclic voltammetry

1. $i_{pc} = i_{pa}$
2. The peak potential, E_{pc} and E_{pa}, are independent of the scan rate
3. $E^{0'}$ is positioned midway between E_{pc} and E_{pa}, so $E^{0'} = (E_{pa} + E_{pc})/2$
4. i_p is proportional to (scan rate)$^{1/2}$
5. The separation between E_{pc} and E_{pa} is 59 mV/n for an n-electron couple

The magnitude of current in cyclic voltammetry is given by the Randles-Sevcik equation

$$i_p = 2.69 \times 10^5 n^{3/2} A C^b D^{1/2} \nu^{1/2} \quad \text{----------2.1}$$

2.1.1.1 Reversible system [31]

The reaction $O \rightleftharpoons R$, assuming semi-infinite linear diffusion and a solution initially containing only species O, with the electrode held initially at a potential E_I, where no electrode reaction occurs. The potential is swept linearly at ν V/sec so that the potential at any time is

$$E(t) = E_I - \nu t \quad \text{----------2.2}$$

The current is given by

$$i_p = 2.69 \times 10^5 n^{3/2} A C^b D^{1/2} \nu^{1/2} \quad \text{----------2.3}$$

2.1.1.2 Quasi-reversible system

The treatment of a quasi-reversible system in which electron transfer kinetic limitations of the reverse reaction have to be considered was first described by Matsuda and Ayaba The equation for this case is

$$D_0(\partial C_0(x,t)/\partial x)_{x=0} = k^0 e^{-\alpha n a F[E(t) - Eo']}\{ C_0(0,t) - C_R(0,t)\, e^{naF[E(t) - E0' ']}\} \text{----------2.4}$$

The current is given by

$$i_p = 0.4463nFAC_0^*(nF/RT)^{1/2}\nu^{1/2} D_0^{1/2}K(\Lambda,\alpha) \text{---------- 2.5}$$

2.1.1.3 Totally reversible system

For a totally irreversible reaction (O +ne $\rightarrow$ R), the equation is

$$i/nFA = k_f(t)C_0(0,t) \text{ ---------- 2.6}$$

The peak current is given by

$$i_p = (2.99 \times 10^5)n(\alpha n_a)^{1/2}A\, C_0^*\, D_0^{1/2}\nu^{1/2} \text{ ---------- 2.7}$$

For the totally irreversible wave, i_p is also proportional to C_0^* and $\nu^{1/2}$

2.1.1.4 Adsorption

2.1.1.4.1 Cyclic voltmmetry: Only Adsorbed O and R Electroactive-Nernstain Reaction

When the sweep rate is so large that no appreciable diffusion of O at the electrode surface occurs, then only adsorbed O is electroactive. Alternatively, the wave for adsorbed O could be shifted to potentials well before the reduction wave dissolved O. The conditions for such behavior will be given below.

There are also cases where adsorption is so strong that the adsorbed layer of O can form even when the solution concentration is so small that the contribution to the current from dissolved O is negligible.

The peak current is given by

$$i_p = n^2F^2(\nu\Gamma)/4RT \text{----------2.8}$$

Note that the peak current, and indeed the current at all points on the wave, is proportional to ν, in contrast to $\nu^{1/2}$ dependence observed for Nernstain waves of diffusion species.

2.1.1.4.2 Cyclic voltmmetry: Only Adsorbed O Electroactive-Irreversible Reaction

For the case where adsorbed O is reduced in a totally irreversible reaction. The peak current is given by

$$i_p = n\alpha nF^2A\nu\Gamma^*_0 / 2.718RT \text{----------2.9}$$

Again i_p is proportionally to ν, but the wave is shifted from the reversible value and is distorted from its symmetrical parabolic shape.

สถาบันวิทยบริการ
จุฬาลงกรณ์มหาวิทยาลัย

2.1 2 Amperometry [30]

This is the usual name of the analytical application of the chronoamperometric technique. With certain cell and electrode configurations, the decaying current reaches an approximately steady state after a certain time. This is shown by the shaded part of the curve in Figure 2.2. The current has become effectively independent of time, as indicated by the equation 2.10.

$$i = \frac{nFADCox}{\delta} \qquad \text{----------2.10}$$

where δ is a constant related to the diffusion layer thickness. This relationship is much more useful for analytical work, even though the current has decayed considerably from its highest values.

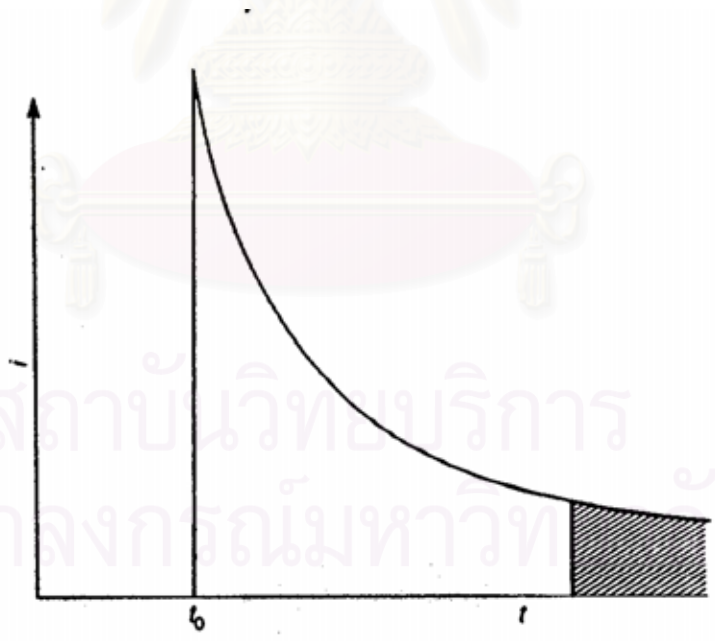

Figure 2.2 The current-time profile associated with a potential step redox process.

2.2 Flow injection analysis (FIA)

Flow injection analysis was defined by Ruzicka and Hansen in 1975. It is a simple and versatile analytical technique for automating wet chemical analysis. It is based on the physical and chemical manipulation of a dispersed sample zone formed from the injection of the sample into a flowing carrier stream with detection downstream.

The schematic diagram below (Figure 2.3) groups the FIA process into three stages to help visualize how the FIA performs a method or analysis.

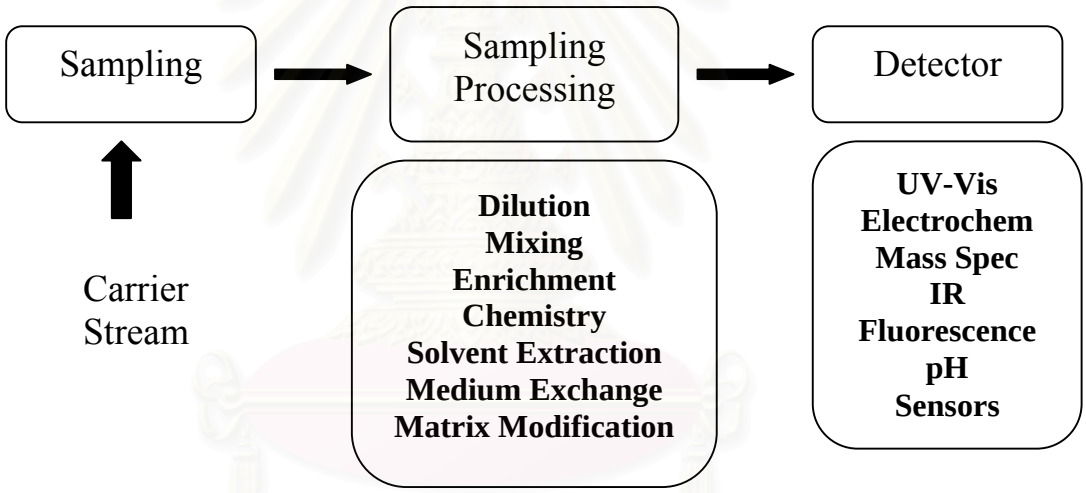

Figure 2.3 Schematic diagram of generic description of FIA

First is sampling, where the sample is injected into the flowing carrier stream (thus, the name Flow Injection Analysis). This step is generally performed with a sample injection valve. The second stage is called sample processing. The purpose of this step is to transform the analyte into a species that can be measured by the detector and manipulate its concentration into a range that is compatible with the detector, using one or more of the indicated processes. The third stage is detection where the

analyte, or a derivative of it, generates a signal peak which is used for quantitation. As indicated, a large variety of detectors can be used in FIA.

The power of FIA as an analytical tool lies in its ability to combine these analytical functions in a wide variety of different ways to create a broad range of different methodologies, and perform these methodologies rapidly and automatically with minute and low amounts of sample.

The thin-layer cell design [32] is commonly used as an amperometric detector for liquid chromatography and was also employed in this study. The basic functioning of this mode of detection is depicted schematically in Figure 2.4. As illustrated, an electrochemically active substance passes over an electrode held at a potential sufficient great (positive or negative) for an electron transfer (either oxidation or reduction) to occur. An amperometric current is produced that is proportional to the concentration of analyte entering the thin-layer cell.

สถาบันวิทยบริการ
จุฬาลงกรณ์มหาวิทยาลัย

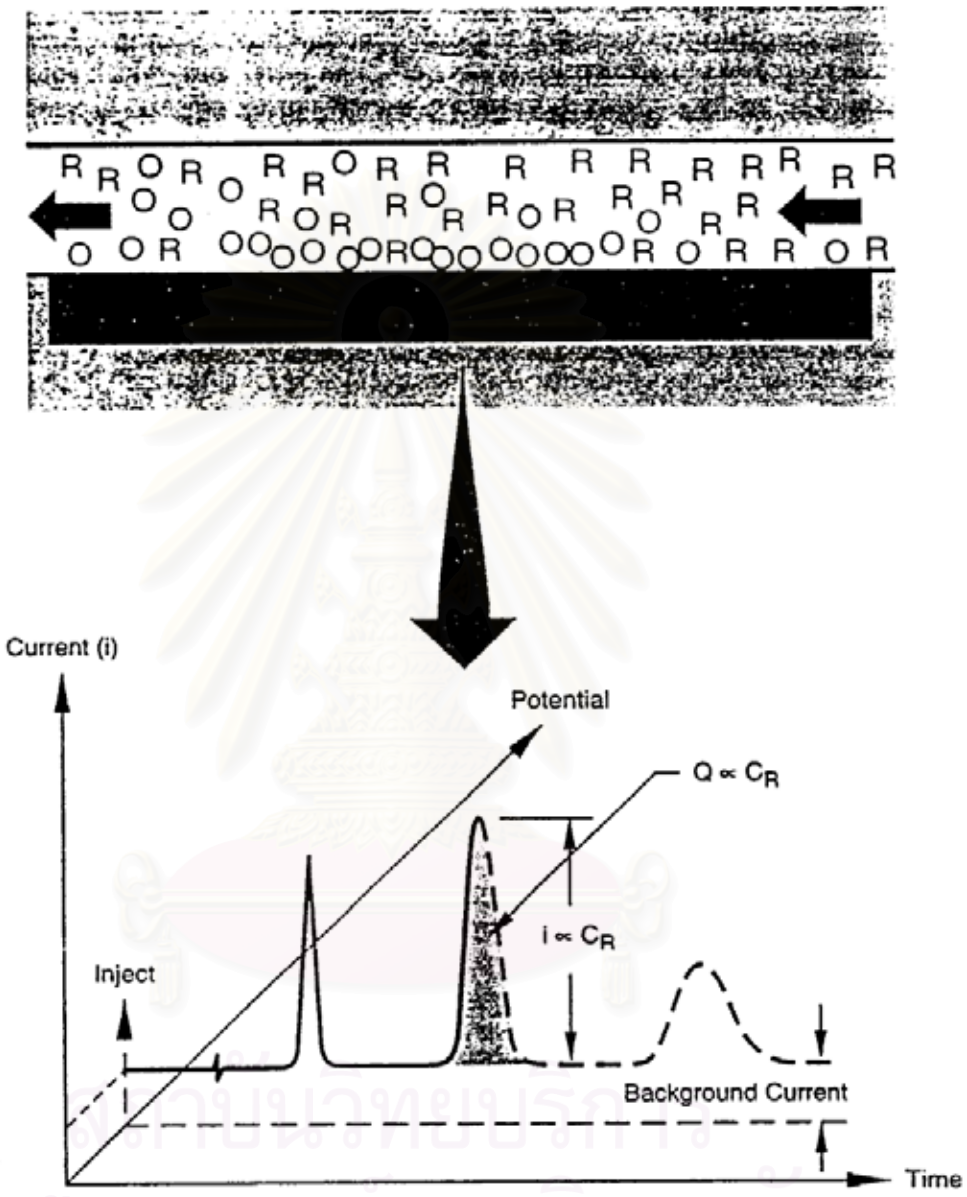

Figure 2.4 At any instant in time, the current in an LCEC experiment reflects the rate of conversion of reactant (R) to product (O).

In thin-layer cells with a downstream auxiliary electrode, the current between the working and auxiliary electrodes passes along a thin-layer channel, including that

portion adjacent to the electrode (Figure 2.5a). Therefore, the potential between the working electrode and the solution is not uniform across the face of the electrode. The potential difference at the downstream edge of the electrode will be closest to the value controlled by the potentiostat, whereas the upstream potential may be insufficient to oxidize or reduce to compounds of interest. The best solution to this problem is to position the auxiliary electrode opposite the working electrode surface (Figure 2.5b). This geometry ensures both that the uncompensated iR drop will be extremely small (due to the thinness of the layer) and that the potential will be uniform at all points on the working electrode surface. Moving the electrodes in relation to each other certainly impacts on the physical properties of the cell as an electronic circuit element. A more detailed treatment of the iR problem requires rather complex mathematics; however, the influence on the design of practical detector cells is important and can be easily understood form a qualitative point of view.

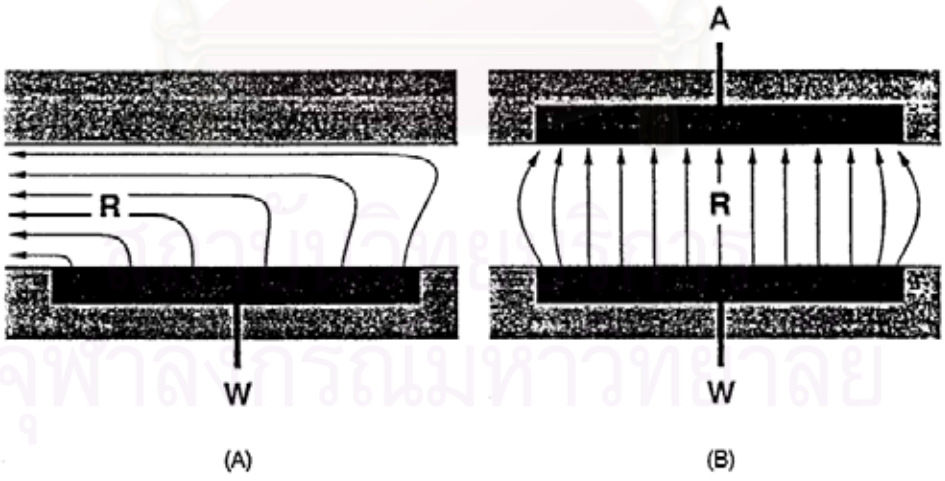

Figure 2.5 Thin-layer experiments are subject to large iR drops under certain condition (A). Placement of the auxiliary electrode across the channel from the working electrode (B) minimizes this problem.

Figure 2.6 illustrates five cross-flow cell geometries that they have been investigated for a number of years and are currently using for various applications. Figure 2.6a illustrates the original geometry employed for LCEC experiments with both the reference (R) and auxiliary (A) electrodes mounted downstream. The design is relatively inexpensive, but can suffer from iR-drop problems. It is important to recognize that for this design the three-electrodes system does not compensate for any significant solution resistance, but does have the advantage of not drawing current through the reference electrode. At low currents, the auxiliary electrode is not needed and the cell can be operated with the reference electrode serving as a classical counter electrode, as in two electrode polarography or Clark amperometric oxygen electrodes. This cell has the disadvantage that it is not suitable for collection of fractions. Figure 2.6b illustrates a simple modification in which a planar auxiliary electrode is placed opposite the working electrode. The thin-layer channel serves as a salt bridge to the reference electrode, but since no current passes along the thin layer, there is no resulting iR drop in the solution. In most instances the transit time across the thin layer of solution. Therefore, no interference occurs between chemical events taking place at the working and auxiliary electrodes. Some attention should be payed to this problem with large electrode areas, low flow rates, and very thin gaskets, in which case the geometry shown in Figure 2.6c can be advantageous. The problem here is that cell construction and maintenance becomes awkward when a porous diffusion barrier must be incorporated in the cell to isolate the auxiliary electrode. Placing the reference electrode probe opposite the working electrode in the wall of the thin channel can best be accomplished by use of an ionic junction constructed from a porous material that permits ions to migrate but blocks the flow of electrolyte solution (Figure 2.6d). Porous Vycor glass or ion exchange membranes are useful for this

purpose. Configuration 2.6e is perhaps most satisfactory from a fundamental point of view because of the uncompensated solution resistance and the compensated resistances are both small. In summary, configurations 2.6 a,b, and e are the most practical approaches to rugged cross-flows cells capable of routine use for many months. With geometry b, the linear range of the detector extents to over six orders of magnitude even in mobile phases with poor conductivity. Configuration a will work for trace applications, and b or e should be used for those cases where either a high background current or high resistance cause significant iR problems.

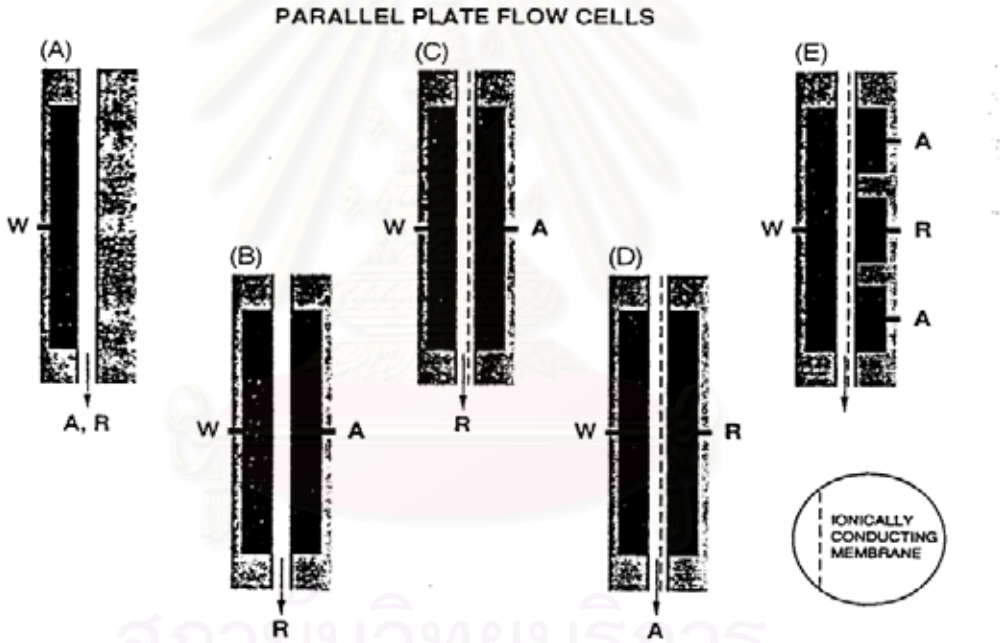

Figure2.6 Five geometries for thin-layer electrochemical cells. Relative placement of the working (W), reference (R), and auxiliary (A) is shown.

Figure 2.7 illustrates an early commercially available detector of type b, marketed by Bioanalytical Systems.

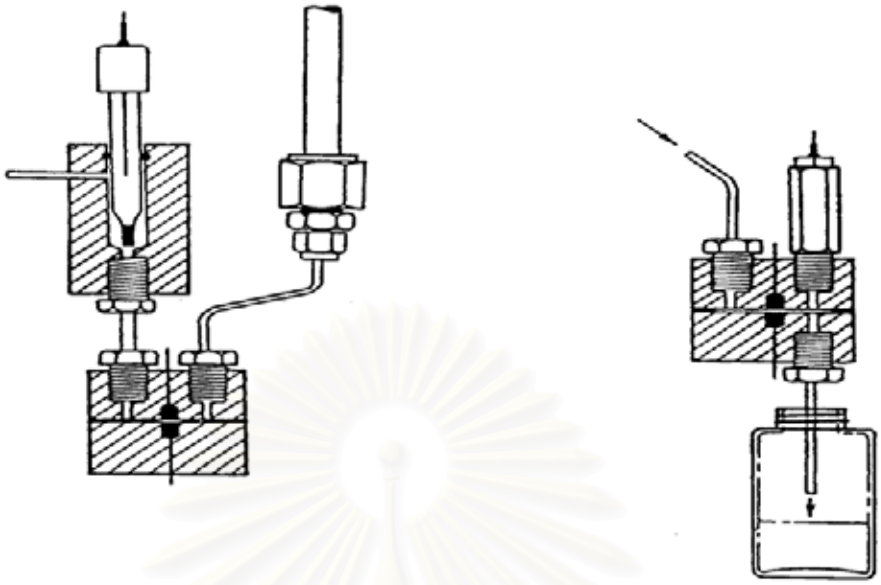

Figure 2.7 Commercial thin layer LCEC detector [Courtesy of Bioanalytical Systems, Inc.]

Figure 2.8 illustrates a more recent cross-flow design with the added features of parallel or series working electrodes. This cell can be used in any situation where a flow through cell is required, e.g., on-line process control. The size of the layer is determined by the thickness of the gasket used in the cell. The stainless steel auxiliary electrode houses a reference electrode compartment. A miniature Ag/AgCl reference is used in this design. The volume of the flow cell is extremely small.

สถาบันวิทยบริการ
จุฬาลงกรณ์มหาวิทยาลัย

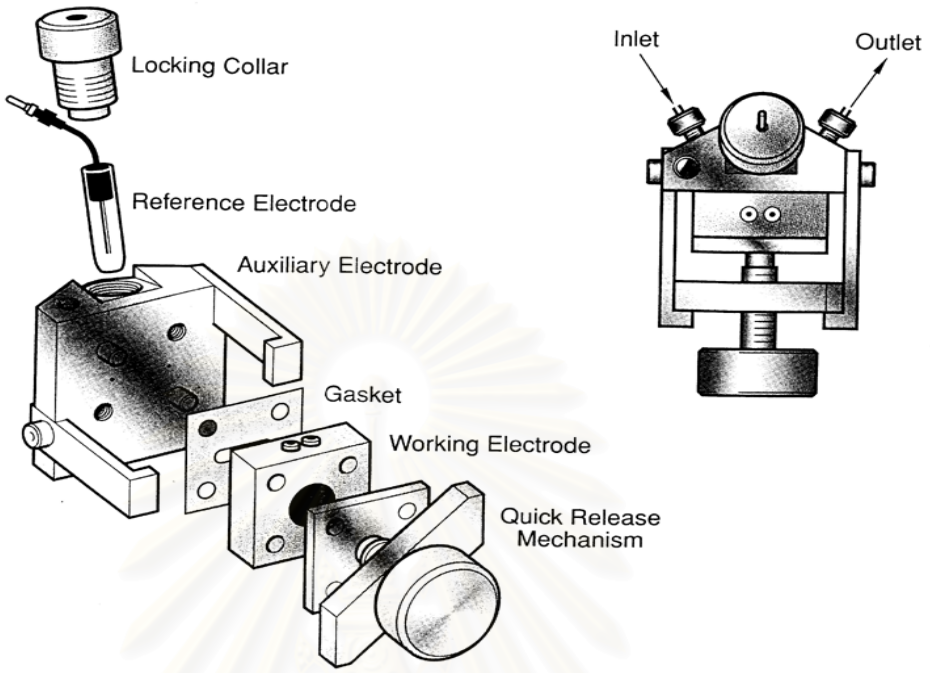

Figure 2.8 Recent cross-flow cell design. (the thin layer flow cell used in this study). Working electrodes may be in parallel or series.

สถาบันวิทยบริการ
จุฬาลงกรณ์มหาวิทยาลัย

2.3 Boron doped diamond thin film electrode

Diamond exhibits several important properties such as high thermal conductivity, extreme hardness, chemical inertness and corrosion resistance. Each carbon atom of diamond is tetrahedral, using sp^3-hybrid orbitals. Microstructure atoms arrange themselves in stacked six-member rings. This structure is different from that of other carbon- based materials (e.g. carbon fibers, glassy carbon and graphite) which have structures consisting of layers of condensed, six member rings with sp^2- hybridized carbon atoms trigonally bonded to one another [33].

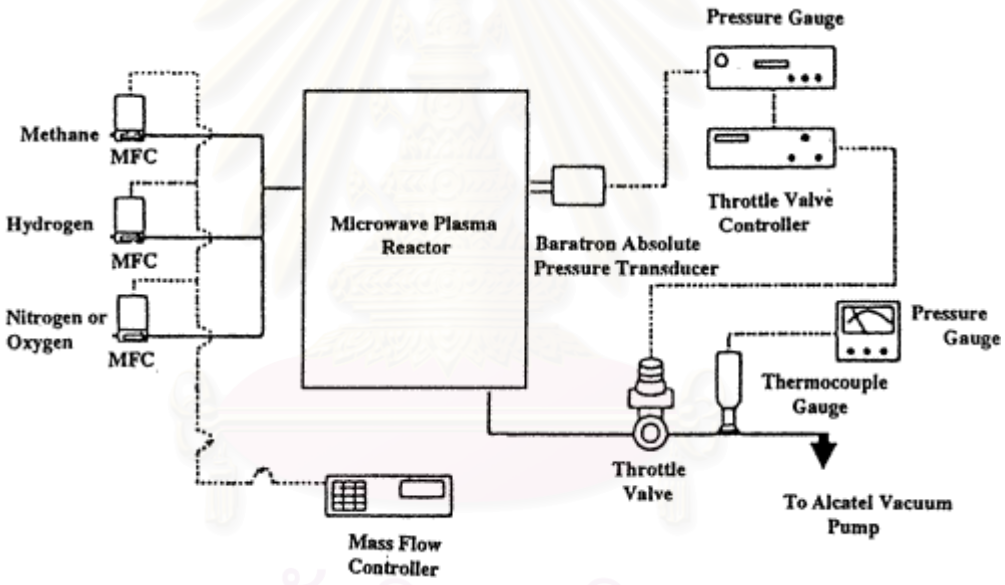

Figure 2.9 Diagram of the microwave plasma-assisted CVD diamond thin film reactor [34].

Recently, chemical vapor deposition (CVD) techniques (Figure 2.9) have afforded the possibility to produce synthetic diamond thin films. Hydrogen incorporation occurs during the film preparation since the presence of atomic hydrogen in the plasma is necessary to promote diamond formation. It was use to

grow on a variety of metal and nonmetal substrates e.g. c-BN, Ni, Cu, Si, Ta, Mo, W and glassy carbon. Diamond is one of nature's best insulating materials. In order to obtain enough conductive films for electrochemical studies, the material must be doped. Boron is most commonly used as the dopant, the resulting films are either p-type semiconductors or have semimetal electronic properties, depending on the doping level.

It has been observed that boron doped diamond thin film posses several unique electrochemical properties. First, diamond electrodes exhibit a lower and more stable background current in both voltammetric and amperometric detection compared with glassy carbon electrodes (Figure 2.10). Enhancement of S/B ratios [34] and long term response stability of several aqueous-based redox analytes were obtained. Second, diamond provides a wide working potential window in aqueous media (2.5 - 3 V) due to the large overpotentials for oxygen and, particularly, hydrogen evolution. This property may allow detecting redox analytes with more positive and negative standard reduction potentials. Third, the diamond surface is resistant to severe morphological damage and corrosion during anodic polarization in acidic fluoride, acidic chloride, and alkaline media [35,36]. Fourth, diamond exhibits a quasi-reversible transfer kinetic for redox analytes such as $Fe(CN)_6^{3-}$/ $Fe(CN)_6^{4-}$, $Ru(NH_3)_6^{2+}$/ $Ru(NH_3)_6^{3+}$ and $IrCl_6^{2-}$/ $IrCl_6^{3-}$. Fifth, it was found that slightly polar molecules adsorb on the diamond surface. Swain and co-workers confirmed this property [37]. Anthraquinonedisulfonate (AQDS) was tested at four electrodes: glassy carbon, hydrogenated glassy carbon, highly oriented pyrolytic graphite and diamond. The results are shown in Figure 2.11. No evidence of adsorption AQDS was found at the hydrogenated glassy carbon and diamond electrodes, while strongly physisorption were observed on glassy carbon and defected highly oriented pyrolytic graphite.

These material properties are the impetus for the use of the diamond electrode in amperometric detectors in flow injection analysis [38,39] and liquid chromatography [40-42].

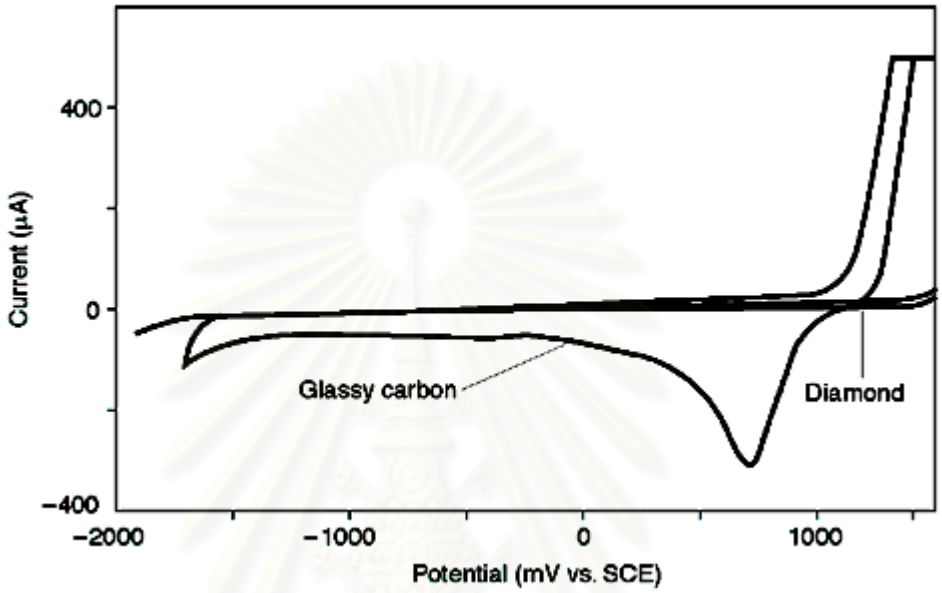

Figure 2.10 Cyclic voltammetric i-E curve for glassy carbon and boron-doped diamond thin film electrodes in 0.1 M KCl.

สถาบันวิทยบริการ
จุฬาลงกรณ์มหาวิทยาลัย

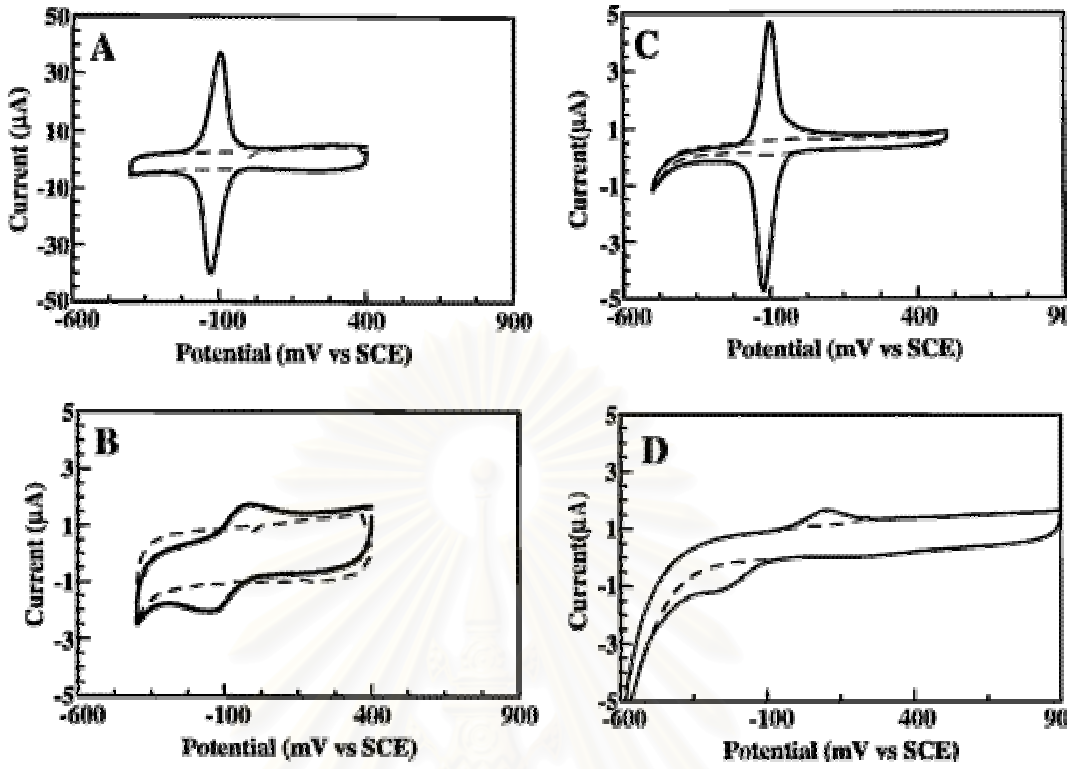

Figure 2.11 Cyclic voltammetric i-E curve for 10 μM AQDS and 0.1 M $HClO_4$ at (A) glassy carbon, (B) hydrogenated glassy carbon, (C) defected highly oriented pyrolytic graphite, and (D) diamond electrodes, Scan rate = 200 $mV.s^{-1}$

The previous work [42] has shown that the diamond electrode provides better performance than the glassy carbon as an amperometric detector. Most of amperometric data was obtained using flow injection analysis e.g. for chlorpromazine, ascorbic acid and 4-methylcatechol. Important parameters for the diamond and freshly polished glassy carbon electrodes are shown in Table 2.2. The diamond electrode has also been applied to ion chromatography for the detection of some ionic species such as azide and nitrite (Figure 2.12). Moreover, the use of diamond for the voltammetric detection of trace metal cations is illustrated (Figure 2.13). It was found

that diamond exhibited excellent performance in use as electrochemical detector for electroanalysis.

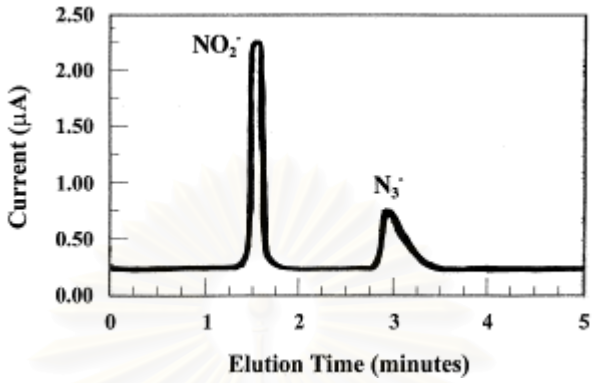

Figure 2.12 Ion chromatograph for 50 μl injections of 100 μM N_3^-, NO_2^- and NO_3^- in 5 mM phosphate buffer Na_2HPO_4, pH 7.2. Amperometric detection with a diamond film at +1.25 V vs Ag/AgCl was used. The flow rate was 2.0 ml/min.

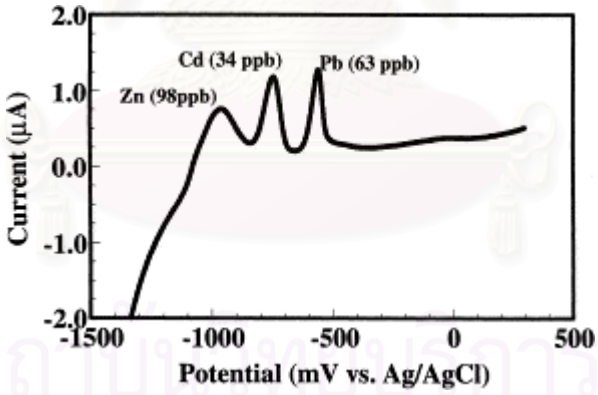

Figure 2.13 Linear sweep voltammetric i-E stripping curve for Zn^{2+}, Cd^{2+} and Pb^{2+} from bare diamond in an acetate buffer of 0.1 M acetate buffer, pH 4.52. The preconcentration was performed for 3 min in quiescent solution at -1300 mV vs SCE. The scan rate was 0.05 V/s.

Table 2.2 Amperometric data for chlorpromazine, ascorbic acid and 4-methylcatechol at diamond and polished glassy carbon electrode obtained in the flow injection system.

	Diamond	Glassy carbon
Chlorpromazine		
Dynamic range (μM)	0.1–3000	0.1–3000
Sensitivity (nA/ μM)	6	5
Detection limit (nM) at S/N = 3	4 (26 pg)	40 (260 pg)
Response variability range (%RSD)	0.3 %	1 %
Ascobic acid		
Dynamic range (μM)	0.1–3000	0.1–3000
Sensitivity (nA/ μM)	10	14
Detection limit (nM) at S/N = 3	12 (43 pg)	46 (162 pg)
Response variability range (%RSD)	0.7 %	0.7 %
4-methylcatechol		
Dynamic range (μM)	0.1–3000	0.1–3000
Sensitivity (nA/ μM)	13	14
Detection limit (nM) at S/N = 3	2.0 (5 pg)	40 (99 pg)
Response variability range (%RSD)	0.6 %	0.9 %

สถาบันวิทยบริการ
จุฬาลงกรณ์มหาวิทยาลัย

2.4 Drugs

Drugs are one type of chemicals that are important for human life because they are used for treatment of many diseases. In this work, drugs that have different functional groups including hydroxyl group, thiol group and keto - enol group were investigated.

2.4.1 Acetaminophen (Figure 2.14a) [43]

Acetaminophen, also called Paracetamol, is a good analgesic and antipyretic drug. It is suitable for the treatment of pains of all kinds such as headaches, dental pain, postoperative pain, pain in connection with colds and posttraumatic pain. For cancer patients, acetaminophen is used for mild pain and it can be administered in combination with opioids. Acetaminophen has been compared to many other analgesic drugs and is considered approximately equipotent to aspirin. It is suitable for use in children and preferred for patients who are sensitive to aspirin. There are no known side effects of the drug when the patients use the appropriate dose. In overdoses, larger amounts of paracetamol are metabolized by oxidation because of saturation of the sulphate conjugation pathway. Therefore, liver glutathione stores become depleted so that the liver is unable to deactivate the toxic metabolite that has a high affinity for cell protein and binds to liver cell macromolecules. The result is disruption of cellular architecture and function.

Several methods including conventional spectrophotometry [44-48], fluorimetry [49], high performance liquid chromatography [9,13,50-53] and capillary electrophoresis [54-56] have been used to determine acetaminophen in the pharmaceutical and medical applications. Electrochemical methods are also general

for this application. Most previous reports were performed using mercury, glassy carbon, carbon paste or platinum electrodes to study the electrochemistry of acetaminophen [16,20-24,57-63]. Most of these electrodes were modified with some chemical such as Nafion/Ruthenium oxide in order to improve the sensitivity. To clean the surface, these electrodes must pretreated with some chemical such as alumina slurries to provide a reproducible and stable response prior to use. Diamond electrodes can overcome this problem, they can be used without any complicated pretreatment even after exposure to the laboratory atmosphere over a month.

2.4.2 D-penicillamine (Figure 2.14 b)

D-penicillamine, D-2-amino-3-mercaptobutanoic acid or 3-mercapto-D-valine, is a chelating agent recommended for removal of excess copper in patients with Wilson's disease [64-66]. It is also used to reduce cystine excretion in cystinuria [67-69] and to treat patients with severe, active rheumatoid arthritis [70,71] unresponsive to conventional therapy.

Various methods have been proposed for the determination of D-penicillamine including high-performance liquid chromatography with pre or post column derivatization [10-12,14,15,72], calorimetry [73,74], fluorometry [75], chemiluminescene [76] and electrophoresis [77,78]. One of the important limitations of liquid chromatography techniques is the fact that this thiol lacks sufficient UV absorption. Therefore, a pre or post-column derivatization procedure is normally required. Electrochemical methods are an alternative for thiol drug determination because they are cheap, simple, fast and sensitive. Mercury and mercury amalgam electrodes were extensively used for thiol-compound determination, however, the mercury has limitations due to its toxicity and the rapid deterioration of the electrode

response. Chemically modified electrodes have also been used to determine D-penicillamine but their use in flow injection analysis and liquid chromatography is limited because of particular mechanical and chemical stability towards the flowing solution.

2.4.3 Barbituric acid (Figure 2.14c)

Barbituric acid analogs are useful for the treatment of benign or malignant tumors such as prostate cancer, breast cancer or leukemia and for the treatment of viral infections, immune disorders or depression associated with HIV-1. Barbituric acid is also a precusor of barbiturate (sleeping pill) and an intermediate for Vitamin B_{12}. It can also be used as a polymerization catalyst and raw material for dyes [79].

Surprisingly, there are few reports of the determination of this compound. Aman, et. al. [80] used spectrophotometry to determine barbituric acid. However, this method was complicated because barbituric acid must be reacted with a derivatization agent by heating for 1 min at 100 degree C to give a compound that can absorb in the UV spectrum. You, et al. [79] determined barbituric acid and 2-thio-barbituric acid by capillary electrophoresis with end-column electrochemical (carbon fiber microdisk electrode) detection. Under the optimum conditions, a detection limit of 0.5 μM of barbituric acid and a linear range over three orders of magnitude was obtained.

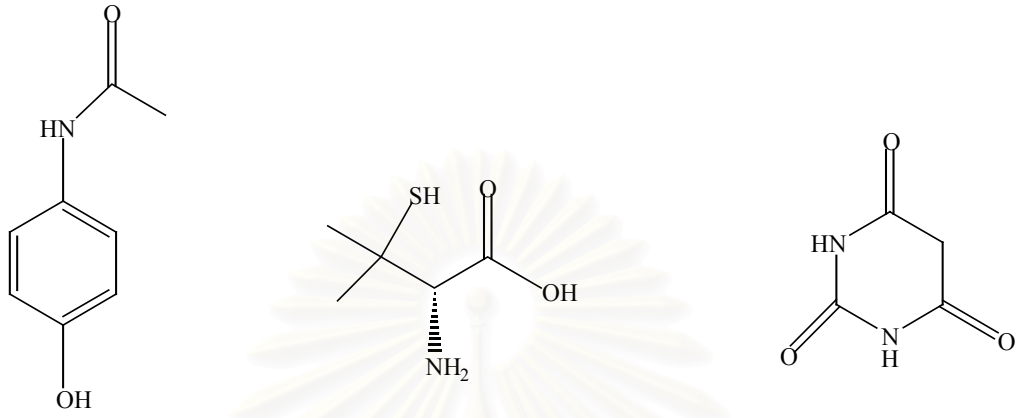

(a) (b) (c)

Figure 2.14 Structures of (a) acetaminophen (b) D-penicillamine and (c) barbituric acid.

สถาบันวิทยบริการ
จุฬาลงกรณ์มหาวิทยาลัย

CHAPTER III

EXPERIMENTAL

3.1 Chemicals and reagents

3.1.1 Acetaminophen (Fluka)

3.1.2 D-penicillamine (Sigma)

3.1.3 Barbituric acid (Fluka, purum)

3.1.4 Potassium dihydrogenphosphate (Merck)

3.1.5 Sodium hydroxide (Merck)

3.1.6 Phosphoric acid (85% Carlo Erba)

3.1.7 Sodium hydrogen carbonate (Baker)

3.1.8 Sodium carbonate (Merck)

3.1.9 Absolute Ethanol (Merck)

3.1.10 Potassium chloride (Merck)

3.1.11 A standard buffer solution pH 4 and 7 (Metrohm)

3.1.12 Lactose (Bacto)

3.1.13 Paracetamol Syrup (Sara)

3.1.14 Penicillamine Capsule (Cuprimine 250 mg)

สถาบันวิทยบริการ
จุฬาลงกรณ์มหาวิทยาลัย

3.2 Apparatus

3.2.1 Boron-doped diamond thin films (BDD) (obtained from Prof A. Fujishima Laboratory, The University of Tokyo) were grown in a chemical vaporization deposition system (CVD). The BDD film contained 10^4 ppm boron. The electrode was rinsed with an ultrapure water prior to use.

3.2.2 A glassy carbon electrode (0.07 cm^2 , Bioanalytical Inc) was pretreated by polishing with alumina powder (1 and 0.05 micron , respectively) slurries in ultrapure water on felt pads and rinsed thoroughly with an ultrapure water prior to use.

3.2.3 A Ag/AgCl electrode (TCI) with a salt bridge

3.2.4 A home-made platinum wire

3.2.5 A home made glass cell

3.2.6 A home made brass holder

3.2.7 An O-ring viton (0.07 cm^2)

3.2.8 A polishing set of 0.05 and 1 micron alumina powder slurry (Bioanalytical Inc.)

3.2.9 An Autolab Potentiostat (PG-100, Methrom)

3.2.10 A reagent delivery module (Water) and using nitrogen gas for driving the mobile phase.

3.2.11 A peristaltic pump (Ismatic)

3.2.12 A Rheodyne injection valve, Model 7125 (Altech), with a 20 μl stainless steel injection loop (0.5 mm. i.d.)

3.2.13 A thin layer flow cell (Bioanalytical Inc.).

3.2.14 A neoprene gasket (Bioanalytical Inc.)

3.2.15 PEEK tubing (0.25 mm. i.d.) and connecting (Upchurch)

3.2.16 Teflon tubing (1/16 inch o.d., Upchurch)

3.2.17 A cutting set (Altech)

3.2.18 A 0.2 μM Nylon membrane filter (Altech).

3.2.19 A 0.45 μM Nylon membrane syringe filter with polypropylene (PP) housing (Orange Scientific filter).

3.2.20 A pH meter (Metrohm)

3.2.21 A sonicator (USA)

3.2.22 An analytical balance (Metler)

3.3 The Preparation of buffer solutions

All solutions were prepared using deionized water obtained from a Milli-Q system (Milford, MA, USA). The preparation of buffer solutions are shown below:

3.3.1 0.1 M Phosphate buffer

Potassium dihydrogen phosphate 13.60 g was dissolved in 1.0 L of deionized water and then adjusting with sodium hydroxide or phosphoric acid to the required pH.

3.3.2 0.1 M Carbonate buffer pH 9.2

Sodium hydrogen carbonate 7.50 g and sodium carbonate 1.70 g were dissolved in 1.0 L of deionized water. The pH was adjusted to pH 9.2 using hydrochloric acid or sodium hydroxide to the required pH.

3.4 Procedures

3.4.1 Cyclic voltammetry

The electrochemical measurements were performed in a single compartment glass cell using a potentiostat. Figure 3.1 showed an electrochemical cell for cyclic votammetric experiment. A Ag/AgCl and platinum wire electrodes were used as reference and auxiliary electrodes, respectively. The diamond and glassy carbon electrodes (0.07 cm^2) were used as working electrodes. The diamond electrode was pressed against a smooth ground joint at the bottom of the cell isolated by an O-ring (area 0.07 cm^2). The exposed geometric area was 0.07 cm^2. Ohmic contact was made by placing the backside of the Si substrate on a brass plate.

Figure 3.1 The electrochemical cell for cyclic voltammetric study

3.4.1.1 Background current.

The experiment was carried out in 0.1 M phosphate buffer (pH 7) using the diamond electrode at the scan rate of 200 mV s^{-1}. Comparison the experiments using the glassy carbon electrode was studied.

3.4.1.2 pH dependence study

These experiments were done to obtain the optimum pH for each analyte at the scan rate of 20 mV s^{-1}. The pH and the concentration of each analyte solutions are shown in Table 3.1

Table 3.1 pH and the concentration of each analyte for the pH dependence experiments

Analyte	Concentration	pH
1. Acetaminophen	1 mM	2.5, 5, 7, 8
2. D-penicillamine	2 mM	5, 7, 8, 9.2
3. Barbituric acid	2 mM	2.5, 5, 7, 8, 9.2
4. Ampicillin sodium	1 mM	2.5, 5, 6, 7

สถาบันวิทยบริการ
จุฬาลงกรณ์มหาวิทยาลัย

3.4.1.3 The electrochemical oxidation of analytes solution.

The 1 mM solutions of the analytes in the chosen buffer solution from the previous experiment (Section 3.4.1.2) were studied using the diamond electrode by cyclic voltammetry. Comparison the experiments with the glassy carbon electrode were carried out. A scan rate of 20 mV s^{-1} was used.

3.4.1.4 The scan rate dependence study

Using 1 mM solutions of analytes, experiments were performed to investigate the adsorption of the analytes on the surface of electrode at various scan rates. The scan rates that were used in these experiments were 10, 20 50, 100, 200 and 300 mV s^{-1}.

3.4.1.5 The analytical performance

Stock solution of 20 mM concentration of each analyte were freshly prepared and diluted to a concentration range between 0.01 and 20 mM. A scan rate of 20 mV s^{-1} was used. These studies were carried out to find the linear ranges and detection limits.

สถาบันวิทยบริการ
จุฬาลงกรณ์มหาวิทยาลัย

3.4.2 Flow injection with amperometric detection

The flow injection analysis system consisted of a thin layer flow cell, an injection port with a 20 μl injection loop, a reagent delivery module or peristaltic pump and an electrochemical detector. The mobile phase was regulated by a reagent delivery module (N_2 gas flow) or a peristaltic pump at a flow rate of 1 ml min^{-1}. Figure 3.2 shows a thin layer flow cell for the flow injection system. The thin layer flow cell consisted of a silicone rubber gasket as a spacer, a Ag/AgCl electrode as the reference electrode and a stainless steel tube as an auxiliary electrode and an outlet of the flow cell. The experiments were performed in a copper faradaic cage to reduce electrical noise.

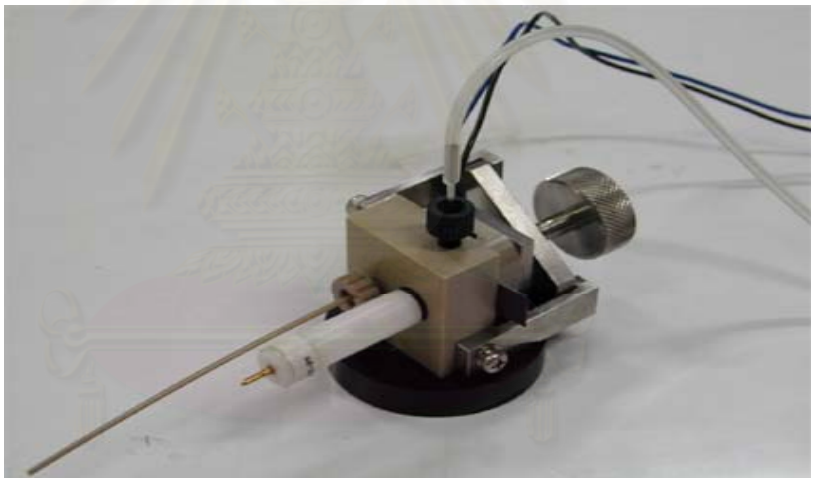

Figure 3.2 The thin layer flow cell

สถาบันวิทยบริการ
จุฬาลงกรณ์มหาวิทยาลัย

3.4.2.1 Hydrodynamic voltammetry

Hydrodynamic voltammetry were carried out for each analyte before the amperometric determination to find the optimum potential that used to set the instrument. The data were obtained by recording the background current at each potential and then injecting a series of four replicates of 20 μl of 100 μM analyte solutions. The peak current after each injection was recorded, together with the corresponding background current. These data were plotted as a function of applied potential to obtain hydrodynamic voltammograms.

3.4.2.2 Calibration and linear range

5 mM stock solutions of each analyte were freshly prepared and then diluted to a concentration range from 10 nM to 2.5 mM. The experiments were carried out by injection 5 replicates of each concentration. Results were used to plot the calibration and find the linear range.

3.4.2.3 Detection limit

The detection limit was carried out by injecting of low concentrations of analyte solutions five replicates under the optimal potential. The detection limit was defined as the concentration that provided a current response higher three replicates than the noise ($S/N \geq 3$).

สถาบันวิทยบริการ
จุฬาลงกรณ์มหาวิทยาลัย

3.4.2.4 Repeatability

The repeatability was studied by injecting of analyte solutions for five replicates. The repeatability is expressed in terms of the relative standard deviation (%RSD), using the following formula:

$$\%RSD = \frac{\text{standard deviation}}{\text{Mean}} \times 100$$

3.4.2.5 Stability of electrode

The stability of the electrode was determined by injecting of 100 μM D-penicillamine 45 replicates using the diamond electrode that continuous used for 1 month. The result obtained was used in calculating the relative standard deviation.

3.4.2.6 Applications

The proposed method was applied to a real sample. The real samples were a drug syrup and a capsule. The standard addition method for finding the amount of drug in the real sample was used.

3.4.2.6.1 The drug syrup

Paracetamol syrup (Sara, USA 5 ml = 120 mg of paracetamol) was used as a model in this study. The sample preparation is described below:

Paracetamol syrup 2 ml was transferred and diluted with 0.1 M phosphate buffer (pH 8) to 100 ml in a volumetric flask. After that, the

solution was further diluted with 0.1 M phosphate buffer (pH 8) to give a final concentration of 1.8 μg/ml.

A stock solution of 1.51 μg/ml acetaminophen in 0.1 M phosphate buffer (pH 8) and a set of six 25 ml volumetric flasks were prepared. 5 ml of sample solution was pipetted in each flask, then 0, 2.5, 5.0, 7.5, 10.0 and 15.0 ml of a stock solution of acetaminophen were added to give the final concentration of standard in the solution of 0, 0.15, 0.30, 0.45, 0.60 and 0.91 μg/ml, respectively.

3.4.2.6.2 The drug capsule

Penicillamine capsule 250 mg (Cuprimine, USA) was used in this study. The sample preparation is described below:

A mass of powder of one capsule of penicillamine (Cuprimine 250 mg) was transferred to a 100 ml volumetric flask and dissolved in 0.1 M phosphate buffer (pH 7), filtrated through a 0.45 μM Nylon membrane syringe filter. Then, the filtrated was further diluted with 0.1 M phosphate buffer (pH 7) to obtain a final concentration of 2.50 μg/ml.

A stock solution of 2.98 μg/ml of D-penicillamine in 0.1 M phosphate buffer (pH 7) and a set of five 25 ml volumetric flasks were prepared. 5 ml of sample solution was pipetted in each flask and then 0, 5.0, 7.5, 10.0 and 12.5 ml of a stock solution of D-penicillamine was added to give final concentrations of the standard 0, 0.60, 0.90, 1.19 and 1.49 μg/ml, respectively.

Interference study was also studied. A stock solution of 37.30 μg/ml (0.25 mM) of D-penicillamine and 34.20 mg/ml (10 mM) of lactose in 0.1 M phosphate buffer (pH 7) were prepared. 5 ml of stock solution of

D-penicillamine was pipetted into each 25 ml of volummetric flask and then 2.5,5.0 and 10.0 and 12.5 ml of lactose solution was added to obtain a concentration ratio between a lactose and D-pencillamine of 20, 40, 80 and 100, respectively. Each flask was adjusted to the volume with 0.1 M phosphate buffer (pH 7).

สถาบันวิทยบริการ
จุฬาลงกรณ์มหาวิทยาลัย

CHAPTER IV

RESULTS AND DISCUSSION

4.1 Cyclic voltammetry

4.1.1 Background current

The preliminary work was focused on a comparison of the background currents that were obtained for the diamond and the glassy carbon electrodes. Figures 4.1 and 4.2 show the background voltammograms of 0.1 M phosphate buffer (pH 7) at the diamond and glassy carbon electrodes, respectively. The background current for the glassy carbon electrode was ~ 10 times higher than that obtained for the diamond electrode. There are three possibilities that can explain the low background current [39]. First, the relative absence of electroactive carbon-oxygen functionalities on the hydrogen-terminated diamond surface as compare with glassy carbon, leads to a lower current but this possibility can explain only some, but not all, of low current for diamond. A second contributing factor may be a lower charge carrier concentration due to the semimetal-semiconductor nature of boron-doped diamond. A lower state at a given potential, or a lower charge carrier concentration, would lead to a reduced accumulation of counterbalancing ions and water dipoles on the solution side of the interface, thereby lowering the background current. A third possible contributing factor could be that the diamond surface is constructed like an array of microelectrodes. In other words, perhaps the diamond surface has "electrochemically

actives" sites separated by less reactive or more insulating regions, in much the same way that composite electrodes have very reactive regions of carbon separated by insulating regions of the support.

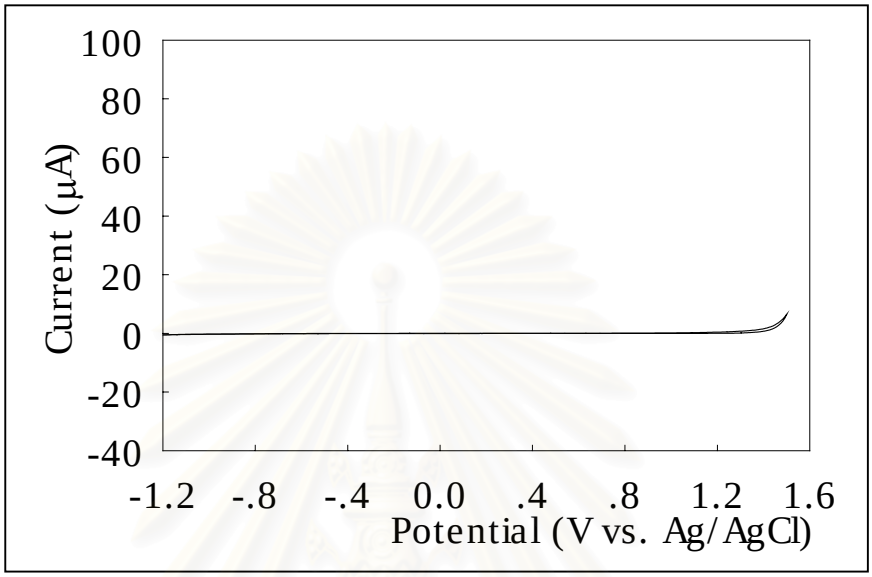

Figure 4.1 Cyclic voltammogram of 0.1 M phosphate buffer (pH 7) at the diamond electrode. The scan rate was 200 mV s^{-1}.

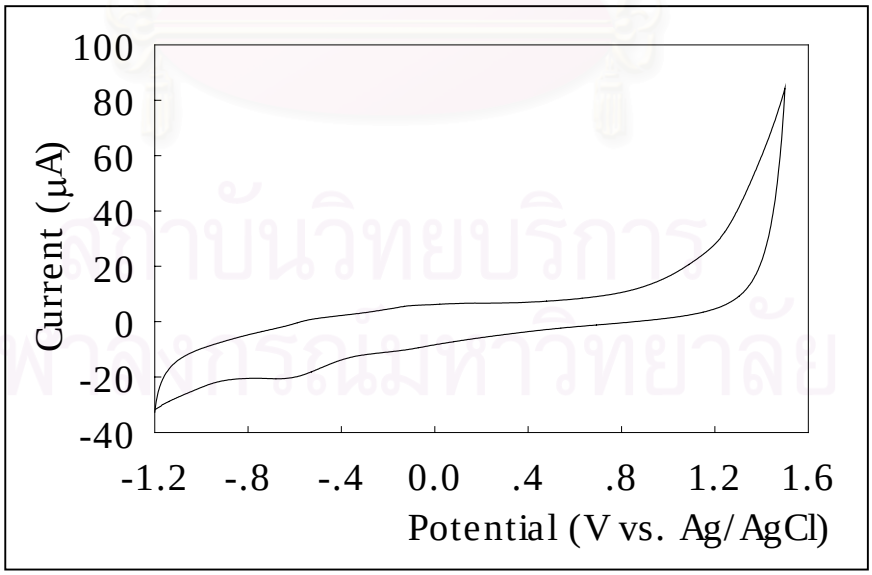

Figure 4.2 Cyclic voltammogram of 0.1 M phosphate buffer (pH 7) at the glassy carbon electrode. The scan rate was 200 mV s^{-1}.

4.1.2 pH dependence study

The influence of pH on the electrode responses of acetaminophen, D-penicillamine and barbituric acid were studied at the diamond electrode.

4.1.2.1 Acetaminophen

Table 4.1 summarizes the electrochemical data obtained from cyclic voltmmograms of 1 mM acetaminophen oxidation at pH 2.5, 5, 7 and 8 at the diamond electrode. It was found that the oxidation potential (positive scan) decreased when the pH of the analyte solution increased. This phenomenon may be because acetaminophen was easier to hydrolyse in an alkaline medium [81]. The proposed oxidation mechanism of acetaminophen is shown in Figure 4.3 [82].

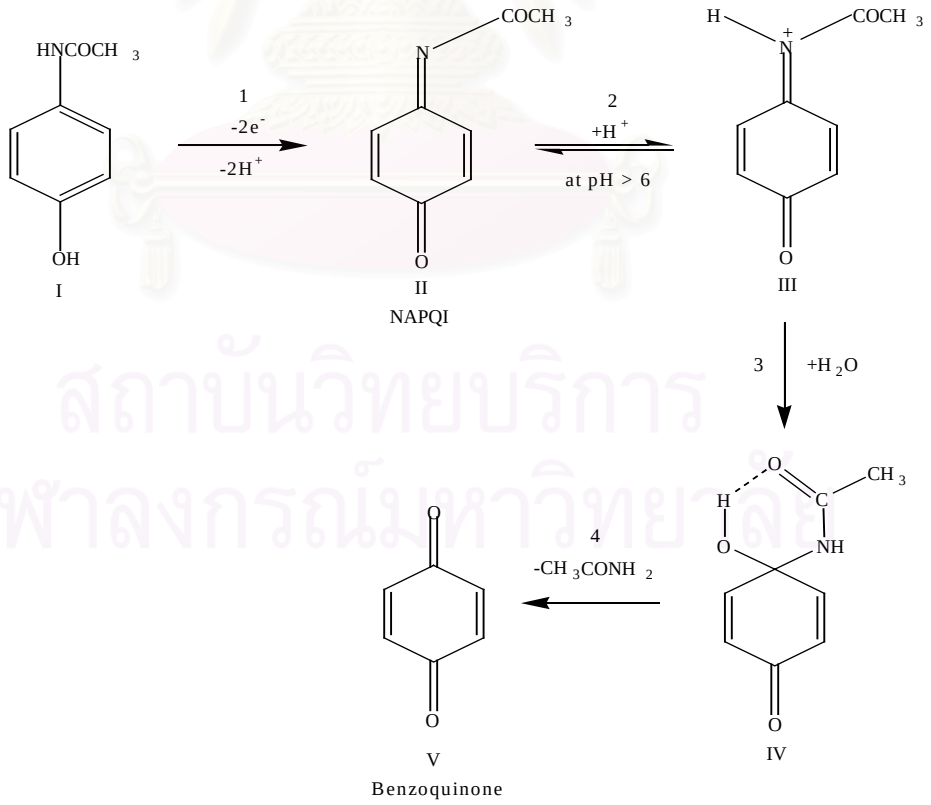

Figure 4.3 The proposed oxidation mechanism of acetaminophen

Acetaminophen is electrochemically oxidized in a pH-dependent, 2-electron, 2 proton process to N-acetyl-p-quinoneimine (NAPQI). The occurrence of follow-up chemical reactions involving NAPQI is pH dependent. At pH > 6, NAPQI exists in the stable unprotonated form (II). Under more acidic conditions, NAPQI is immediately protonated (step2), yielding a less stable but electrochemically active species (III) which rapidly yields (step 3) a hydrated form (IV) that is electrochemically inactive. Hydrated NAPQI (IV) converts (step 4) to benzoquinone. The medium, however, has to be extremely acidic for the rate of the process to be significant enough that reduction of benzoquinone is observed during the cyclic voltammetric experiment.

Table 4.1 Comparison of electrochemical data obtained from the cyclic voltammogram of the 1 mM acetaminophen for the diamond electrode at pH 2.5, 5, 7 and 8 (n = 2)

pH	E_p^{ox} (V vs. Ag/AgCl)	I_p^{ox} (μA)	E_p^{red} (V vs. Ag/AgCl)	I_p^{red} (μA)
2.5	0.786±0.004	10.840±0.390	-0.011±0.000	-0.444±0.082
5	0.761±0.003	10.97±0.240	-0.101±0.002	-2.802±0.976
7	0.694±0.006	8.129±0.584	-0.139±0.003	-4.025±0.200
8	0.610 ±0.023	13.720±0.230	-0.170±0.010	-7.696±0.968

From the Table 4.1, the maximum oxidation current signal at the peak potential about 0.610 V vs. Ag/AgCl was obtained at the pH 8. Hence, this pH was selected as the optimum pH for the study of acetaminophen.

4.1.2.2 D-penicillamine

The effect of the buffer pH was investigated at pH 5, 7, 8 and 9.2 at the diamond electrode. At the buffer pH 7 , 8 and 9.2, the diamond electrode exhibited a well-defined cyclic voltammograms. In the case of buffer pH 5, an ill-defined cyclic voltammogram was obtained.

The changing of buffer pH effected the oxidation peak potential. It was found that increasing the buffer pH from pH 7, decreased the oxidation peak potential, probably due to the facile oxidation of the thiol group in D-penicillamine structure in the alkaline medium. The pH of the buffer also affected the peak current of the cyclic voltammograms. From Table 4.2, the maximum current signal was observed at pH 7. Therefore, this pH was chosen as the optimal pH. The proposed oxidation mechanism of D-penicillamine [83-85], which was similar to other thiol compounds e.g. cysteine reaction mechanisms, is shown in Figure 4.4

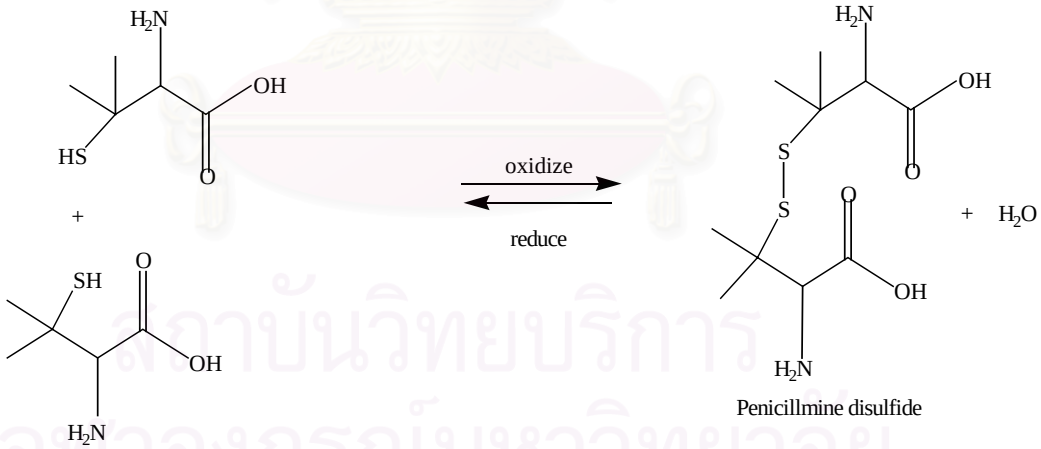

Figure 4.4 The proposed oxidation mechanism of D-penicillamine

Thiols are easily oxidized to give dimers called disulfides. Two thiols join together in this reaction, the hydrogen from each is lost, and the two sulfides bond together. The disulfide bond is week and is easily reduced to give the thiols.

.

Table 4.2 Comparison of electrochemical data obtained from the cyclic voltammograms of 2 mM D-penicillamine for the diamond electrode at pH 5, 7, 8 and 9.2 (n = 2)

pH	E_p^{ox} (V vs. Ag/AgCl)	I_p^{ox} (μA)
5	0.948±0.005	7.621±2.689
7	0.757±0.031	13.500±0.540
8	0.693±0.002	12.215±1.095
9.2	0.674±0.011	11.460±0.430

สถาบันวิทยบริการ
จุฬาลงกรณ์มหาวิทยาลัย

4.1.2.3 Barbituric acid

Table 4.3 summarizes the electrochemical data obtained from the cyclic voltammograms of 2 mM of barbituric acid at pH 2.5, 5, 7, 8 and 9.2 at the diamond electrode. It was found that the higher pH analyte solution, the lower peak potential was obtained, possible due to easier oxidation of barbituric acid in the alkaline solution. From the Table, the maximum oxidation current signal was obtained at pH 8. Therefore, pH 8 was selected for the study of barbituric acid.

Table 4.3 Comparison of electrochemical data obtained from the cyclic voltammetry for the 2 mM of barbituric acid on the diamond electrode at pH 2.5, 5, 7, 8 and 9.2 (n = 2)

pH	E_p^{ox} (V vs. Ag/AgCl)	I_p^{ox} (μA)
2.5	1.265±0.008	19.880±0.230
5	1.259±0.001	17.190±1.670
7	1.140±0.053	19.365±1.495
8	1.065±0.040	22.910±1.600
9.2	1.019±0.012	20.390±0.250

สถาบันวิทยบริการ
จุฬาลงกรณ์มหาวิทยาลัย

4.1.3 The electrochemical oxidation of analytes solution.

The electrochemical oxidation of 0.1 mM of acetaminophen, 0.1 mM of D-penicillamine and 0.1 mM of barbituric acid at the diamond and the glassy carbon electrodes were studied. The electrochemical data obtained from cyclic voltammograms of 0.1 mM acetaminophen, 0.1 mM D-penicillamine, and 0.1 mM barbituric acid at diamond and glassy carbon electrodes are shown in Table 4.4. It was found that the diamond electrode provided higher S/B ratios for acetaminophen, D-penicillamine and barbituric acid than the glassy carbon electrode.

Figure 4.5 – 4.10 show cyclic voltammograms obtained for 0.1 mM 0.1 mM acetaminophen, 0.1 mM D-penicillamine, and 0.1 mM barbituric acid at diamond and glassy carbon electrodes. Well-defined quasi-irreversible cyclic voltammograms were obtained at both diamond (Figure 4.5) and glassy carbon electrodes (Figure 4.6) for acetaminophen. However, the diamond electrode provided a better S/B ratio current signal. A well-defined irreversible cyclic voltammogram was obtained at the diamond electrode (Figure 4.7) while an ill-defined irreversible cyclic voltammogram was obtained at the glassy carbon electrode (Figure 4.8) for D-penicillamine. Well-defined irreversible cyclic voltammograms were obtained at both dimond (Figure 4.9) and glassy carbon electrodes (Figure 4.10) for barbituric acid. However, the diamond electrode again provided a better S/B ratio current signal.

Table 4.4 The electrochemical data of 0.1 mM acetaminophen, 0.1 mM, D-penicillamine and 0.1 mM barbituric acid at the diamond and the glassy carbon electrodes (n = 2).

Analyte	Electrode	E_p^{ox} (V)*	I_p^{ox} (μA)	E_p^{red} (V)*	I_p^{red} (μA)	S/B[a]
Acetaminophen	BDD	0.426 ±0.010	2.680 ±0.086	-0.079 ±0.011	-1.063 ±0.065	38.26 ±0.83
	GC	0.325± 0.003	1.532± 0.066	0.131 ±0.014	-0.716 ±0.036	4.46 ±0.61
D-penicillamine	BDD	0.812± 0.006	0.810 ±0.013	-	-	27.63 ±1.27
	GC	0.801 ±0.011	0.745 ±0.078	-	-	1.04 ±0.01
Barbituric acid	BDD	1.044 ±0.000	0.641 ±0.000	-	-	7.14 ±0.01
	GC	0.981 ±0.013	0.998 ±0.066			0.77 ±0.05

* potential (V) vs. Ag/AgCl
[a] calculated from I_p^{ox}/Background current

สถาบันวิทยบริการ
จุฬาลงกรณ์มหาวิทยาลัย

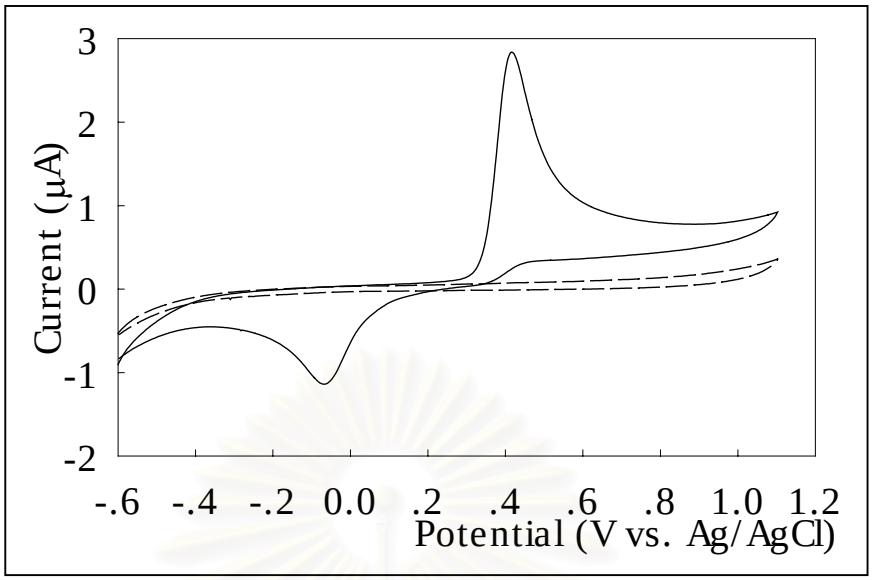

Figure 4.5 Cyclic voltammogram of 0.1 mM acetaminophen in 0.1 M phosphate buffer (pH 8) at the diamond electrode (solid line). The scan rate was 20 mV s^{-1}. Background voltammogram (0.1 M phosphate buffer, pH 8) is also shown in this Figure (dash line).

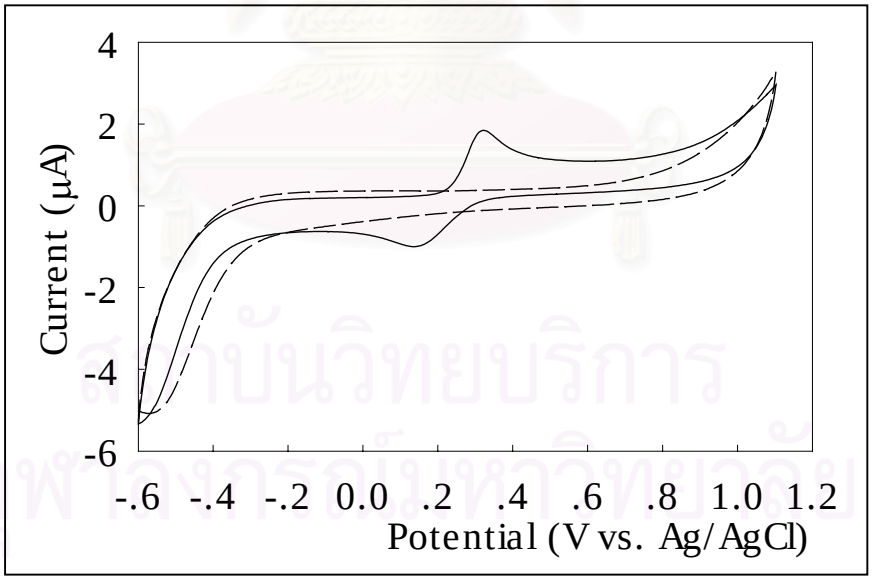

Figure 4.6 Cyclic voltammogram of 0.1 mM acetaminophen in 0.1 M phosphate buffer (pH 8) at the glassy carbon electrode (solid line). The scan rate was 20 mV s^{-1}. Background voltammogram (0.1 M phosphate buffer, pH 8) is also shown in this Figure (dash line).

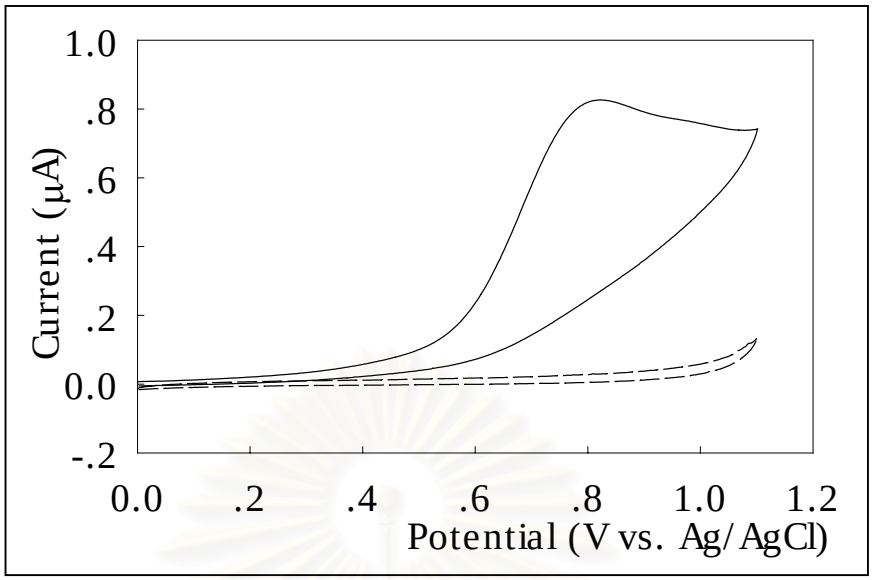

Figure 4.7 Cyclic voltammogram of 0.1 mM D-penicillamine in 0.1 M phosphate buffer (pH 7) at the diamond electrode (solid line). The scan rate was 20 mV s^{-1}. Background voltammogram (0.1 M phosphate buffer, pH 7) is also shown in this Figure (dash line).

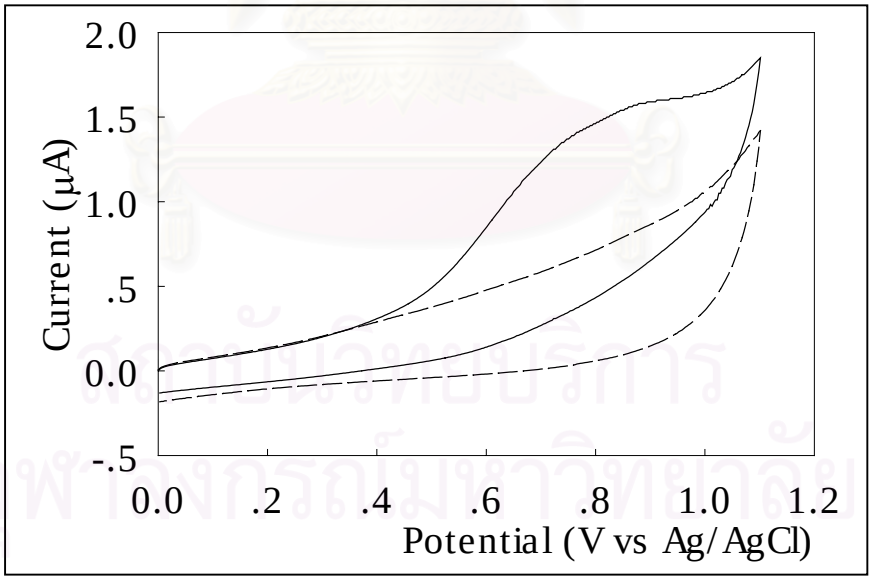

Figure 4.8 Cyclic voltammogram of 0.1 mM D-penicillamine in 0.1 M phosphate buffer (pH 7) at the glassy carbon electrode (solid line). The scan rate was 20 mV s^{-1}. Background voltammogram (0.1 M phosphate buffer, pH 7) is also shown in this Figure (dash line).

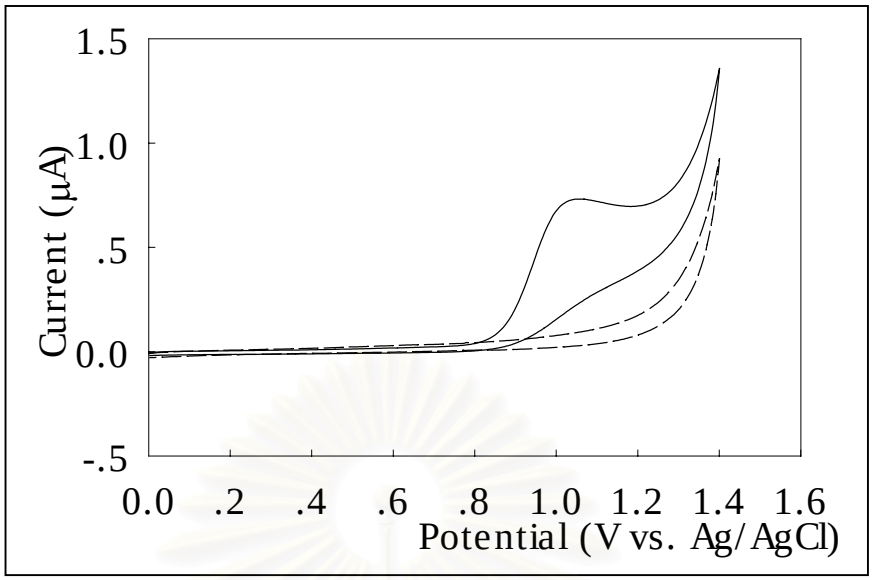

Figure 4.9 Cyclic voltammogram of 0.1 mM barbituric acid in 0.1 M phosphate buffer (pH 8) at the diamond electrode (solid line). The scan rate was 20 mV s^{-1}. Background voltammogram (0.1 M phosphate buffer, pH 8) is also shown in this Figure (dash line).

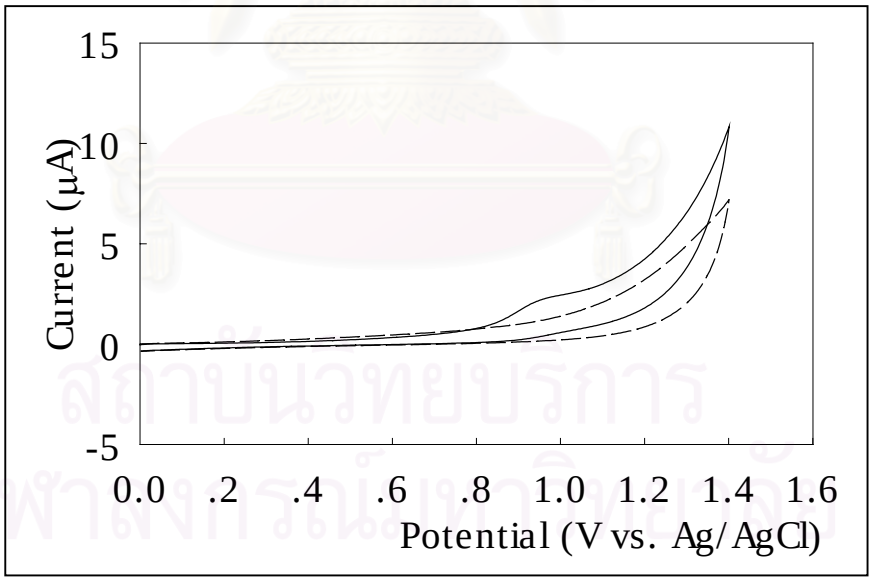

Figure 4.10 Cyclic voltammogram of 0.1 mM barbituric acid in 0.1 M phosphate buffer (pH 8) at the glassy carbon electrode (solid line). The scan rate was 20 mV s^{-1}. Background voltammogram (0.1 M phosphate buffer, pH 8) is also shown in this Figure (dash line).

4.1.4 The scan rate dependence study

In this study, 1 mM of acetaminophen, D-penicillamine and barbituric acid were investigated by varying the scan rate from 10 to 300 $mV.s^{-1}$. The equations used for describing the relationship between the current signal and scan rate are shown below [31]:

4.1.4.1 Quasi-reversible system

$$i_p \text{ (diffusion)} = 0.4463nFAC_0^*(nF/RT)^{1/2}\nu^{1/2} D_0^{1/2}K(\Lambda,\alpha)\text{------- 4.1}$$

The analyte in this system was acetaminophen. From equation 4.1, the current (diffusion) is expected to be proportional to square root of scan rate, $\nu^{1/2}$. Figures 4.11 and 4.12 show the relationship between current and square root of scan rate for acetaminophen at the diamond and the glassy carbon electrodes, respectively. The currents were proportional to the square root of the scan rate at the diamond and the glassy carbon electrodes. It can be concluded that acetaminophen underwent quasi-reversible reaction and also that there was indicated semi-infinite linear diffusion of reactant to the electrode surface at the diamond and the glassy carbon electrodes.

สถาบันวิทยบริการ
จุฬาลงกรณ์มหาวิทยาลัย

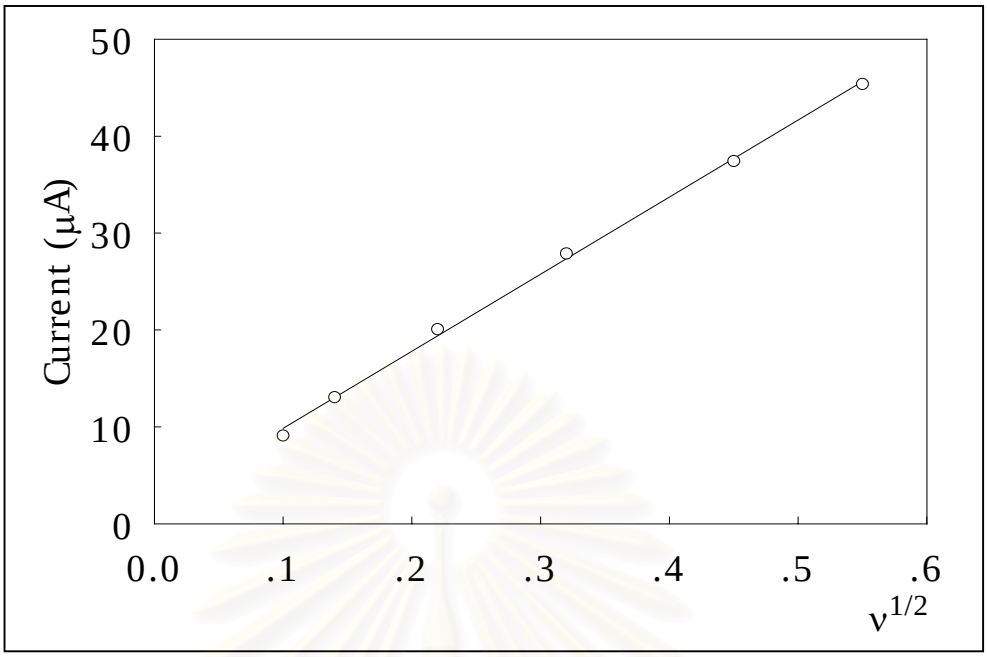

Figure 4.11 The current vs. square root of scan rate ($\nu^{1/2}$) curve of 1 mM acetaminophen in 0.1 M phosphate buffer (pH 8) at the diamond electrode.

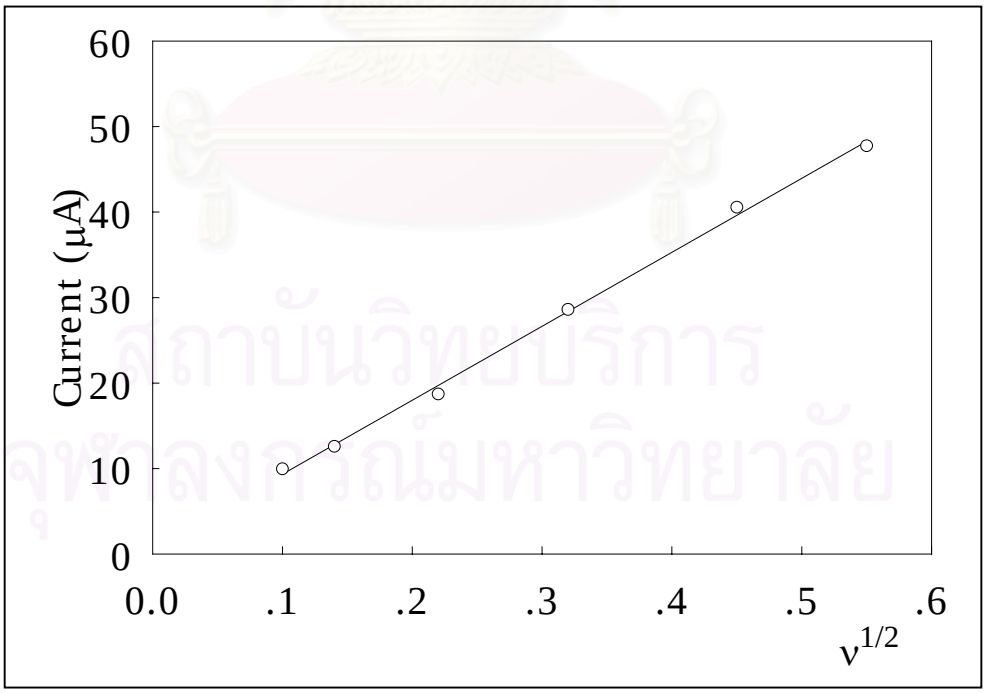

Figure 4.12 The current vs. square root of scan rate ($\nu^{1/2}$) curve of 1 mM acetaminophen in 0.1 M phosphate buffer (pH 8) at the glassy carbon electrode.

4.1.4.2 Totally irreversible

i_p (diffusion) = $(2.99 \times 10^5)n(\alpha n_a)^{1/2} A C_0^* D_0^{1/2} \nu^{1/2}$ ----------4.2

i_p (adsorption) = $n\alpha n F^2 A \nu \Gamma^*_0 / 2.718RT$----------4.3

The analytes that exhibited this behavior were D-penicillamine and barbituric acid . From equation 4.2, the current (diffusion) is expected to be proportional to the square root of scan rate, $\nu^{1/2}$. At the diamond electrode the relationship between the current and the square root of scan rate was linear with $R^2 >$ 0.998 for D-penicillamine and barbituric acid as shown in Figure 4.13 and 4.14, respectively. It can be concluded that D-penicillamine and barbituric acid underwent irreversible reaction and also that there was semi-infinite linear diffusion of reactant to the diamond electrode surface.

For the glassy carbon electrode, D-penicillamine can not provide a linear relationship between current and square root of scan rate because at higher the scan rate, the shape of the cyclic voltammograms were ill-defined and hard to define the current. Interestingly, barbitruic acid did not provide a linear relationship between current and the square root of scan rate (Figure 4.15) however the current was proportional to scan rate (Figure 4.16). It can be concluded that barbituric acid was adsorbed on the electrode surface (electrode fouling) (equation 4.3).

สถาบันวิทยบริการ
จุฬาลงกรณ์มหาวิทยาลัย

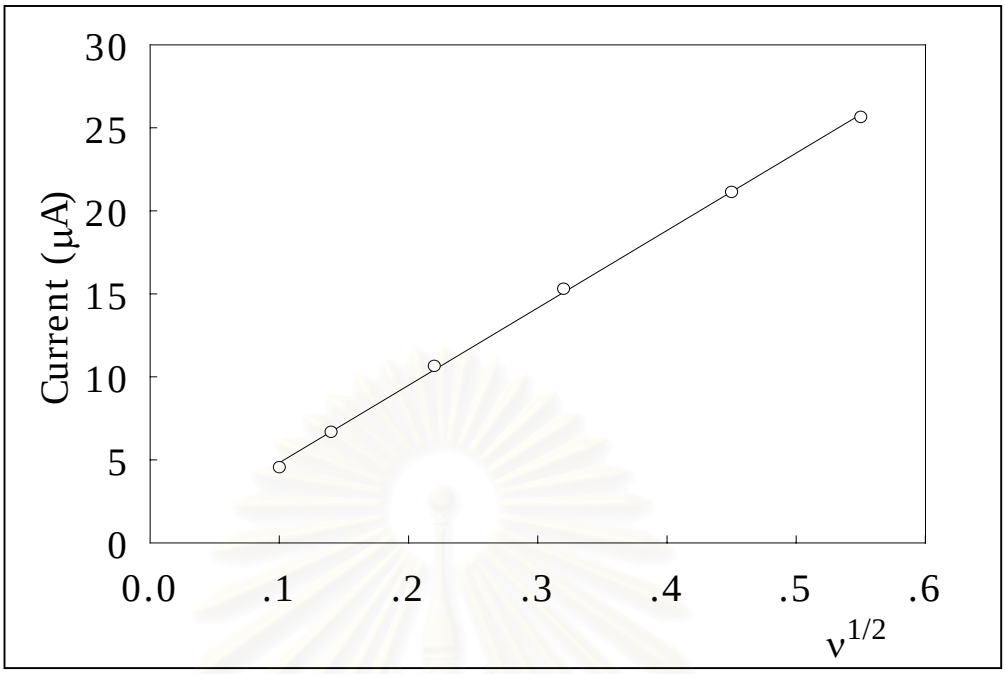

Figure 4.13 The current vs. square root of scan rate ($\nu^{1/2}$) curve of 1 mM D-penicillamine in 0.1 M phosphate buffer (pH 7) at the diamond electrode.

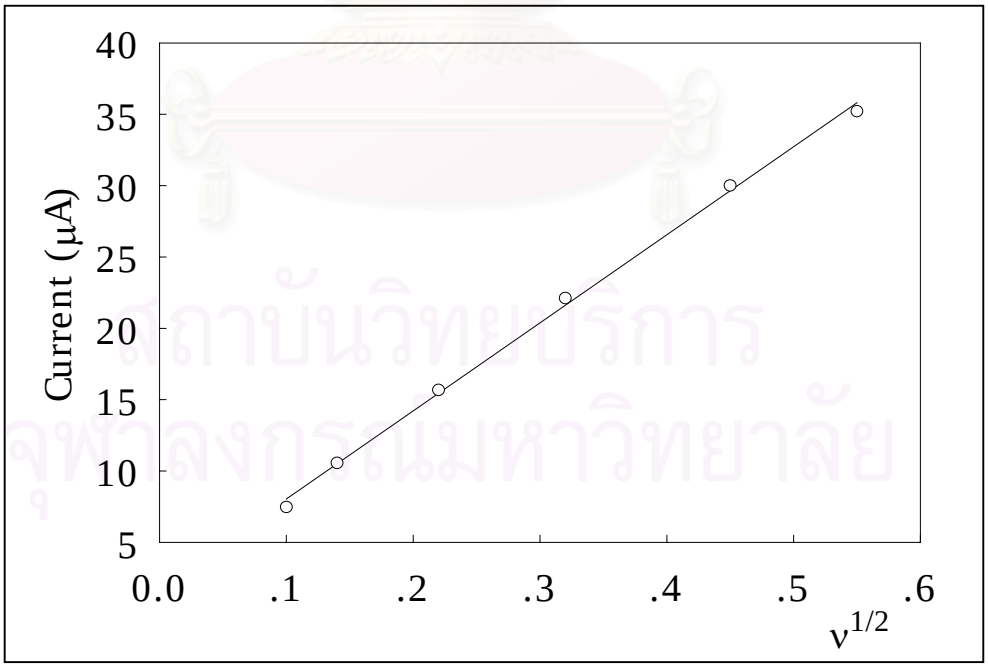

Figure 4.14 The current vs. square root of scan rate ($\nu^{1/2}$) curve of 1 mM barbituric acid in 0.1 M phosphate buffer (pH 8) at the diamond electrode.

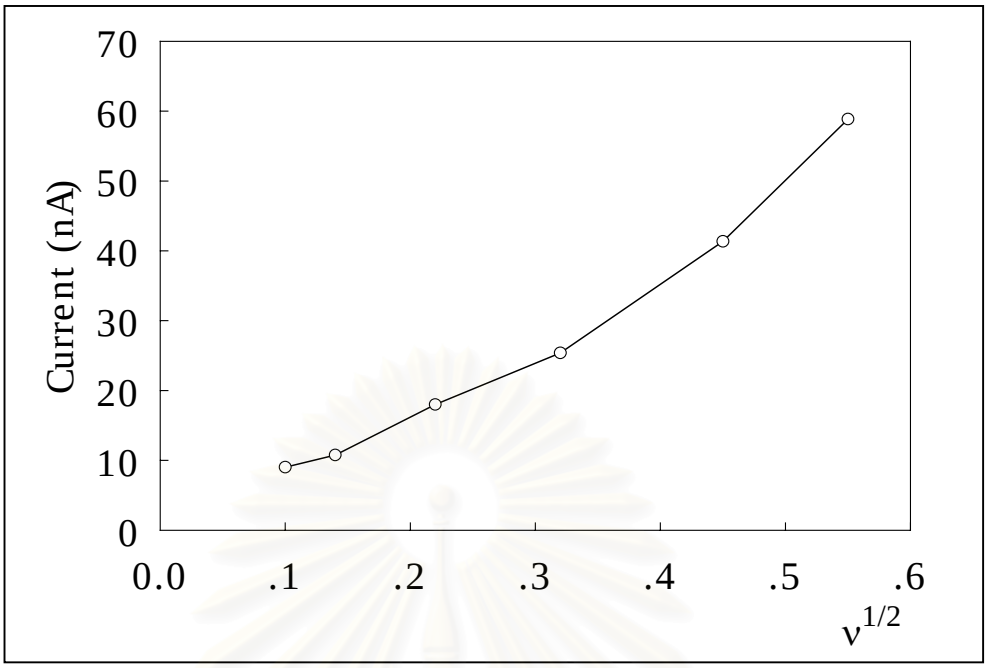

Figure 4.15 The current vs. square root of scan rate ($\nu^{1/2}$) curve of 1 mM barbituric acid in 0.1 M phosphate buffer (pH 8) at the glassy carbon electrode

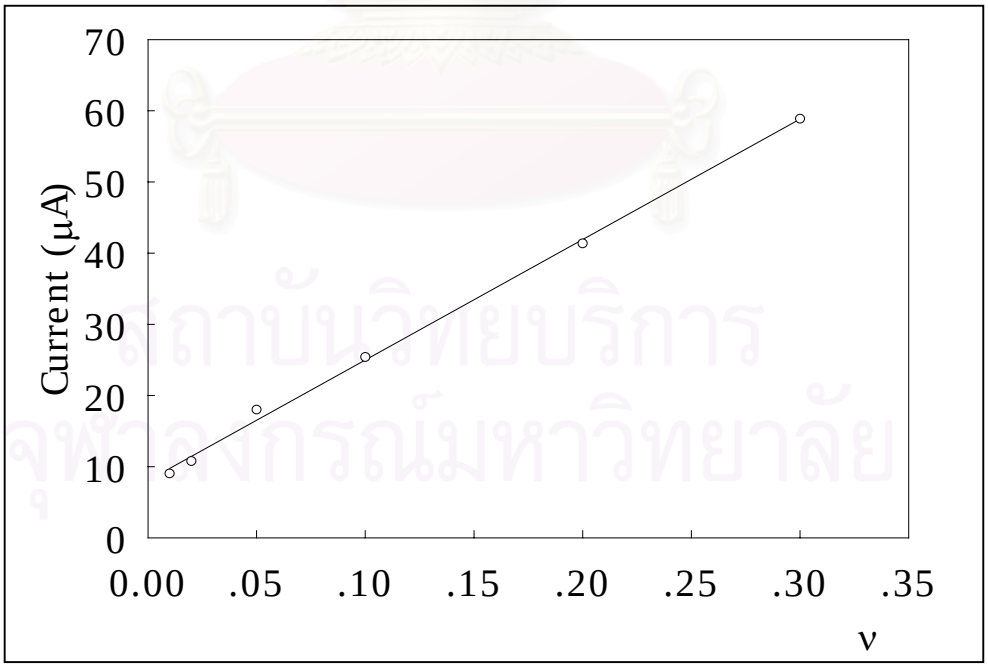

Figure 4.16 The current vs. scan rate (ν) curve of 1 mM barbituric acid in 0.1 M phosphate buffer (pH 8) at the glassy carbon electrode.

4.1.5 The analytical performance

Table 4.5 summarizes the analytical figures of merit of acetaminophen, D-penicillamine and barbituric acid at the diamond and the glassy carbon electrodes by cyclic voltammetry.

4.1.5.1 Acetaminophen

Acetaminophen was determined using concentrations from 0.010 to 10 mM at the diamond and the glassy carbon electrodes. From the calibration curve, a good linear response within the concentration range 0.1 -8 mM (Figure 4.17) and 0.5-5 mM (Figure 4.18) were obtained for the diamond and the glassy carbon electrodes, respectively. The sensitivity, as the slope of calibration plot of acetaminophen at the diamond electrode (10.14±0.70 μA/mM) was close to the glassy carbon electrode (10.36±0.59 μA/mM) with the same correlation coefficient of 0.995 (Table 4.5). However, the diamond electrode provided a lower detection limit than the glassy carbon electrode by a factor of 10. The detection limit (LoD) is defined as the concentration that provides a ratio of current signal to background current of at least 3 (S/B ≥ 3). The LoD for the diamond electrode was 0.01 mM (10 μM) (Figure 4.19) while the LoD obtained at the glassy carbon electrode was 0.1 mM (100 μM) (Figure 4.20). This was due the high background current of the glassy carbon electrode.

Table 4.5 Analytical figures of merit of acetaminophen, D-penicillamine and barbituric acid at the diamond and the glassy carbon electrodes by cyclic voltammetry (n = 2).

Analyte	BDD				GC			
	Linear range (mM)	Sensitivity (μA/mM)	R^2	LoD (mM)	Linear range (mM)	Sensitivity (μA/mM)	R^2	LoD (μM)
Acetaminophen	0.1 – 8	10.14± 0.70	0.9952 ± 0.0029	0.010	0.5 - 5	10.36± 0.59	0.9948 ± 0.0030	0.100
D-penicillamine	0.5 - 10	3.60± 0.55	0.9979 ± 0.0002	0.025	-	-	-	0.500
Barbituric acid	0.05 - 20	9.19 ±0.06	0.9952 ± 0.0029	0.050	3- 20	7.53 ±0.44	0.9988 ± 0.0002	0.500

สถาบันวิทยบริการ
จุฬาลงกรณ์มหาวิทยาลัย

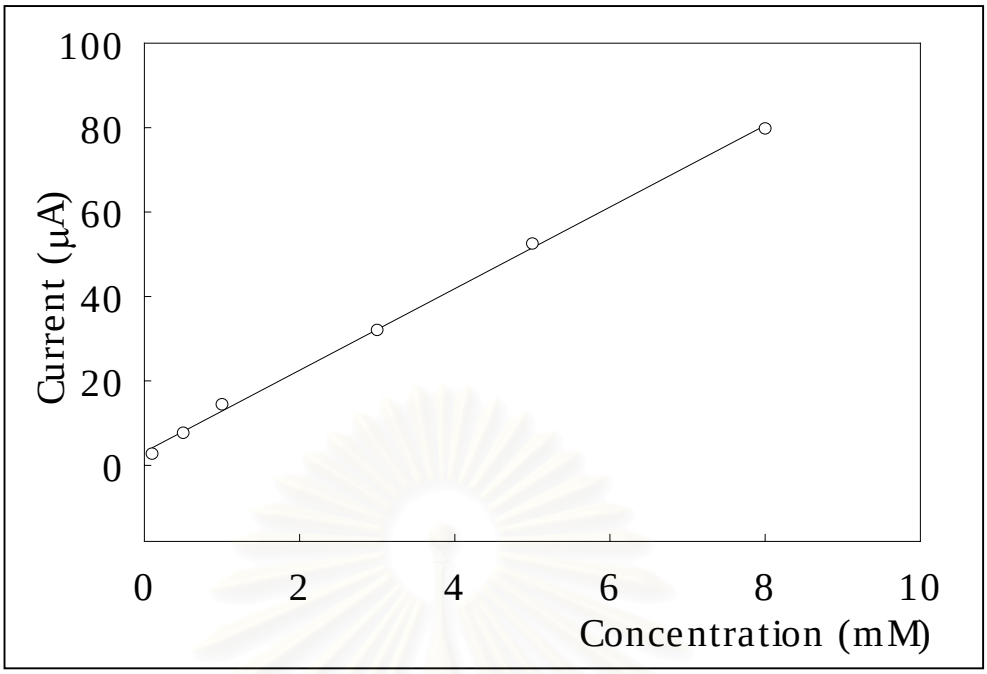

Figure 4.17 Calibration curve of acetaminophen (0.1 - 8 mM) in 0.1 M phosphate buffer (pH 8) at the diamond electrode. The scan rate was 20 mV s^{-1}

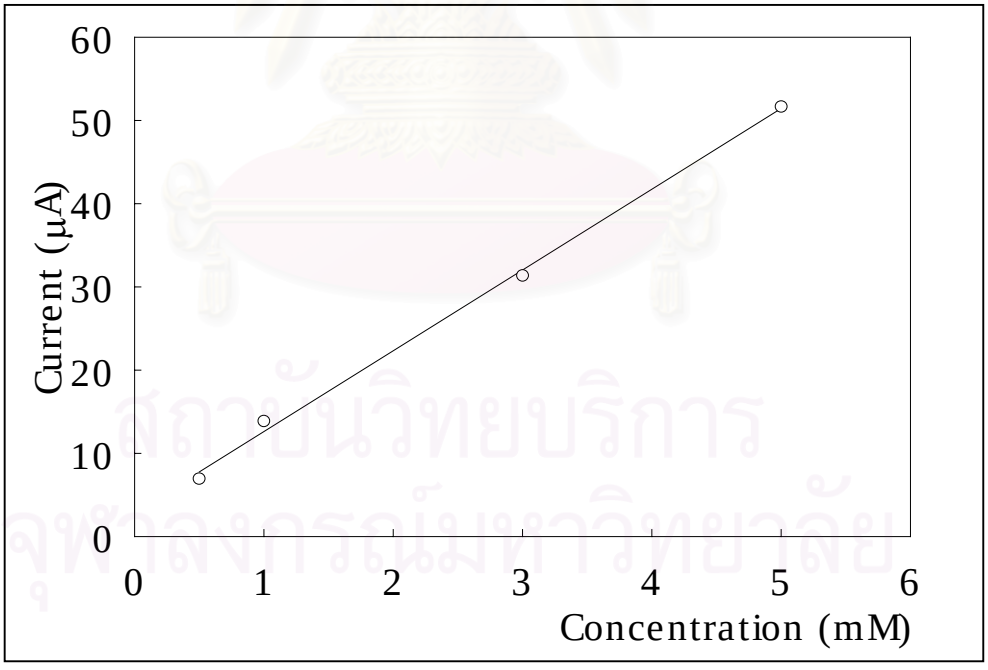

Figure 4.18 Calibration curve of acetaminophen (0.5 – 5 mM) in 0.1 M phosphate buffer (pH 8) at the glassy carbon electrode. The scan rate was 20 mV s^{-1}.

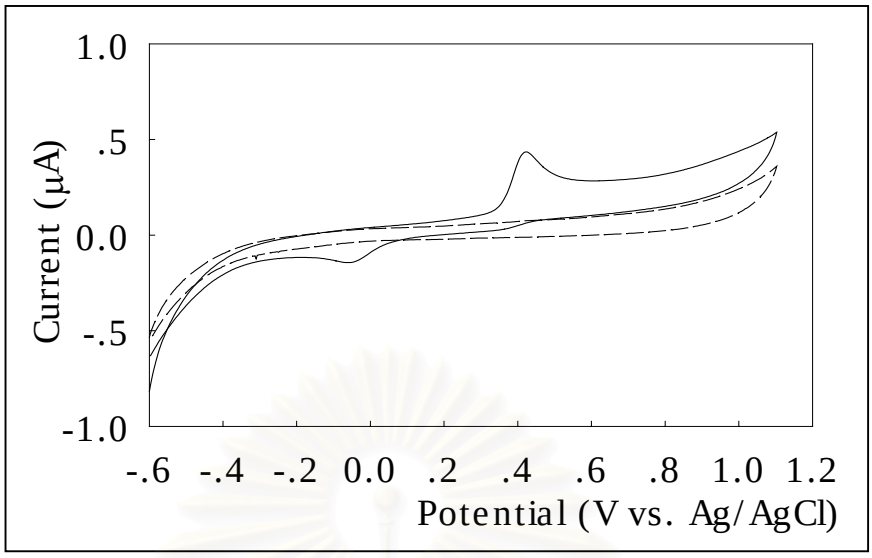

Figure 4.19 Cyclic voltammogram of 0.01 mM (10 μM) acetaminophen in 0.1 M phosphate buffer (pH 8) at the diamond electrode (solid line). The scan rate was 20 $mV.s^{-1}$. Background voltammogram (0.1 M phosphate buffer, pH 8) is also shown in this Figure (dash line).

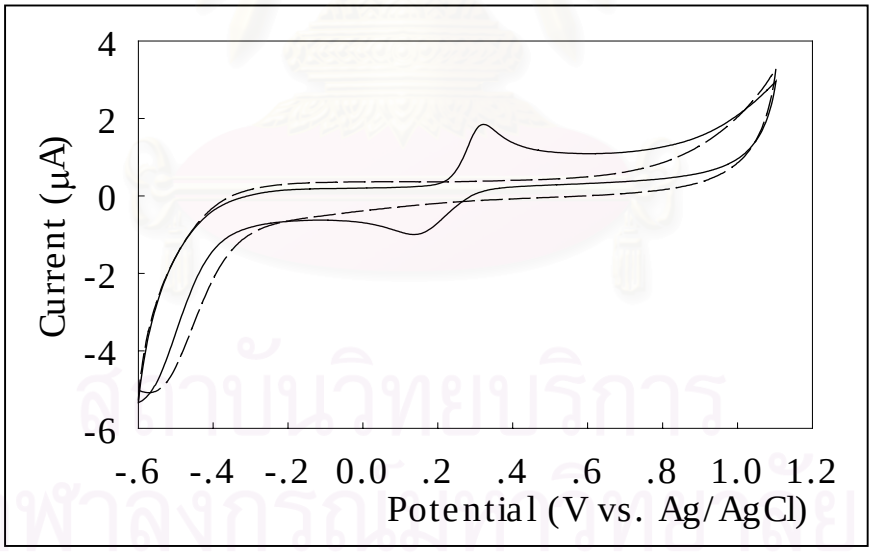

Figure 4.20 Cyclic voltammogram of 0.1 mM (100 μM) acetaminophen in 0.1 M phosphate buffer (pH 8) at the glassy carbon electrode (solid line). The scan rate was 20 mV s^{-1}. Background voltammogram (0.1 M phosphate buffer, pH 8) is also shown in this Figure (dash line).

4.1.5.2 D-penicillamine

The oxidation peak current was investigated with the concentration range from 0.025 to 15 mM D-penicillamine at the diamond and the glassy carbon electrodes. Linear regression analysis of current (μA) versus the concentration (mM) profiles showed a reasonable linearity from 0.5 to 10 mM for the diamond electrode (Figure 4.21) while the glassy carbon electrode provided no linear relationship between the oxidation current and the concentration (Figure 4.22). This may be due to the electrode fouling. The sensitivity, as slope of this calibration plots, is 3.60±0.55 μA/mM with the correlation coefficient of 0.998. At a concentration as low as 0.025 mM (25 μM) (Figure 4.23) and above, a well-defined peak with the S/B ratios > 3 could be obtained at the diamond electrode while the glassy carbon electrode provided detection limit at the concentration of 0.5 mM (500 μM) (Figure 4.24).

สถาบันวิทยบริการ
จุฬาลงกรณ์มหาวิทยาลัย

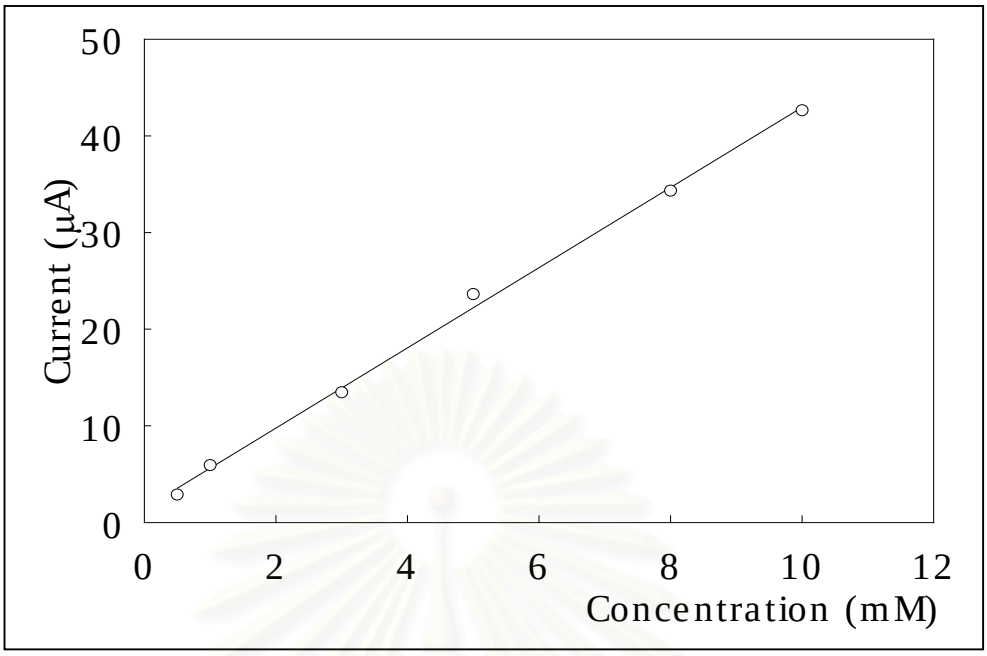

Figure 4.21 Calibration curve of D-penicillamine (0.5 - 10 mM) in 0.1 M phosphate buffer (pH 7) at the diamond electrode. The scan rate was 20 mV s^{-1}.

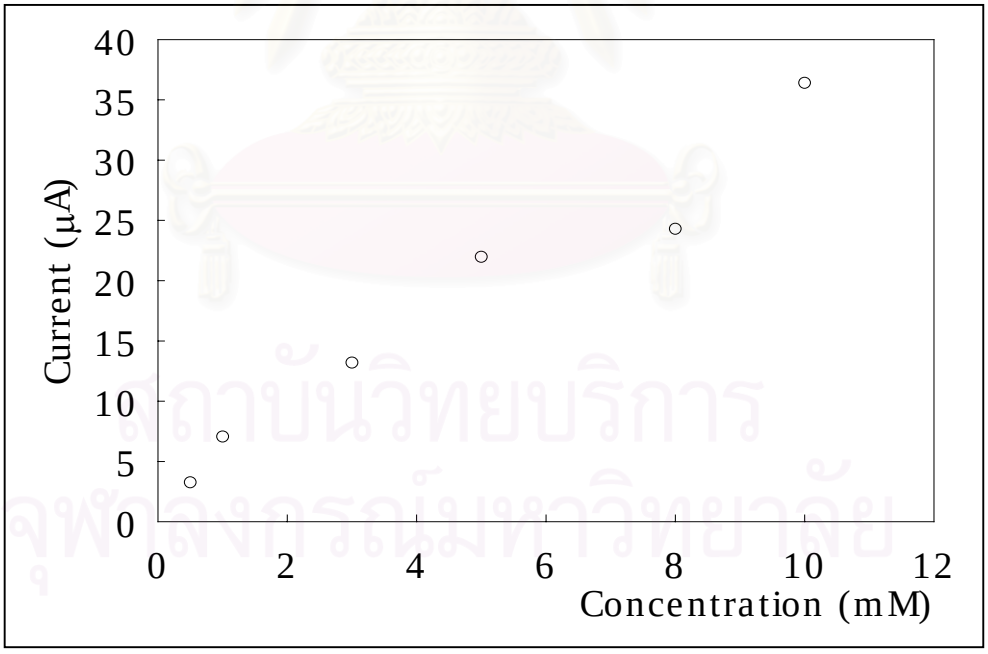

Figure 4.22 Calibration curve of D-penicillamine (0.5 -10 mM) in 0.1 M phosphate buffer (pH 7) at the glassy carbon electrode. The scan rate was 20 mV s^{-1}.

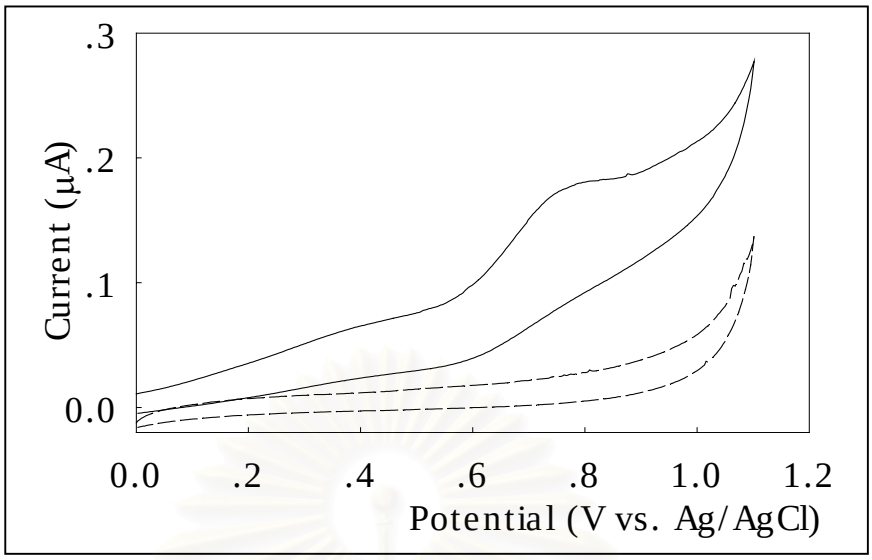

Figure 4.23 Cyclic voltammogram of 0.025mM (25 μM) D-penicillamine in 0.1 M phosphate buffer (pH 7) at the diamond electrode (solid line). The scan rate was 20 mV s^{-1}. Background voltammogram (0.1 M phosphate buffer, pH 7) is also shown in this Figure (dash line).

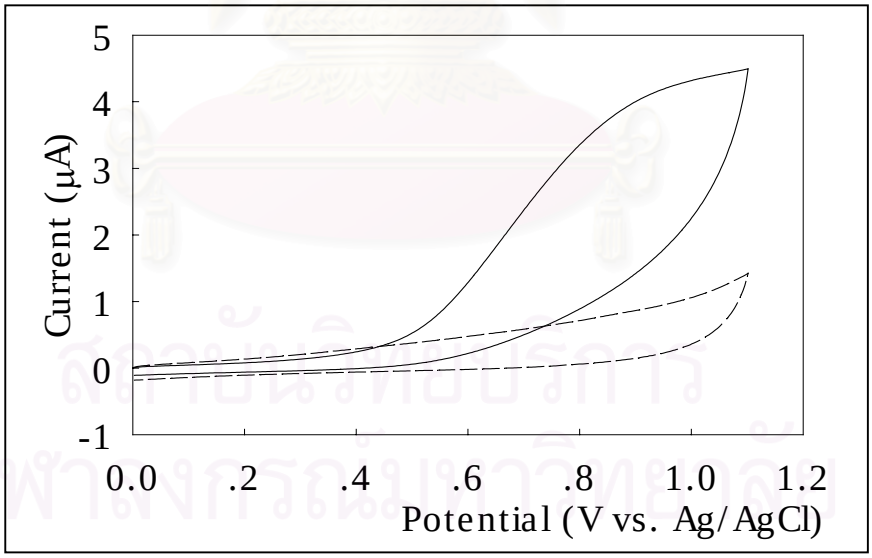

Figure 4.24 Cyclic voltammogram of 0.5 mM (500 μM) D-penicillamine in 0.1 M phosphate buffer (pH 7) at glassy carbon electrode (solid line). The scan rate was 20 mV s^{-1}. Background voltammogram (0.1 M phosphate buffer, pH 7) is also shown in this Figure (dash line).

4.1.5.3 Barbituric acid

The oxidation peak current was investigated with a concentration range of 0.05 to 20 mM barbituric acid at the diamond and the glassy carbon electrode. The current signal and concentration relationship was linear from 0.05 - 20 mM for the diamond electrode (Figure 4.25) while for the glassy carbon electrode, it was 3- 20 mM (Figure 4.26). The sensitivities, as the slope of these calibration plots, are 9.19±0.06 μA/mM with the correlation coefficient of 0.996 and 7.53 ±0.44 μA/mM with the correlation coefficient of 0.999 for diamond and glassy carbon electrode, respectively. The narrow linear range and low sensitivity at the glassy carbon electrode (Table 4.5) may be due to the electrode fouling. The LoD of barbituric acid at diamond electrode was 0.05 mM (50 μM) (Figure 4.27) while the LoD obtained at the glassy carbon electrode was 0.5 mM (500 μM) (Figure 4.28).

สถาบันวิทยบริการ
จุฬาลงกรณ์มหาวิทยาลัย

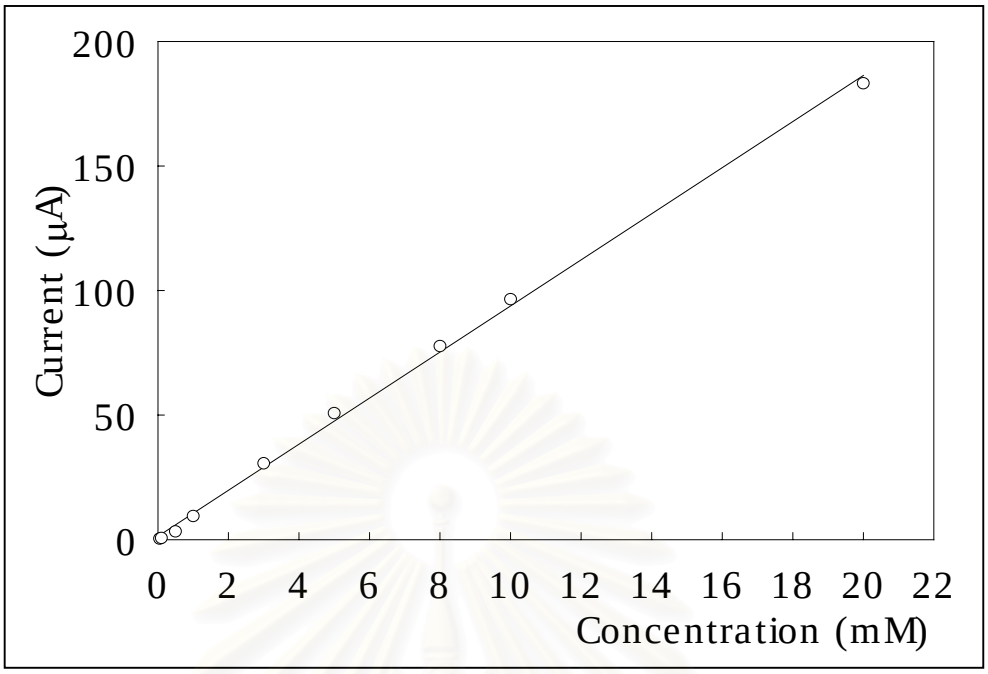

Figure 4.25 Calibration curve of barbituric acid (0.05 - 20 mM) in 0.1 M phosphate buffer (pH 8) at the diamond electrode. The scan rate was 20 mV s^{-1}.

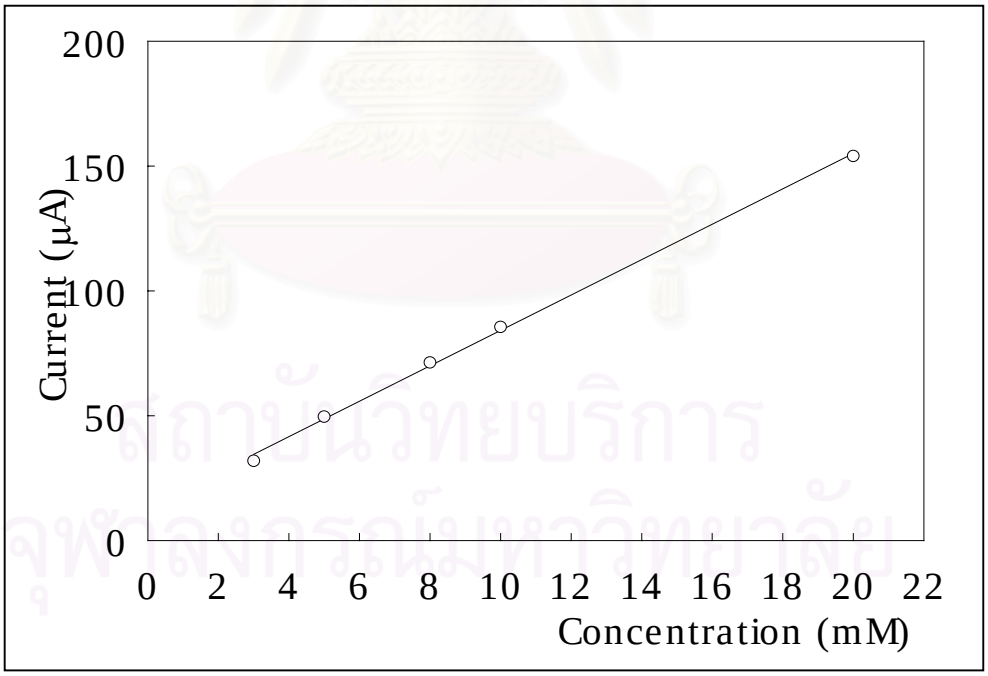

Figure 4.26 Calibration curve of barbituric acid (3 -20 mM) in 0.1 M phosphate buffer (pH 8) at the glassy carbon electrode. The scan rate was 20 mV s^{-1}.

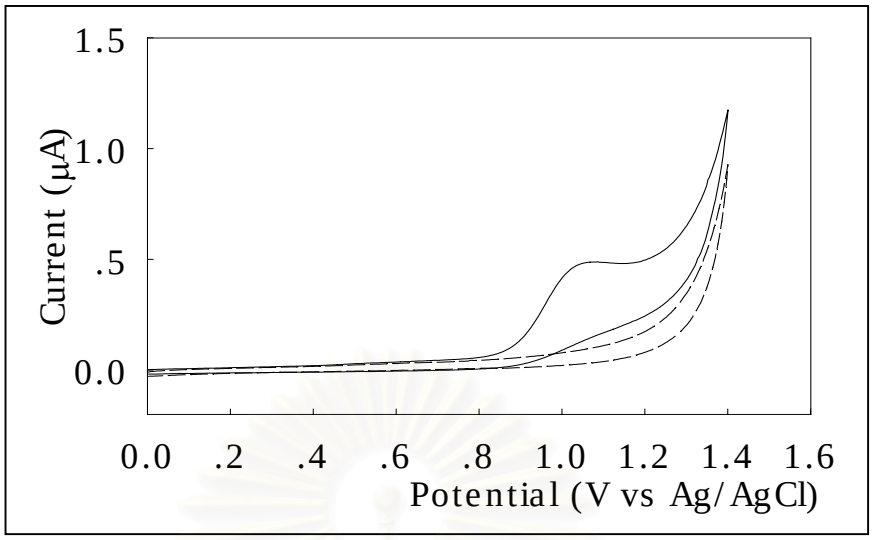

Figure 4.27 Cyclic voltammogram of 0.05 mM (50 μM) barbituric acid in 0.1 M phosphate buffer (pH 8) at the diamond electrode (solid line). The scan rate was 20 mV s^{-1}. Background voltammogram (0.1 M phosphate buffer, pH 8) is also shown in this Figure (dash line).

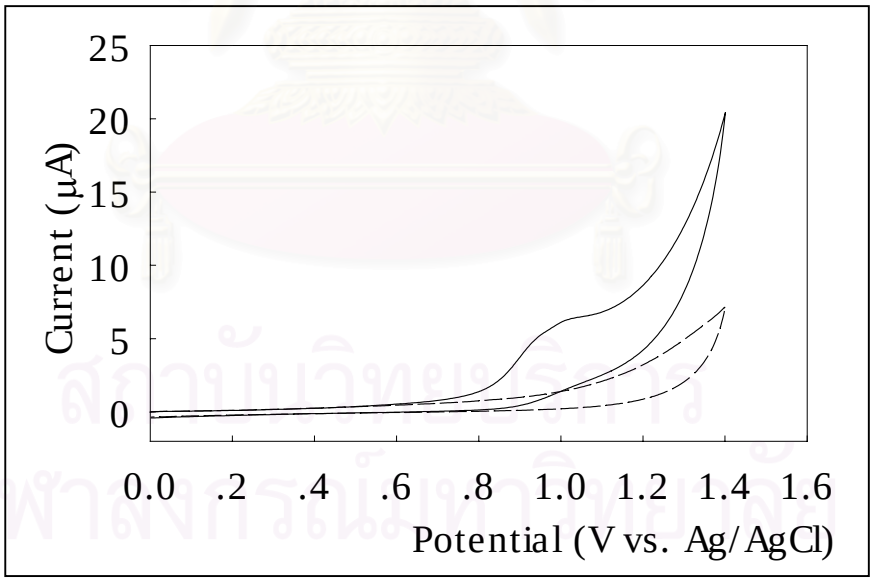

Figure 4.28 Cyclic voltammogram 0.5 mM (500 μM) barbituric acid in 0.1 M phosphate buffer (pH 8) at the glassy carbon electrode (solid line). The scan rate was 20 mV s^{-1}. Background voltammograms (0.1 M phosphate buffer, pH 8) is also shown in this Figure (dash line).

4.2 Flow injection with amperometric detection

4.2.1 Hydrodynamic voltammetry

4.2.1.1 Acetaminophen

Figure 4.30 shows the hydrodynamic voltammetric i-E curve obtained at the diamond electrode for 20 μl injection of 100 μM of acetaminophen in 0.1 M of phosphate buffer (pH 8). 0.1 M phosphate buffer (pH 8) was used as the carrier solution. Each datum represents the average of four injections. The magnitude of the background current at each potential is also shown in this Figure 4.29. The hydrodynamic voltammogram of acetaminophen at the diamond electrode exhibited a well-defined sigmodal shape with a half peak potential at about 0.5 V vs. Ag/AgCl. The half peak that was obtained for acetaminophen is near to the peak potential observed in the corresponding cyclic voltammogram at the same concentration. The S/B ratio was calculated from Figure 4.29. The S/B ratio reached a maximum value at a potential of 0.55 V vs. Ag/AgCl as shown in Figure 4.30. Therefore, this potential was fixed for the amperometric potential detection in flow injection analysis experiments.

สถาบันวิทยบริการ
จุฬาลงกรณ์มหาวิทยาลัย

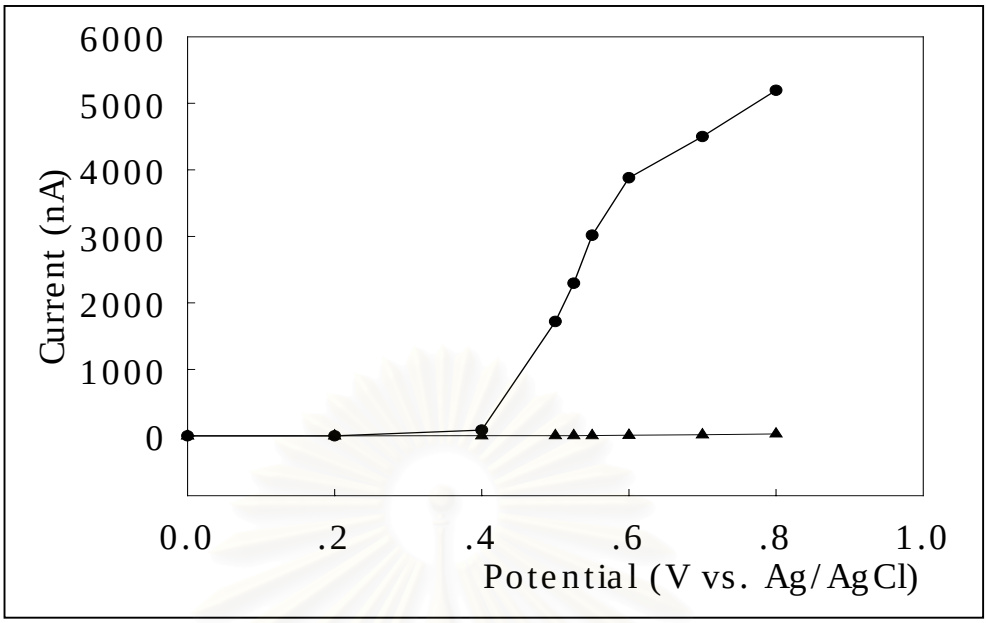

Figure 4.29 Hydrodynamic voltammogram of (-•-) 100 μM of acetaminophen in 0.1 M phosphate buffer (pH 8) and (-▲-) 0.1 M phosphate buffer (pH 8, background current) with 4 injections of analyte. 0.1 M phosphate buffer (pH 8) was used as a carrier solution, flow rate 1 ml min^{-1}.

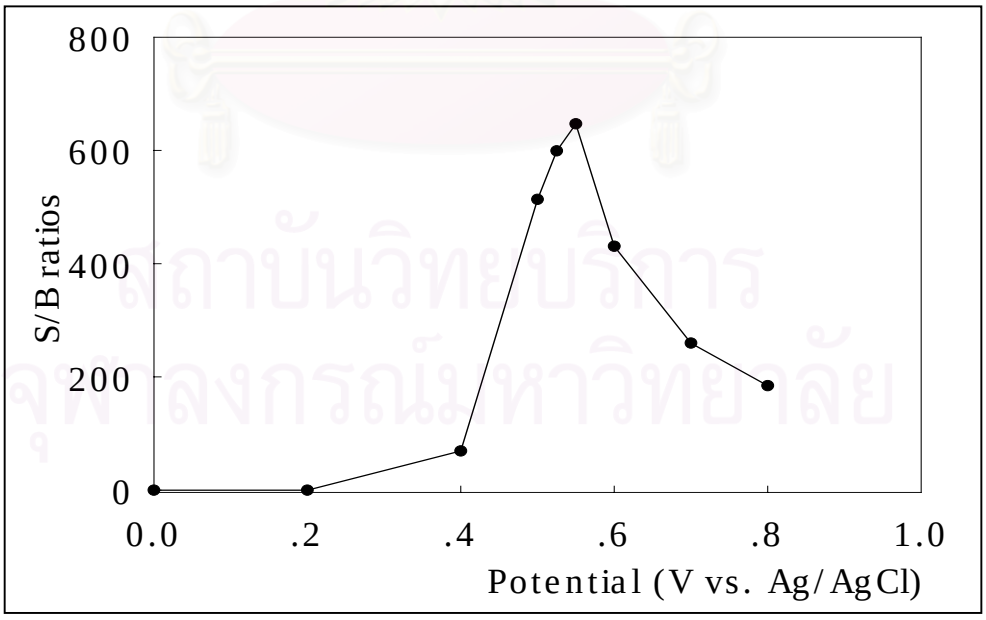

Figure 4.30 Plot of the S/B ratios calculated from Figure 4.29 vs. the applied potential.

4.2.1.2 D-penicillamine

Figure 4.31 shows a hydrodynamic voltammetric i-E curve obtained at the diamond electrode for 20 μL injections of 100 μM D-penicillamine in 0.1 M phosphate buffer (pH 7). 0.1 M phosphate buffer (pH 7) was used as the carrier solution. Each datum represents the average of four injections. The absolute magnitude of background current at each potential is also shown for comparison. The hydrodynamic voltammogram for D-penicillamine did not produce a sigmodal shape. The S/B ratio was calculated from Figure 4.31 at each potential. The S/B ratio vs. potential curve is shown in Figure 4.32, which indicates the maximum S/B ratio at 0.75 V. vs. Ag/AgCl. Hence, this potential was fixed as the amperometric potential detection in flow injection analysis experiments.

สถาบันวิทยบริการ
จุฬาลงกรณ์มหาวิทยาลัย

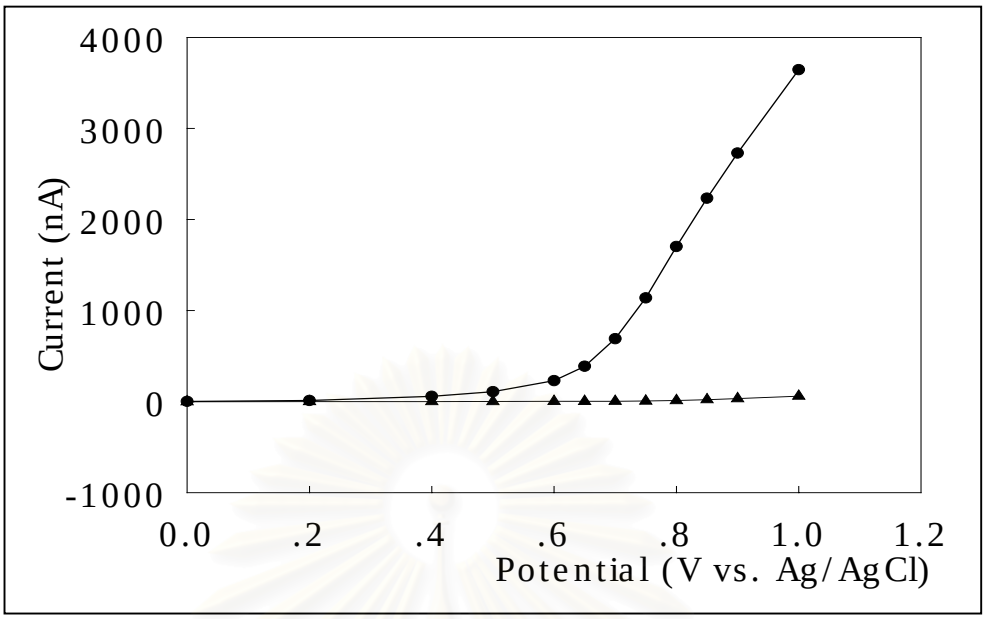

Figure 4.31 Hydrodynamic voltammogram of (-•-) 100 μM of D-penicillamine in 0.1 M phosphate buffer (pH 7) in (-▲-) 0.1 M phosphate buffer (pH 7, background current) with 4 injections of analyte. 0.1 M phosphate buffer (pH 7) was used as a carrier solution, flow rate 1 ml min^{-1}.

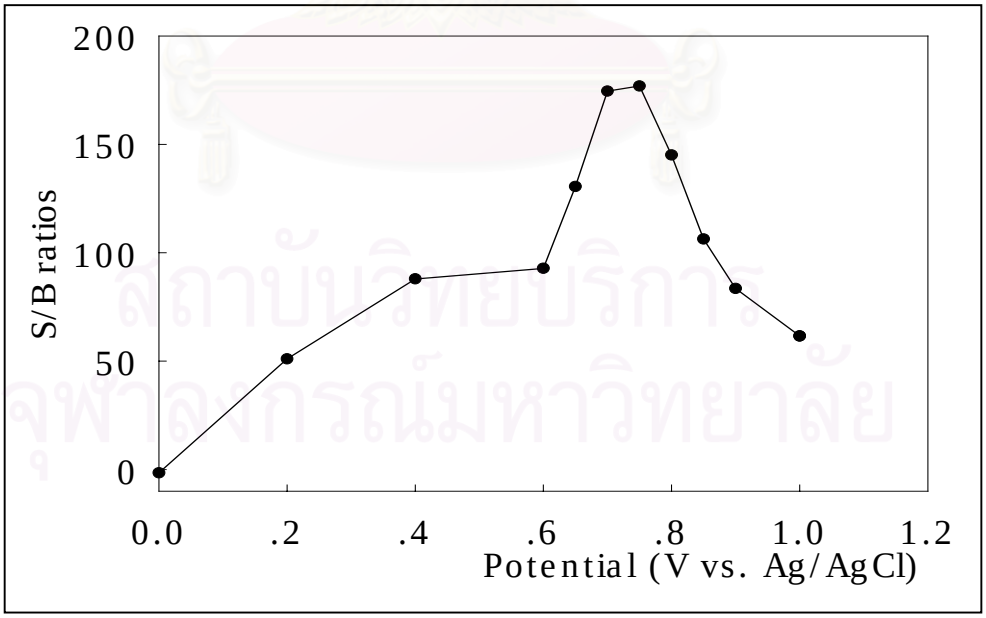

Figure 4.32 Plot of the S/B ratios calculated from Figure 4.31 vs. the applied potential.

4.2.1.3 Barbituric acid

Figure 4.33 shows a hydrodynamic voltammetric i-E curve obtained at the diamond electrode for 20 μL injections of 100 μM barbituric acid in 0.1 M phosphate buffer (pH 8). 0.1 M phosphate buffer (pH 8) was used as the carrier solution. Each datum represented the average of four injections. The corresponding background current was also shown for comparison. The hydrodynamic voltammogram for barbituric did not produce an expected sigmodal shape, probably due to the high oxidation potential. The S/B ratio was calculated from Figure 4.34 as a function of potential. The S/B ratio reached a maximum value at 1.075 V vs. Ag/AgCl as shown in Figure 4.34. Hence, this potential was selected for the amperometric potential detection in flow injection analysis experiments.

สถาบันวิทยบริการ
จุฬาลงกรณ์มหาวิทยาลัย

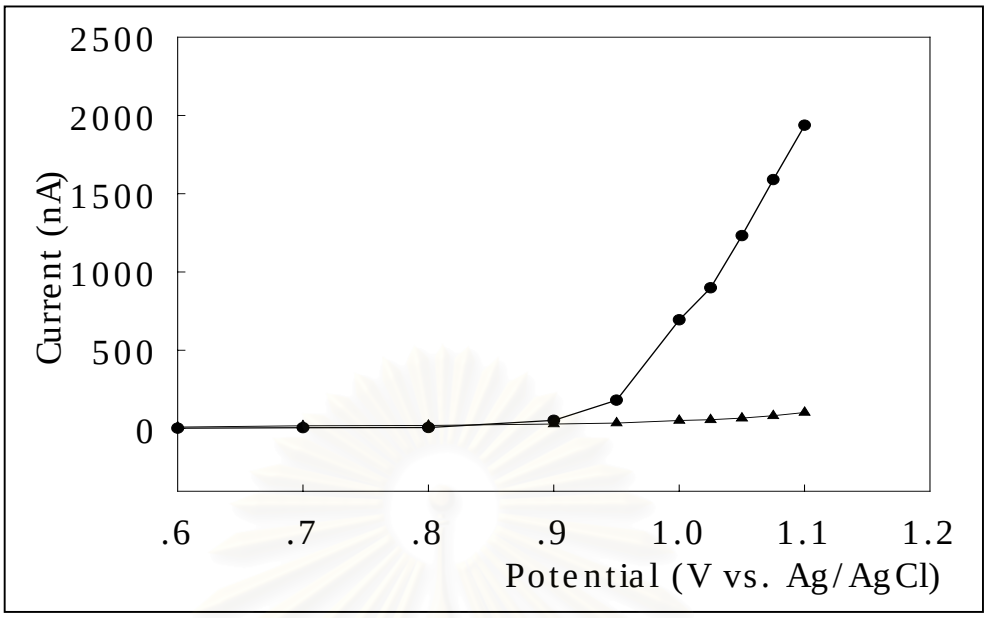

Figure 4.33 Hydrodynamic voltammogram of (-•-) 100 μM of barbituric acid in 0.1 M phosphate buffer (pH 8) and (-▲-) 0.1 M phosphate buffer (pH 8, background current) with 4 injections of analyte. 0.1 M phosphate buffer (pH 8) was used as a carrier solution, flow rate 1 ml.min^{-1}.

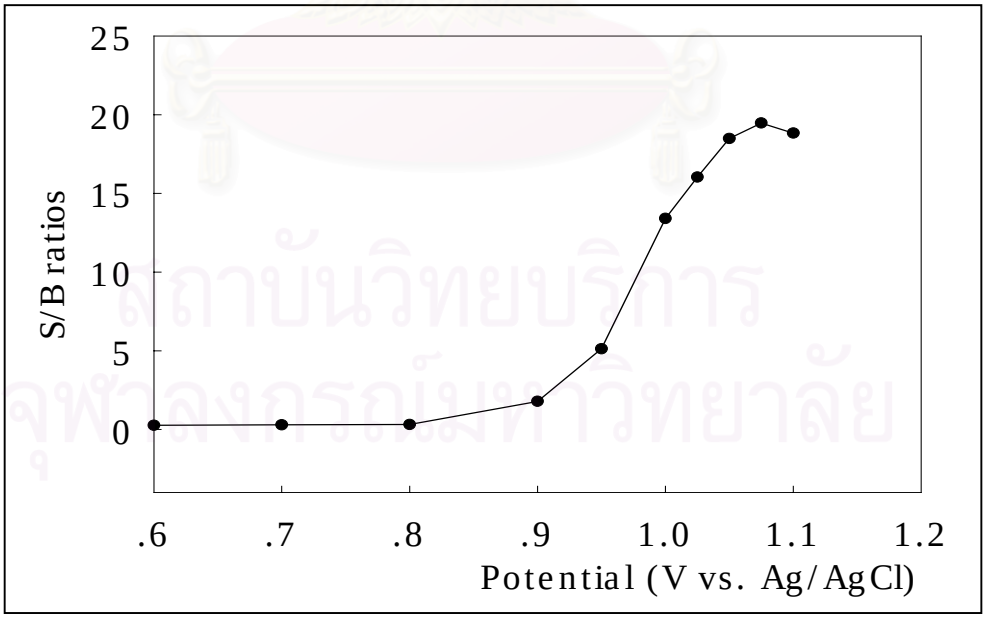

Figure 4.34 Plot of the S/B ratios calculated from Figure 4.33 vs. the applied potential.

After the optimum potential was obtained by hydrodynamic voltammetry, then this potential was used to set the instrument for the amperometric detection.for quantitative analysis of acetaminophen, D-penicillamine and barbituric acid for the rest of the flow injection experiments with amperometric detection experiments.

4.2.2 Calibration and linearity

Calibration curve was obtained from injection of five injections 20 μl of a concentration range of 10 nM to 2.5 mM of analyte solutions. The peaks obtained were sharp without tailing. A linear dynamic range was obtained over 2 - 3 orders of magnitude. The linear regression equation was obtained by least square adjustment as following:

$$i = ax+b$$

where i - current signal (nA),

a - slope or sensitivity (nA/μM),

x - analyte concentration (μM) and b is intercept (nA).

The effect of concentration of acetaminophen, D-pencillamine and barbitruric acid on peak current are shown in Figure 4.35 – 4.37. Flow injection with amperometric detection provided a linear dynamic range of 0.5 - 50 μM, 0.5 -50 μM and 0.5 -100 μM for acetaminophen, D-penicillamine and barbituric acid, respectively. The sensitivity, as the slope of these calibration plots, are 22.08±3.62 nA/μM for acetaminophen, 14.69± 2.57 nA/μM for D-penicillamine and 30.12±0.81 nA/μM for barbituric acid, with correlation coefficients of 0.999. The regression parameters are summarized in Table 4.6.

Table 4.6 Regression statistics for acetaminophen, D-penicillamine and barbituric acid (n = 2).

Analytes	Linear dynamic range (μM)	Sensitivities (nA/μM)	Intercept (nA)	R^2
Acetaminophen	0.5 - 50	22.08±3.62	12.55±0.94	0.9991±0.0003
D-penicillamine	0.5 - 50	14.69± 2.57	2.36± 0.79	0.9996±0.0000
Barbituric acid	0.5 -100	30.12±0.81	71.66±10.24	0.9993±0.0000

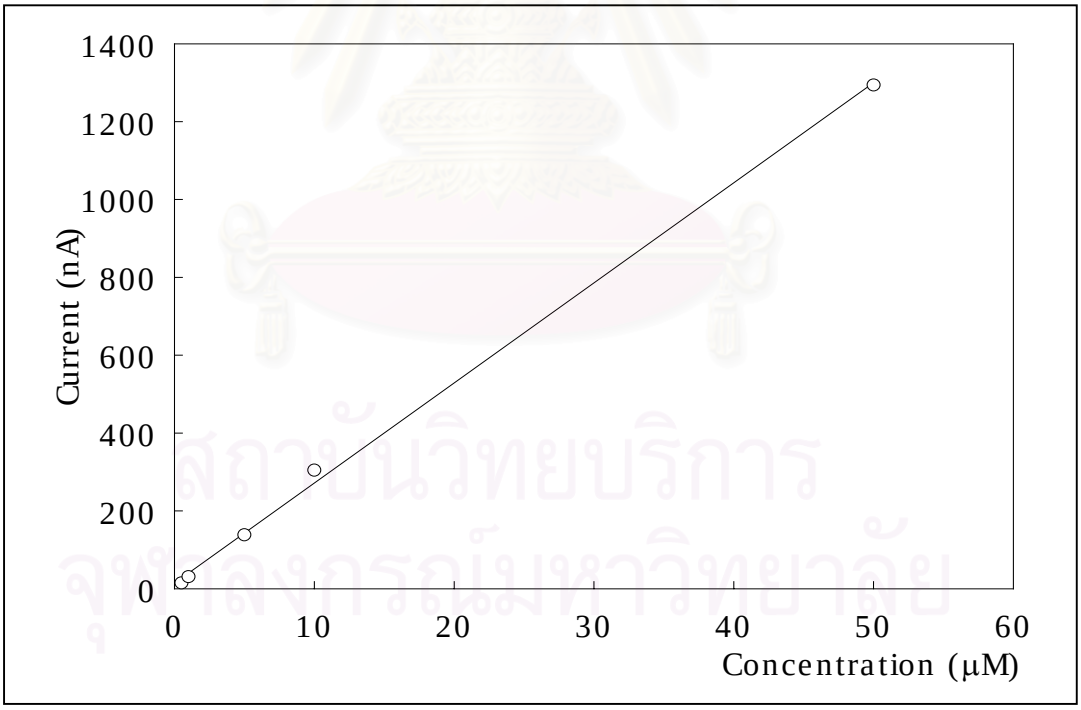

Figure 4.35 Calibration curve (0.5 - 50 μM) of acetaminophen

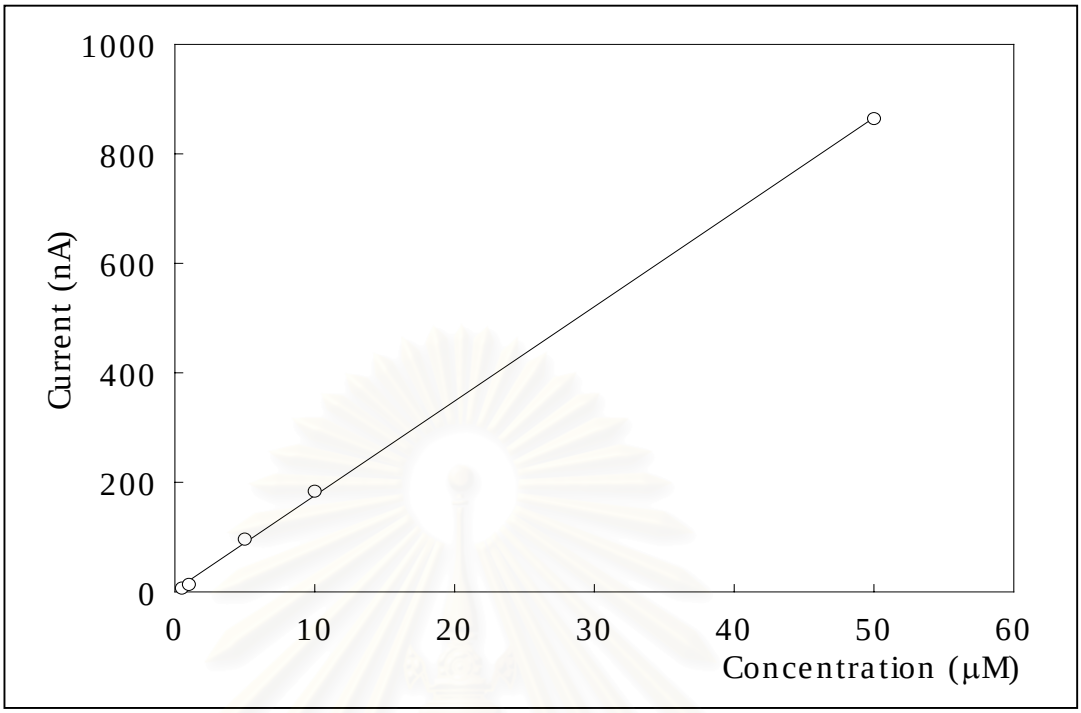

Figure 4.36 Calibration curve (0.5 - 50 μM) of D-penicillamine.

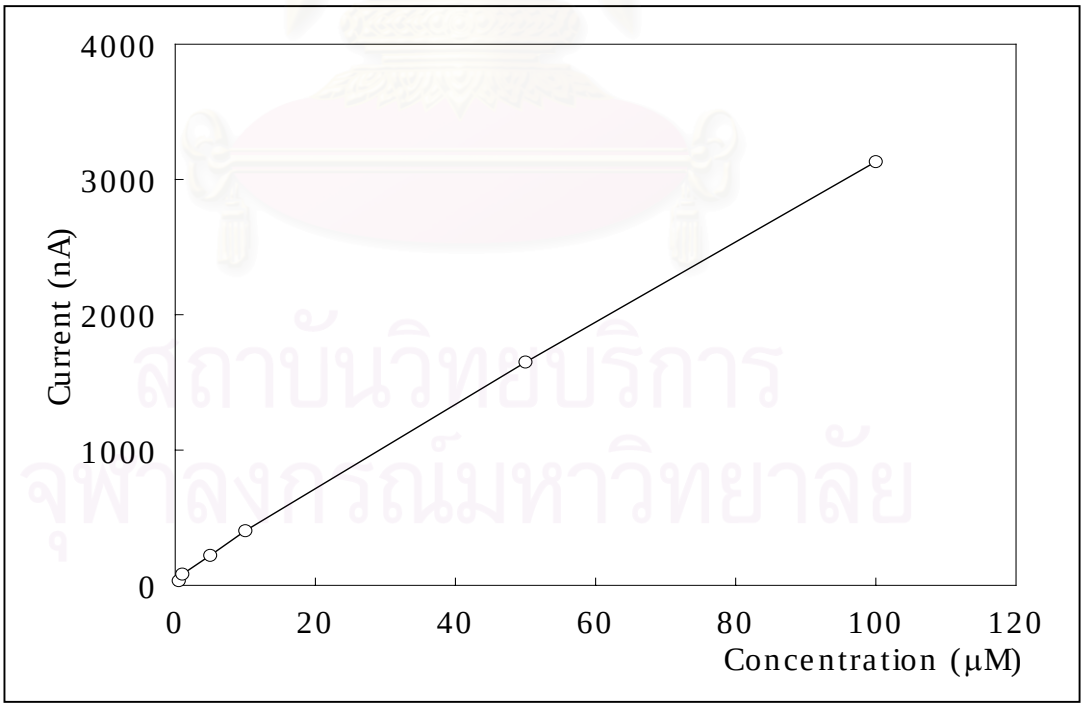

Figure 4.37 Calibration curve (0.5 - 100 μM) of barbituric acid

4.2.3 Detection limit (LoD)

LoD is defined as the concentration, which provides at least three times of the ratio of the analyte current to noise signal ($S/N \geq 3$). Interestingly, LoD that obtained from this proposed method was as low as 10 nM for acetaminophen, D-penicillamine and barbituric acid. The results were shown in Figure 4.38.

4.2.4 Repeatability

The repeatability is defined as relative standard deviation value or peak variability. The repeatability of 2.5 mM of each analyte was examined and the results were shown in the Table 4.7. The relative standard deviations were 1.8% for acetaminophen, 0.8% for D-penicillamine and 1.1% for barbituric acid. The peak variability is effected by the past electrochemical history of the diamond film and the manual injection valve of the flow injection system.

Table 4.7 % RSD of 2.5 mM acetaminophen, D-penicillamine and barbituric acid

Analyte	%RSD
Acetaminophen	1.8
D-penicillamine	0.8
Barbituric acid	1.1

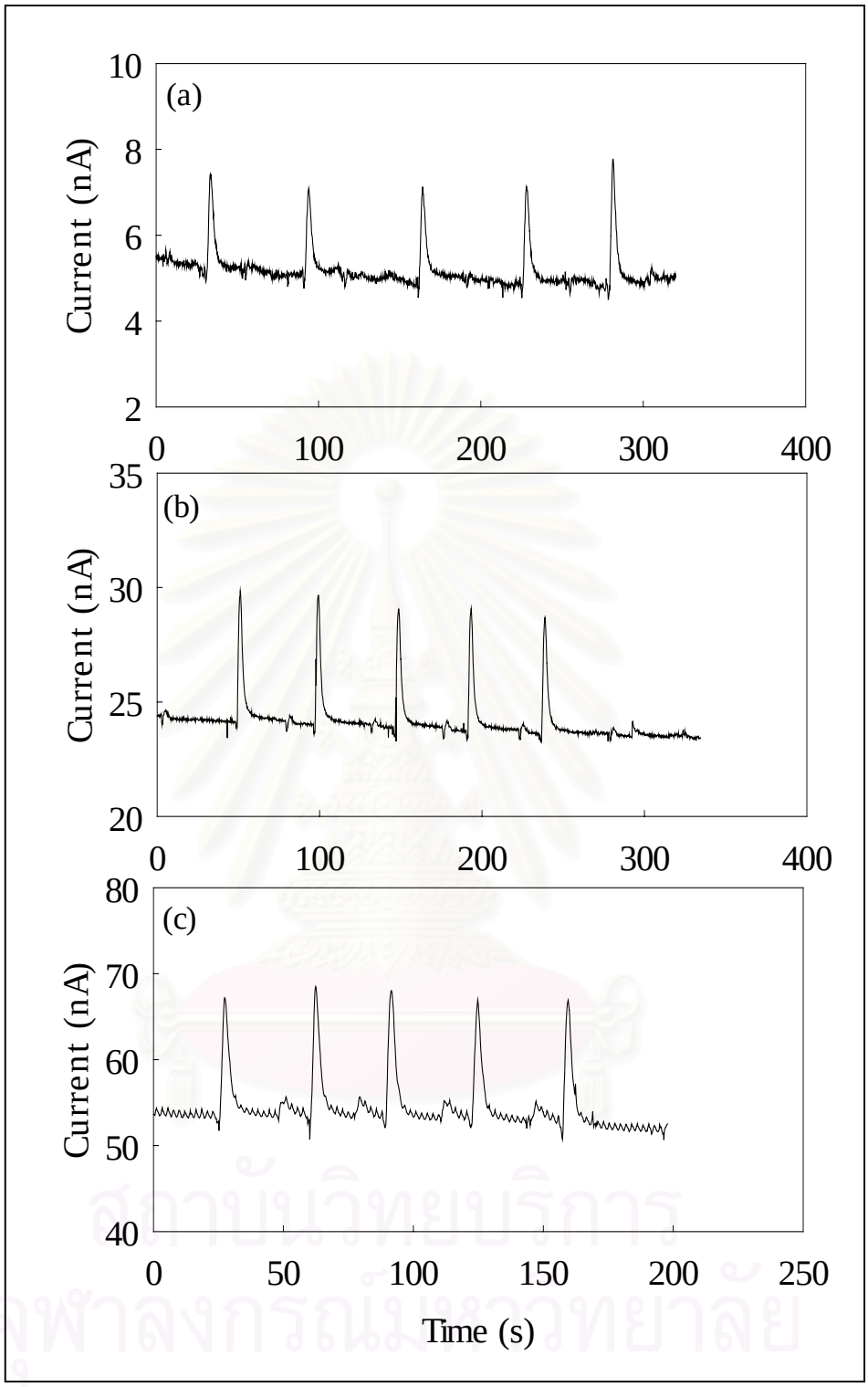

Figure 4.38 Flow injection with ampemetric detection results for (a) 10 nM acetaminophen in 0.1 M phosphate buffer (pH 8) (b) 10 nM D-penicillamine in 0.1 M phosphate buffer (pH 7) and (c) 10 nM barbituric acid in 0.1 M phosphate buffer (pH 8). The flow rate was 1 ml min^{-1}.

4.2.5 Stability of electrode

The diamond electrode that was used with amperometric detection of acetaminophen, D-penicillamine and barbituric acid was very stable, even with continuous use for 1 month. The result of flow injection with amperometric detection obtained from 45 repetitive injections of 100 μM of D-penicillamine at the diamond electrode after 1 month of continuous use provided the peak variation or percent relative standard deviation of only about 1.8% (Figure 4.39). The result indicated that diamond electrode was very stable with high reproducibility. This unique response stability was also reported by previous studies [35,36,86].

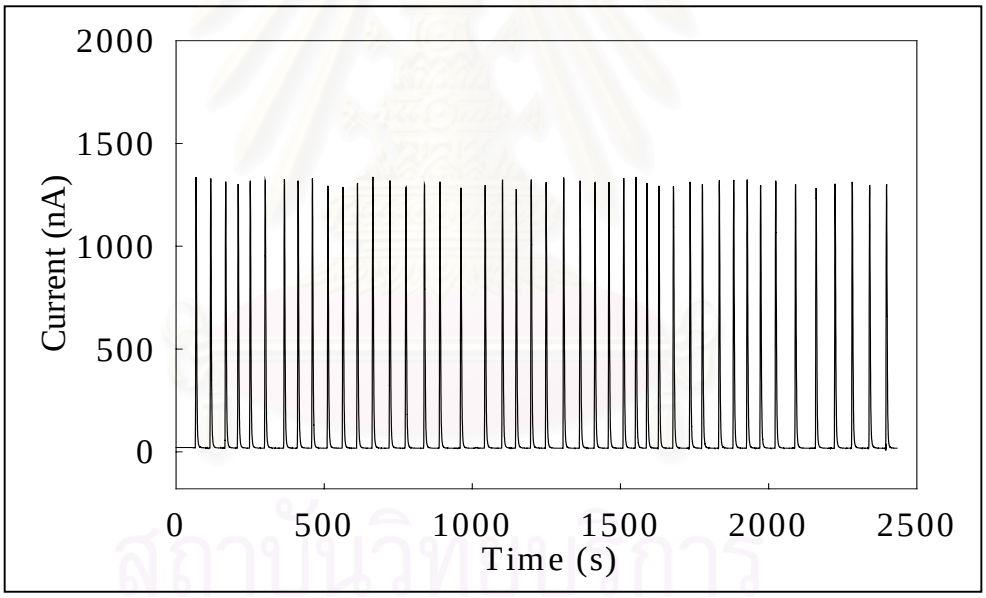

Figure 4.39 Flow injection with amperometric detection result for 100 μM D-penicillamine (45 injections) in 0.1 M phosphate buffer (pH 7). The flow rate was 1 ml min^{-1}.

4.2.6 Applications

Flow injection with amperometric detection was applied to determination of drug formulation samples, which were paracetamol syrup and penicillamine capsule. The standard addition method was used to determine the amount of analyte in the sample.

4.2.6.1 The drug syrup (Paracetamol syrup)

Figure 4.40 shows the standard addition graph of paracetamol syrup. It was found that slope was 131.96 nA ml/ μg and the intercept 32.2 nA. The amounts of acetaminophen obtained from the graph were compared to those labeled in the syrup sample (24 mg/ml). Relative errors compared with the claimed amount were lower than 5%.

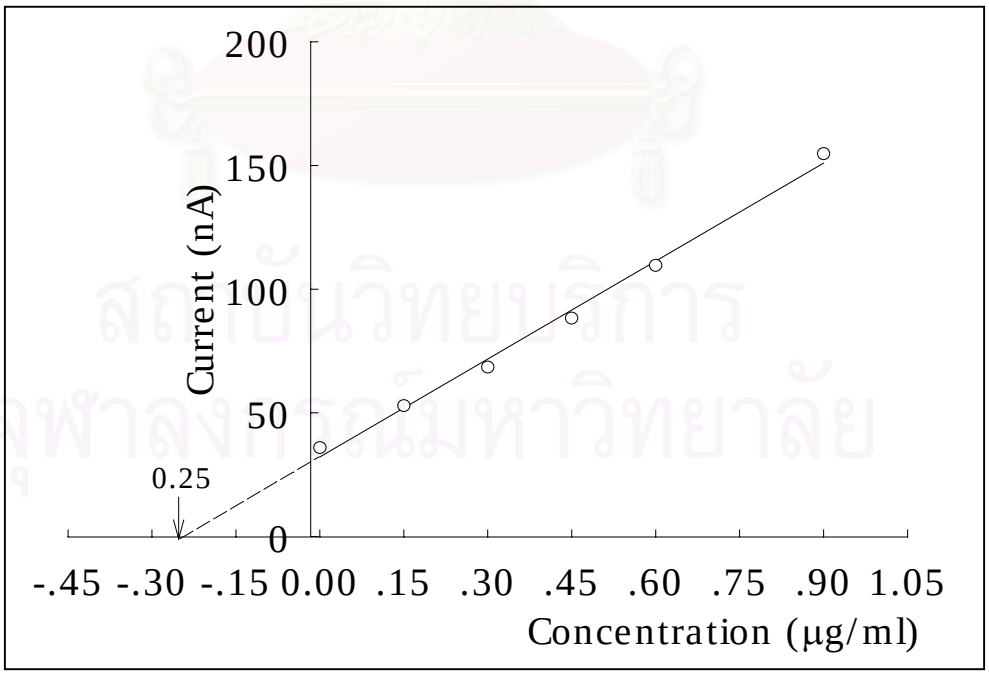

Figure 4.40 Standard addition graph of paracetamol syrup.

In order to verify the accuracy and precision of the proposed method, intra- and inter-day, recovery experiments with the standard addition were carried out. The results of intra- and inter- assays are summarized in Table 4.8. Recovery was studied by addition of 4 standard concentrations (0.30, 0.45, 0.60 and 0.91 μg/ml) in real samples. Recoveries ranging from 94 - 103% and 95 - 105 % were obtained for the intra- and inter-assay studies, respectively.

The precision of the method was defined as the percent relative standard deviation. Three concentrations of added solution (0.15, 0.45 and 0.60 μg/ml) were chosen. Results obtained from 10 injections gave 1.8 - 2.3% and 1.7 - 2.5% for the inter- and intra- assay studies, respectively.

The results intra- and inter-assay studies were satisfactory. This proposed method is very precise for paracetamol syrup analysis.

สถาบันวิทยบริการ
จุฬาลงกรณ์มหาวิทยาลัย

Table 4.8 Recovery of paracetamol syrup sample with amperometric detection using the diamond electrode applied to flow injection system of the intra- assay study (n = 2) and inter-assay study (n = 2).

Amount of added (μg/ml)	Intra-assay		Inter-assay	
	Amount of found (μg/ml)	Percent of recovery (%)	Amount of found (μg/ml)	Percent of recovery (%)
0.30	0.28±0.01	93.66±1.34	0.30±0.01	96.20±2.84
0.45	0.44±0.01	97.52±2.36	0.44±0.02	97.76±2.98
0.60	0.58±0.00	96.10±0.74	0.59±0.01	97.23±1.48
0.91	0.93±0.01	102.71±1.26	0.92±0.01	102.11±1.32
24 mg/ml	24.68±0.26	102.83±1.08	24.82±0.28	103.43±1.13

สถาบันวิทยบริการ
จุฬาลงกรณ์มหาวิทยาลัย

4.2.6.2 The drug capsule (Penicillamine capsule)

Figure 4.41 shows the standard addition graph of penicillamine syrup. It was found that slope was 82.81 nA ml/ μg and the intercept 42.2 nA. The amounts of D-penicillamine obtained from the graph were compared to those labeled in the capsule sample (250 mg/tablet). Relative errors compared with the claimed amount were lower than 6%.

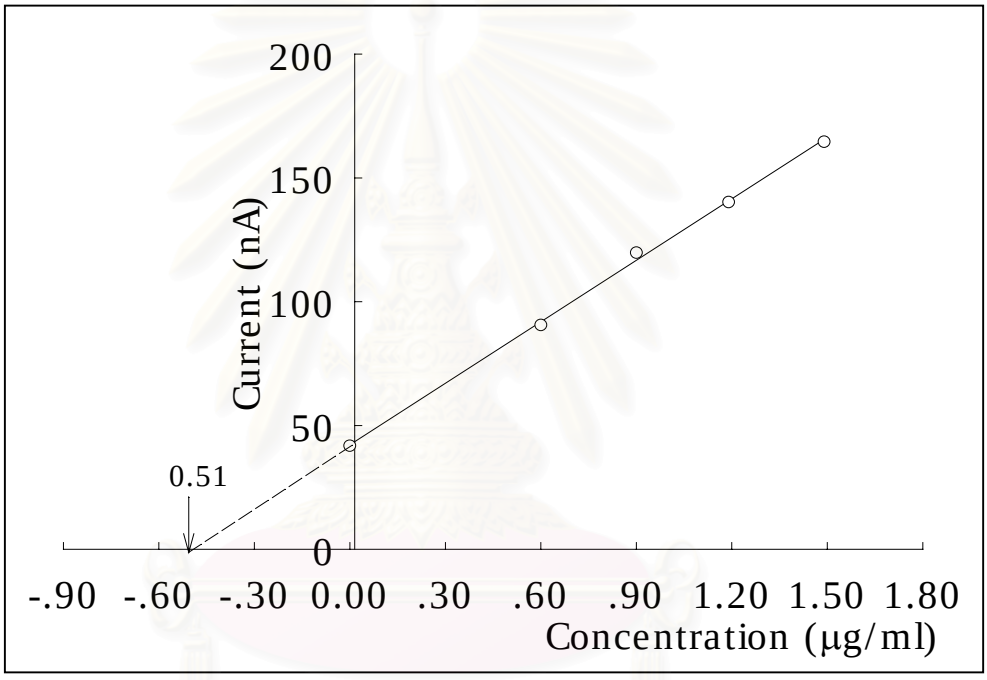

Figure 4.41 Standard addition graph of penicillamine capsule.

In order to verify the accuracy and precision of the proposed method, intra- and inter-day recovery experiments with the standard addition method were carried out. The results of intra- and inter- assays are summarized in Table 4.9. Recovery was also studied by addition of 4 standard concentrations (0.60, 0.9, 1.19 and 1.49 μg/ml) to real samples. Recoveries obtained ranged from 98 - 105% for both the intra- and inter-assay studies.

The precision of the method was defined as the percent relative standard deviation. Three concentrations of added solution (0, 0.60 and 1.49 μg/ml) were chosen. Results obtained from 10 injections gave 1.5 - 2.1% and 1.7 -2.5% for the inter- and intra- assay studies, respectively.

The results of intra- and inter-assay studies were satisfactory. This proposed method is very precise for penicillamine capsule analysis.

Table 4.9 Recovery of penicillamine capsule sample with amperometric detection using the diamond electrode applied to flow injection system of the intra- assay study (n = 2) and inter-assay study (n = 2).

Amount of added (μg/ml)	Intra-assay		Inter-assay	
	Amount of found (μg/ml)	Percent of recovery (%)	Amount of found (μg/ml)	Percent of recovery (%)
0.60	0.59±0.01	98.68±0.93	0.58±0.01	98.04±0.94
0.90	0.94±0.01	104.04±0.65	0.91±0.03	101.30±3.06
1.19	1.19±0.01	99.62±0.39	1.17±0.02	99.07±1.45
1.49	1.48±0.01	98.84±0.33	1.50±0.03	100.43±1.98
250 mg/tablet	255.62±0.14	102.11±0.55	255.55±2.50	102.22±0.99

Table 4.10 Influence of lactose on D-penicillamine determination

[lactose]/[D-penicillamine]	%error
20:1	0.69
40:1	1.60
80:1	3.89
100:1	5.95

The selectivity of the proposed method was investigated by studying interferences from other species accompanying D-penicillamine in the pharmaceutical preparation. From the pencillamine capsule label, there are some inactive ingredients including titanium dioxide, magnesium stearate and lactose in capsule. Only lactose can dissolve in aqueous solution and therefore lactose was used in the interference study. This effect was studied by adding different amounts of lactose to a solution containing standard D-penicillamine 7.46 μg/ml (50 μM). The results obtained are shown in Table 4.10. The proposed method provided a tolerance limit at a [lactose]/[D-penicillamine] ratio equal to 80:1. The tolerance limit is defined as the concentration causing an error not exceeding ± 5% in the determination of D-penicillamine. The proposed method showed a very good tolerance level to lactose. This level was higher than the concentration of lactose that found in the capsules. Hence, the proposed method was selective for the determination of D-penicillamine in this drug capsule.

CHAPTER V

CONCLUSION AND SUGGESTION FOR FURTHER WORK

5.1 Conclusion

Boron-doped diamond thin film electrodes showed excellent properties for applications in electrochemical analysis of drugs including acetaminophen, D-penicillamine and barbituric acid. Electrochemical applications require stable, conductive, chemically robust, and economical electrodes. Diamond electrode exhibited a well-defined cyclic voltammogram with higher S/B ratios than those obtained from the glassy carbon electrode. The advantages of the diamond electrode over the glassy carbon electrode are:

1. Lower background currents and noise signals, which lead to improved S/B and S/N ratios, and lower detection limit.
2. Good electrochemical activity without the need for pretreatment.
3. Chemically inert surface that is resistant to fouling.
4. Wider linear range over 1-3 order of magnitude.

Flow injection analysis with amperometric detection using the diamond electrode for the determination of acetaminophen, D-penicillamine and barbituric acid also enhanced the sensitivity and improved the detection limit (as low as 10 nM) with a reproducible response and without any pretreatment or modification of the electrode or using pulse technique.

The purposed method was further applied to real drug samples in pharmaceutical preparation. These were paracetamol syrup and penicillamine capsule. The method was very precise with good recovery results. Interference was also studied for the pencillamine capsule. No interference was observed from the commonly present inactive ingredient in pharmaceutical formulation.

5.2 Suggestion for further work.

The real samples studied in this work were drug formulation (syrup and capsule). Other samples such as human blood serum and urine are complicated, which may limit this method. The limitation of this method is interference by electrochemically active species, which have potential peaks close to the potential peak of the analyte. However, these interferences can be separated out by high performance liquid chromatography or by connecting the separation column to separate the matrices before the analyte goes to the detection unit.

สถาบันวิทยบริการ
จุฬาลงกรณ์มหาวิทยาลัย

REFERENCES

1. Fujishima, A., et. al. Electroanlaysis of dopamine and NADH at conductive diamond electrode. J. Electroanal. Chem. 473 (1999): 179-185.
2. Rao, T. N.; Yagi, I.; Miwa, T.; Tryk D. A.; and Fujishima, A. Electrochemical oxidation of NADH at highly boron-doped diamond electrodes. Anal. Chem. 71 (1999): 2506-2511.
3. Popa, E.; Yoshinobu, K.; Tryk, D. A.; and Fujishima, A. Selective voltammetric and amperometric detection of uric acid with oxidized diamond electrodes. Anal. Chem. 72 (2000): 1724-1727.
4. Spataru, N.; Sarada, B. V.; Popa, E.; Tryk, D. A.; and Fujishima, A. Voltammetric determination of L-cysteine at conductive diamond electrodes. Anal. Chem. 73 (2001): 514-519.
5. Swain, G. M., et. al. Boron-doped diamond thin film electrodes Anal. Chem. 69 (1997): 591A-597A.
6. Yano, T.; Tryk, D. A.; Hashimoto, K.; and Fujishima, A. Electrochemical behavior of highly conductive boron-doped diamond electrodes for oxygen reduction in alkaline solution. J. Electrochem. Soc. 145 (1998): 1870-1876.
7. Koppang, M. D.; Witek, M.; Blau, J.; and Swain, G. M. Electrochemical oxidation of polyamine at diamond thin-film electrodes. Anal. Chem. 71 (1999), 1188-1195.
8. Sarada, B.V.; Rao, T. N.; Tryk, D. A.; and Fujishima, A. Electrochemical oxidation of histamine and serotonin at highly boron doped diamond electrodes. Anal. Chem. 72 (2000), 1632-1638.

9. Meyer, J.; and Karst, U. Determination of paracetamol (acetaminophen) by HPLC with post-column enzymatic derivatization and fluorescence detection. Chromatographia 54 (2001): 163-167.

10. Miners, J. O. et. al. Analysis of D-penicillamine in plasma by fluorescence derivatisation with N-[p-(2-benzoxazolyl)-phenyl] maleimide and high-performance liquid chromatography J. Chromatogr. 275 (1983): 89-96.

11. Zhang, Z. D.; Baeyens, W. R. G.; Zhang, X. R.; and Weken, G. V. der. HPLC determination of penicillamine in human urine applying a chemiluminescent detection system. Biomed. Chromatogr. 11 (1997): 113-114.

12. Nakashima, K.; Umekawa, C. Nakatsuji, S.; Akiyama, S.; and Givens, R.S. High-performance liquid chromatography/chemiluminescence determination of biological thiols with N-[4-(6-dimethylamino-2-benzofuranyl)phenyl] maleimide. 3 (1989): 90-93.

13. Girolamo, A. D.; O'Neil, W. M.; and Wainer, I. W. A validated method for the determination of paracetamol and its glucoronide and sulphate metabolites in the urine of HIV + / AIDS patients using wavelength-switching UV detection. J. Pharm. Biomed. Anal. 17 (1998): 1191-1197.

14. Ercai, N.; Yang, P.; and Aykin, N. Determination of biological thiols by high-performance liquid chromatography following derivatization by ThioGlo maleimide reagents. J. Chromatogr. B 753 (2001): 287-292.

15. Beales, D; Finch, R. McLean, A. E. M.; Smith, M.; and Wilson, I. D. Determination of penicillamine and other thiol by combined high-performance liquid chromatography and post-column reaction with Ellman's reagent application to human urine. J. Chromatogr. 226 (1981): 498-503.

16. Walash, M. I.; Elbrashy, A. M.; and Sultan, M. A. Polarographic-behavior and determination of paracetamol and salicylamide after treatment with nitrous acid. Mikrochim. Acta 113 (1994): 113-124.

17. Rabenstein. D. L.; and Yamashita, G. T. Determination of homocysteine, penicillamine, and their symmetrical and mixed disulfides by liquid chromatography with electrochemical detection. Anal. Biochem. 180 (1989): 259-263.

18. Yamahita, G. T.; and Robenstein, D. L. Determination of penicillamine, penicillamine disulfide and pencillamine-glutathione mixed disulfide by high-performance liquid chromatography with electrochemical detection. J. Chromatogr. 491 (1989): 341-354. (amalgum)

19. Rabenstein, D. L.;andYamashita, G. T. Determination of homocysteine, penicillamine, and their symmetrical and mixed disulfides by liquid chromatography with electrochemical detection Anal. Biochem. 180 (1989): 259-263.

20. Zen, J. M.; and Ting, Y. S. Simultaneous determination of caffeine and acetaminophen in drug formulations by square-wave voltammetry using chemically modified electrode. Anal. Chim. Acta 342 (1997): 175-180.

21. Gilmartin, M. A. T.; Hart, J. P. Rapid detection of paracetamol using a disposable, surface-modified screen-printed carbon electrode Analyst 119 (1994): 2431-2437.

22. Christie, I. Leeds, S.; Baker, M.; Keedy, F.; and Vadgama, P. Direct electrochemical determination of paracetamol in plasma. Anal. Chim. Acta 272 (1993): 145-150.

23. Shi, G. Y.; Xu, F.; Xue, J.; and Jin, L. T. High performance liquid chromatography-electrochemical detection (HPLC-ECD) for the pharmacokinetic studies of acetaminophen with microdialysis. Electroanalysis (1999): 432-437.

24. Inoue, T.; and Kirchhoff, J. R. Electrochemical detection of thiols with a coenzyme pyrroloquinoline quinone modified electrode. Anal. Chem. 72 (2000): 5755-5760.

25. Favaro, G.; and Fiorani, M. Determination of pharmaceutical thiols by liquid chromatography with electrochemical detection: Use of an electrode with a conductive carbon cement metrix, chemically modified with cobalt phtahlocyanine. Anal. Chim. Acta 332 (1996): 249-255.

26. Zhang, S., et. al. Determination of thiocompounds by liquid chromatography with amperometric detection at a nafion indium hexacyanoferrate film modified electrode. Anal. Chim. Acta 286 (1999): 21-30.

27. Sawyer, D. T.; Sobkowiak, A.; and Roberts, J. L., Jr. Electrochemistry for chemists 2nd Ed. New York John: Wiley & Sons, Inc., 1995.

28. Monk, P. M. S. Fundamentals of Electroanalytical Chemistry New York: John Wiley & Sons, Inc., 2001.

29. Skoog, D. A. and Leary, J. J. Principles of Instrumental Analysis 4th Ed. New York: Harcourt Brace College Publishers, 1992

30. Eggins, Brain Biosensers: An Introduction New York: John Wiley & Sons, Inc., 1996.

31. Bard, A. J.; and Faulkner, L. R. Electrochemical Methods. New York: John Wiley & Sons, 1980.

32. Kissinger, P.T. ; and Heineman W. R. Laboratory Techniques in Eelctroanalytical Chemistry 2nd Ed New York: Marcel Dekker, Inc., 1996.

33. Swain, G. M.; and Ramesham, R. The electrochemical activity of boron-doped polycrystalline diamond thin-film electrodes Anal. Chem. 65 (1993): 345-351.

34. Stojek, J.W.; Granger, M. C.; Swain G. M.; Dallas. T.; and Holtz, M. W. Enhanced signal-to-background ratios in voltammetric measurements made at diamond thin-film electrochemical interfaces. Anal. Chem. 68 (1996): 2031-2037.

35. Swain, G. M. The susceptibility to surface corrosion in acidic fluoride media: A comparison of diamond, HOPG, and glassy carbon electrodes. J. Electrochem. Soc. 141 (1994): 3382-3392.

36.Chen, Q.; Granger, M. C.; Lister, T. E.; and Swain, G. M. Morphological and microstructural stability of boron-doped diamond thin film electrodes in an acidic chloride medium at high anodic current densities. J. Electrochem. Soc. 144 (1997): 3806-3812.

37. Xu, J. S.; Chen, Q. Y.; Swain, G. M. Anthraquinonedisulfonate electrochemistry: A Comparison of glassy carbon, hydrogenated glassy carbon, and diamond electrodes Anal. Chem. 70 (1998): 3146-3154.

38. Jolley, S.; Koppang, M.; Jackson, T.; and Swain, G. M. Flow injection analysis with diamond thin-film detectors. Anal. Chem. 69 (1997): 4099-4107.

39. Xu, J. Z.; and Swain, G. M. Oxidation of azide anion at boron-doped diamond thin-film electrodes. Anal. Chem. 70 (1998): 1502-1510.

40. Rao, T. N.; Sarada, B.V. Tryk,, D. A.; Fujishima, A. Electrochemical study of sulfa drugs at diamond electrodes and their determination by HPLC with amperometric detection. Anal. Chim. Acta 491 (2000): 175-181.

41. Davila-Jimenez,M. M.; Elizalde-Gonzalez, M.P.; Gutierrez-Gonzalez, A.; and Pelaez-Cid A.A. Electrochemical treatment of textile dyes and their analysis by high-performance liquid chromatography with diode array detection. J. Chromatogr. A 889 (2000): 253-259.

42. Granger, M. C.; Xu, J. S.; Strojek, J. W.; and Swain G. M. Polycrystalline diamond electrodes: basic properties and applications as amperometric detectors in flow injection analysis and liquid chromatography. Anal. Chim. Acta 398 (1999): 145-161.

43. Vale, J. A.; and Proudfoot, A. T. Paracetamol (acetaminophen) poisoning. Lancet. 346, (1995): 547-552.

44. Afshari, J. T.; and Liu, T. Z. Rapid spectrophotometric method for the quantitation of acetaminophen in serum. Anal. Chim. Acta 443 (2001): 165-169.

45. Nagaraja, P.; Murthy, K. C. S.; and Rangappa, K. S. Spectrophotometric method for the determination of paracetamol and phenacetin. J. Pharm. Biomed. Anal. 17 (1998): 501- 506.

46. Ozgur, M. U.; Alpdogan, G.; and Asci, B. A rapid spectrophotometric method to resolve ternary mixture of propylphenazone, caffeine, and acetaminophen in tablets. Monatsh. Chem. 133 (2002): 219-223.

47. Amin, A.S. Sensitive spectrophotometric determination microamounts of paracetamol using an indirect redox technique. Quim. Anal. 19 (2000): 135-138.

48. Simultaneous spectrophotometric determination of acetylsalicylic acid, paracetamol and caffeine in pharmaceutical preparations. Chem. Anal-Warsaw. 44 (1999): 1041-1048.

49. Vichez, J. L.; Blanc, R.; Avidad, R.; and Navalon, A. Spectrofluorometric determination of paracetamol in pharmaceuticals and biological-fluid. J. Pharm. Biomed. Anal. 13 (1995): 1119-1125.

50. Aukunuru, J. V.; Kompella, U. B.; and Betageri, G. V. Simultaneous high performance liquid chromatographic analysis of acetaminophen, salicylamide, phenyltoloxamine, and related products. J. Liq. Chromtogr. 23 (2000): 565-578.

51. Abu-Qure, A. W.; and Abou-Donia, M. B. A validation HPLC method for the determination of pyridostigmine bromide, acetaminophen, acetylsalicylic acid and caffeine in rat plasma and urine. J. Pharm. Biomed. Anal. 26 (2001): 939-947.

52. Shervington, L. A.; and Sakhnini, N. J. A quantitative and qualitative high performance liquid chromatographic determination of acetaminophen and five of its para-substituted derivatives. Pharm. Biomed. Anal. 24 (2000): 43-49.

53. Masuda, M.; Satoh, T.; Handa, M.; Itoh, Y.; Sagara, K. Simultaneous determination of the components in an anti-cold drug by gradient HPLC. Bunseki Kagaku 46 (1997): 777-783.

54. Bohnenstengel, F.; Kroemer, H. K.; and Sperker, B. In vitro cleavage of paracetamol glucuronide by human liver and kidney beta-glucoronidase: determination of paracetamol by capillary electrophoresis. J. Chromatogr. B 721 (1999): 295-299.

55. Yururi, M.; Nakanishi, H.; and Taniguchi, K. Simultaneous analysis of ingredients in anti-cold preparations using capillary electrophoresis Bunseki Kaguku 43 (1994): 575-580.

56. Kunkel, A.; Gunter, S.; and Watzig, H. Determination of pharmaceuticals in plasma by capillary electrophoresis without sample pretreatment reproducibility, limit of quantitation and limit of detection. Electrophoresis 18 (1997): 1882-1889.

57. Shearer, C. M.; Christenson, K.; Mukherji, A.; and Papariello, G. J. Peak voltammetry at glassy carbon electrode of acetaminophen dosage forms. J. Pharm. Sci. 61 (1972): 1627-1630.

58. Lau, O. W.; Luk, S. F.; Simultaneous determination of ascorbic acid, caffeine and paracetamol in drug formulations by differential-pulse voltammetry using a glassy carbon electrode And Cheng, Y. M. Analyst 114 (1989): 1047-1051.

59. Bramwell, H.; Cass, A. E.; Gibbs, P. N.; and Green, M. J. Method for determining paracetamol in whole blood by chronoamperometry following enzymatic hydrolysis Analyst 114 (1990):185-188.

60. Wang, C. Y.; Hu, X. Y.; Leng, Z. Z.; Yang, G. J.; and Jin, G. D. Differential pulse voltammetry for determination of paracetamol at a pumice mixed carbon paste electrode. Anal. Letts. 34 (2001): 2747-2759.

61. Munson, J. W.; and Abdine, H. Direct determination of acetaminophen in plasma by differential pulse voltammetry. J. Pharm. Sci. 67 (1978): 1775-1776.

62. Danet, A. F.; David, V.; and David, I. Acetaminophen determination by flow injection analysis with biamperomtric detection. Rev. Roum. Chim. 43(1998): 811-816.

63.Peng, W.; Li, T.; Li, H.; and Wang, E. Direct injection of urine and determination of acetaminophen by micellar liquid chromatography with a wall-jet cell/ carbon fibre microelectrode. Anal. Chim. Acta 298 (1994): 415-421.

64.Falkmer, S.; Samueleson, and G. Sjolin, S. Penicillamine treatment of Wilson's disease. Lakartidningen 66 (1969): 2097-2105.

65. Loudianos, G.; and Gitlin, J. D. Wilson's disease. Semin. Liver Dis. 20 (2000): 353-364.

66. Modai, I.; Karp, L.; Liberman, U. A.; and Munitz, H. J. Penicillamine therapy for schizophreniform psychosis in Wilson's disease Nerv. Ment. Dis.173 (1985): 698-701.

67. Carwhall, J. C.; and Watts, R. W. Cystinuria Am. J. Med. 45 (1968): 736-755.

68. Purkiss, R.; and Watts, R. W. Low dose D-penicillamine in cystinuria. Proc. R. Soc. Med. (1977): 27-30.

69. Frimpter, G. M. Medical management of cystinuria J. Med. Sci. 255 (1968): 348-357.

70. Gordon, M. H.; and Ehrlich, G. E. Penicillamine of treatment of rheumatoid arthritis Jama 229 (1974): 1342-1343.

71. Golding, J. R et. al. Rheumatoid arthritis treated with small doses of penicillamine Proc. R. Soc. Med. 70 (1977): 131-135.

72. Beales, D.; Finch, R.; Mclean, A. E.; Smith, M.; and Wilson, I. D. Determination of penicillamine and other thiols by combined high-performance liquid chromatography and post-column reaction with Ellman's reagent: application to human urine. J. Chromatogr. 226 (1981): 498-503

73. Mann, J.; and Mitchell, P. D. A simple calorimetric method for the estimation of D(--) penicillamine in plasma J. Pharm. Pharmacol. 31 (1979): 420-421.

74. Raggi, M. A.; and Cavrini, V.; Di Pietra, A. M. Calorimetric determination of penicillamine in pharmaceutical preparations. Pharm. Acta Helv. 58 (1983): 94-96.

75. Marnela, K. M.; Isomaki, H.; Takalo, R.; and Vapaatalo, H. Determination of D-penicillamine with an amino acid analyzer using fluorescence detection J. Chromatogr. 380 (1986): 170-176.

76. Vinas, P.; Lopez Garcia, I.; and Martinez Gil, J. A.Determination of thiol-containing drugs by chemiluminescene-flow injection analysis. J. Pharm. Biomed. Anal. 11 (1993): 15-20.

77. Gotti, R.; Pomponio, R.; Andrisano, V.; and Cavrini, V. Analytical study of penicillamine in pharmaceuticals by capillary zone electrophoresis J. Chromatogr. A 844(1999): 361-369

78. Russell, J; and Rabenstein, D. L. Speciation and quantitation of underivatized and Ellman's derivatized biological thiols and disulfides by capillary electrophoresis. Anal. Biochem. 242 (1996): 136-144.

79. You, T.; Yang, X.; and Wang, E. Determination of barbituric acid and 2-thiobarbituric acid with end-column electrochemical detection by capillary electrophoresis. Talanta 51 (2000): 1213-1218.

80. Aman, T.; Khan, I. U.; and Parveen, Z. Spectrophotometric determination of barbituric acid Anal. Letts. 30 (1997): 2765-2777.

81. Sandulescu, R.; Mirel, S.; and Oprean, R. The development of spectrophotometric and electroanalytical methods for ascobic acid and acetaminophen and their applications in the analysis of effervescent dosage forms. J. Pharm. Biomed. Anal. 23 (2000): 77-87.

82. Benschoten, J. J. V.; Lewis, J. Y.; Heineman, W. R.; Roston, D. A.; and Kissinger, P. T. Cyclic voltammetry experiment. J. Chem. Ed. 60 (1983): 772-776.

83. Wade, L. G., Jr. Organic chemistry. 3 rd. Ed. New Jersey: Prentice Hall Inc., 1995.

84. Streitwieser, A.; Heathcock, C. H.; and Kosower, E. W. Introduction to Organic Chemistry. 4 th Ed. New York: Macmillan Publishing Company, 1992.

85. McMurry, J.; and Castellion, M. E. Fundamentals of Organic and Biological Chemistry. New Jersey: Prentice Hall Inc., 1994.

86.Wu, J.; Zhu, J.; Shan, L.; amd Cheng, N. Voltammetric and amperometric study of electrochemical activity of boron-doped polycystalline diamond thin film electrodes. Anal. Chim. Acta. 333 (1996): 125-130.

สถาบันวิทยบริการ
จุฬาลงกรณ์มหาวิทยาลัย

APPENDICES

สถาบันวิทยบริการ
จุฬาลงกรณ์มหาวิทยาลัย

APPENDIX A

Cyclic voltammetric results (pH dependence)

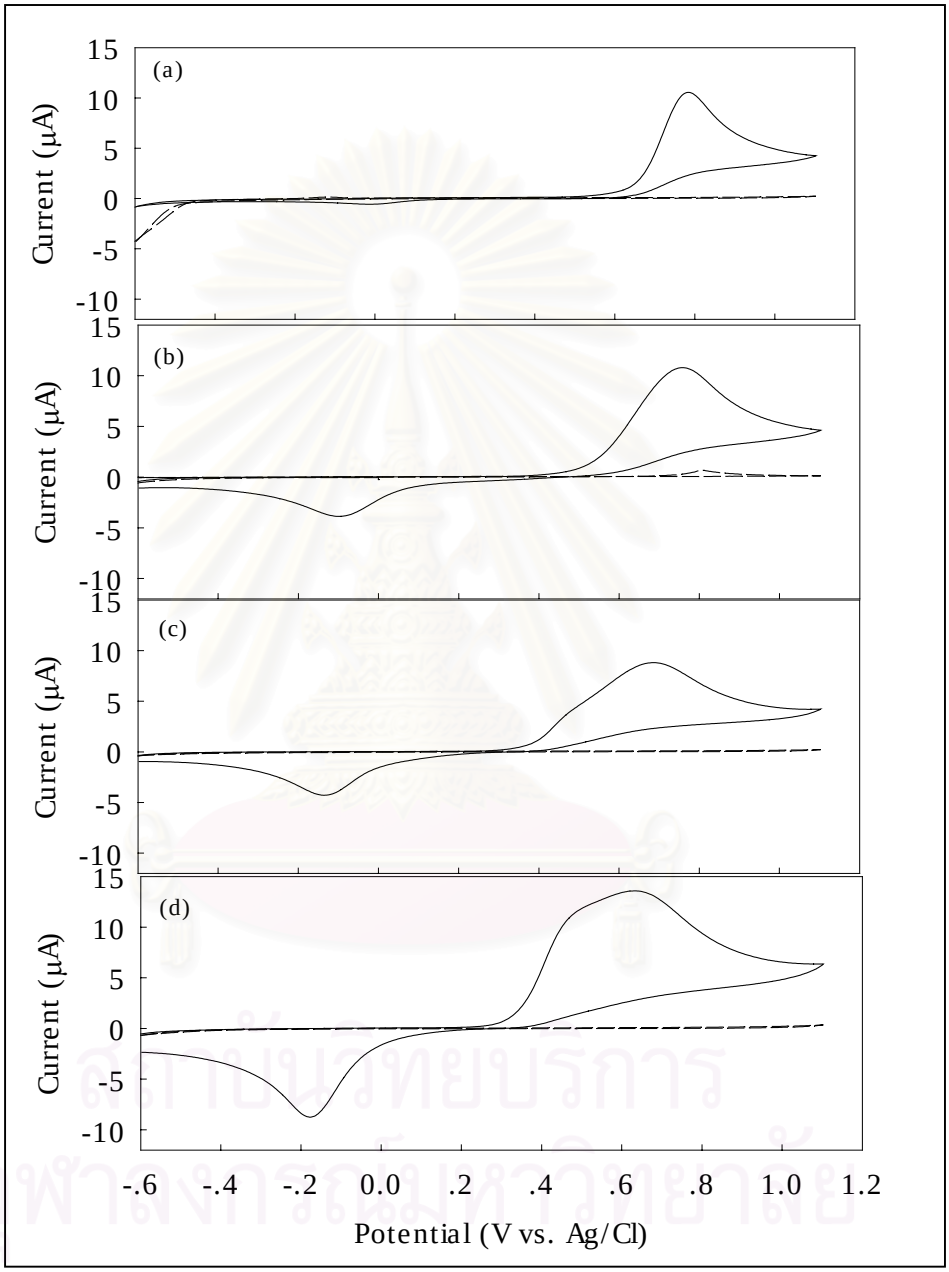

Figure A1 Cyclic voltammograms of 1 mM acetaminophen in 0.1 M phosphate buffer (a) pH 2.5 (b) pH 5 (c) pH 7 and (d) pH 8 at the diamond electrode. Background voltammograms are also shown in this Figure (dashed line.). The scan rate was 20 mV s^{-1}.

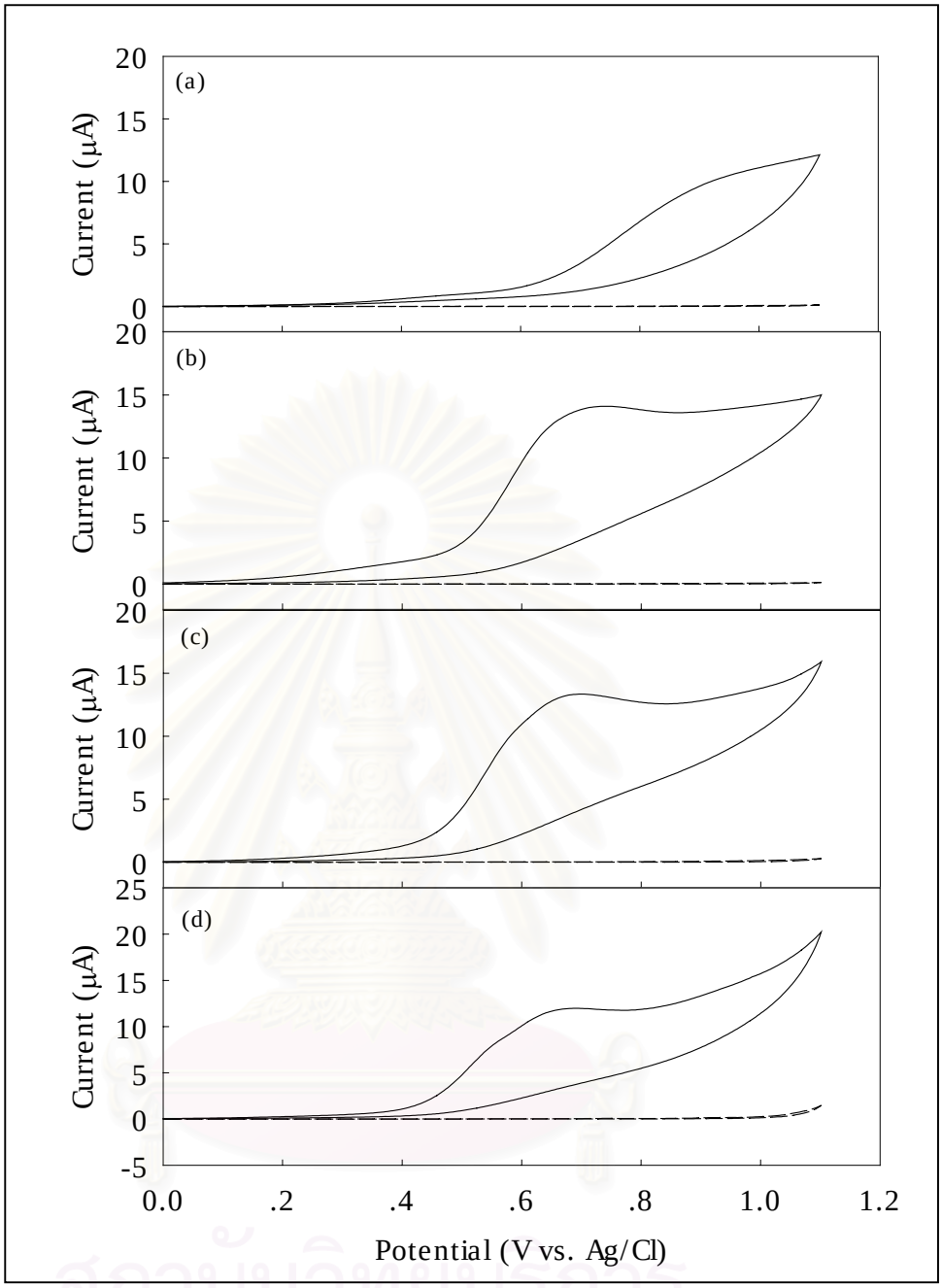

Figure A2 Cyclic voltammograms of 2 mM D-penicillamine in (a) 0.1 M phosphate buffer pH 5 (b) 0.1 M phosphate buffer pH 7 (c) 0.1 M phosphate buffer pH 8 and (d) 0.1 M carbonate buffer pH 9.2 at the diamond electrode. Background voltammograms are also shown in this Figure (dashed line.). The scan rate was 20 mV s^{-1}.

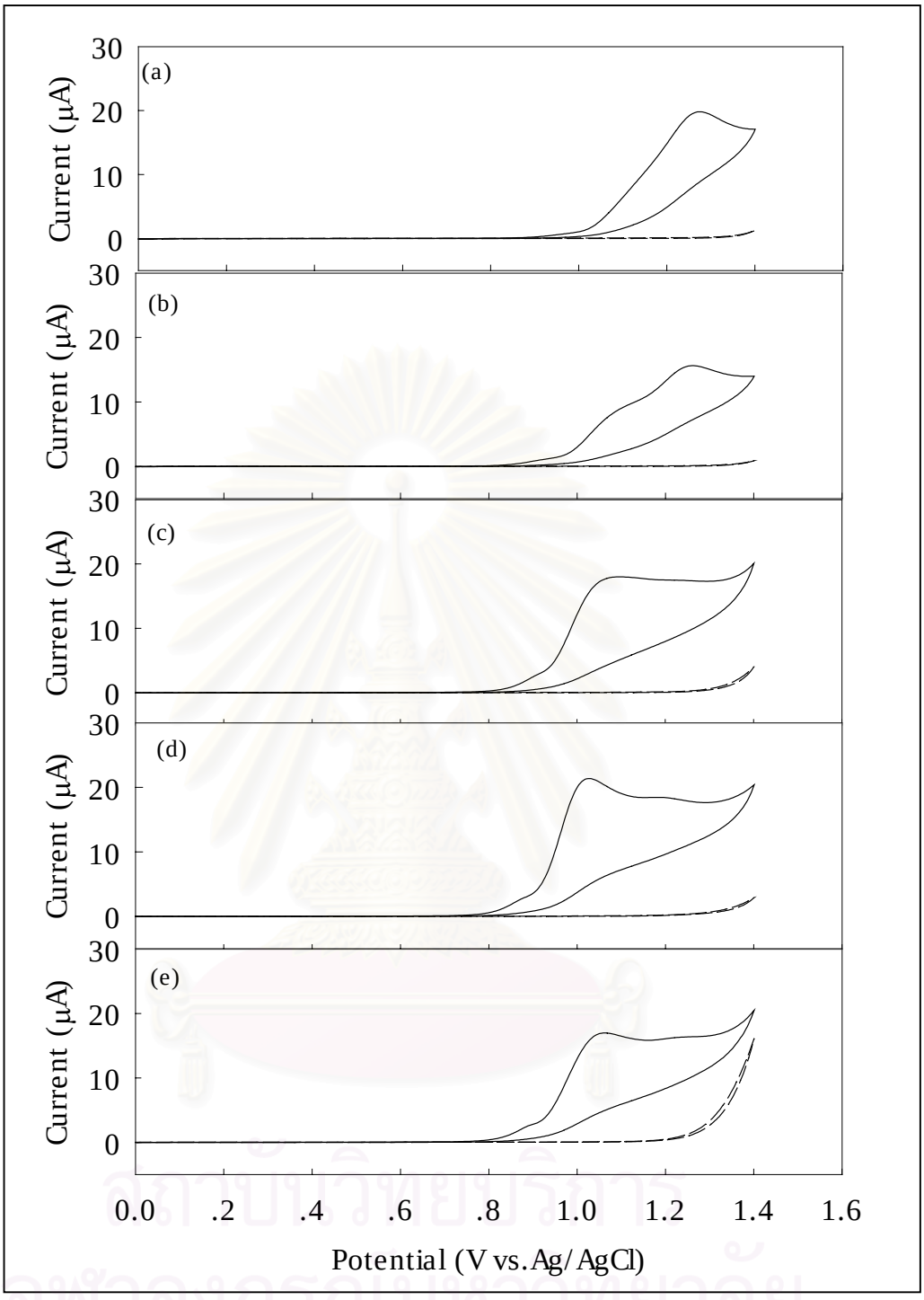

Figure A3 Cyclic voltammograms of 2 mM barbituric acid in (a) 0.1 M phosphate buffer pH 2.5 (b) 0.1 M phosphate buffer pH 5 (c) 0.1 M phosphate buffer pH 7 (d) 0.1 M phosphate buffer pH 8 and (e) 0.1 M carbonate buffer pH 9.2 at the diamond electrode. Background voltammograms are also shown in this Figure (dashed line.). The scan rate was 20 mV s^{-1}.

APPENDIX B

Cyclic voltammetric results (Scan rate dependence)

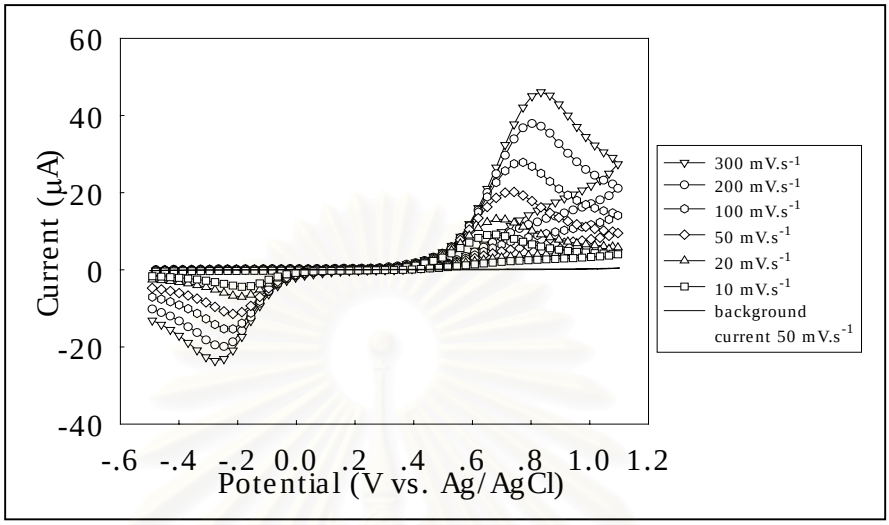

Figure B1 Cyclic voltammograms of 1 mM acetaminophen in 0.1 M phosphate buffer (pH 8) at the diamond electrode. The scan rate was varied from 10 -300 mV s^{-1}. Background cyclic voltammogram at 50 mV s^{-1} is also shown in this Figure (solid line).

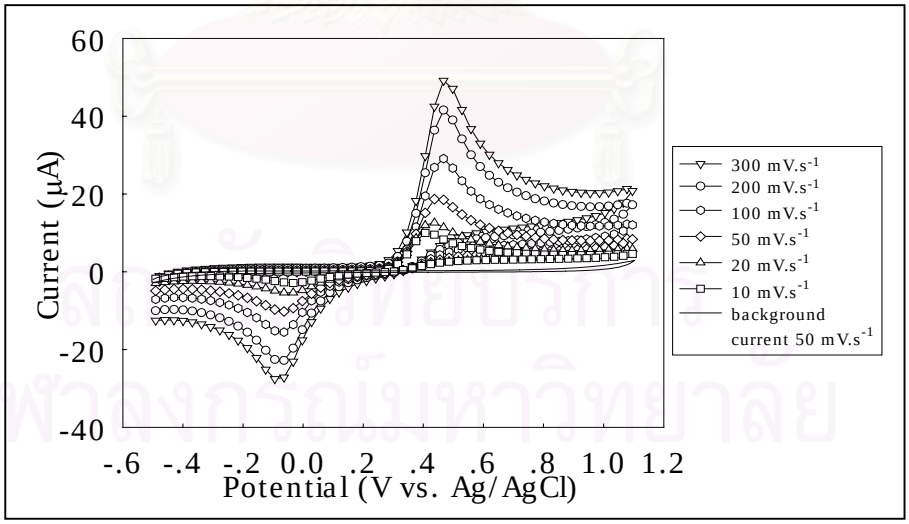

Figure B2 Cyclic voltammograms of 1 mM acetaminophen in 0.1 M phosphate buffer (pH 8) at the glassy carbon electrode. The scan rate was varied from 10 -300 mV s^{-1}. Background cyclic voltammogram at 50 mV s^{-1} is also shown in this Figure (solid line).

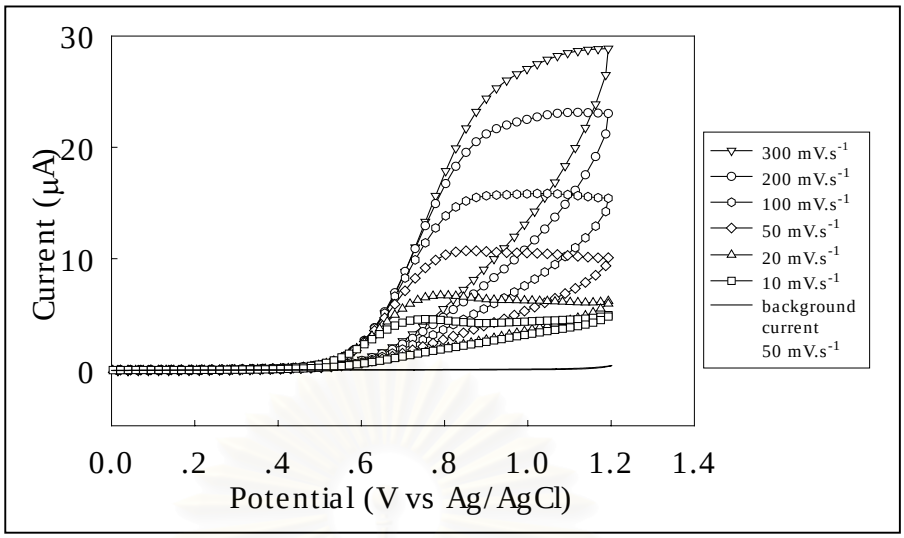

Figure B3 Cyclic voltammograms of 1 mM D-penicillamine in 0.1 M phosphate buffer (pH 7) at the diamond electrode. The scan rate was varied from 10 -300 mV s^{-1}. Background cyclic voltammogram at 50 mV s^{-1} is also shown in this Figure (solid line).

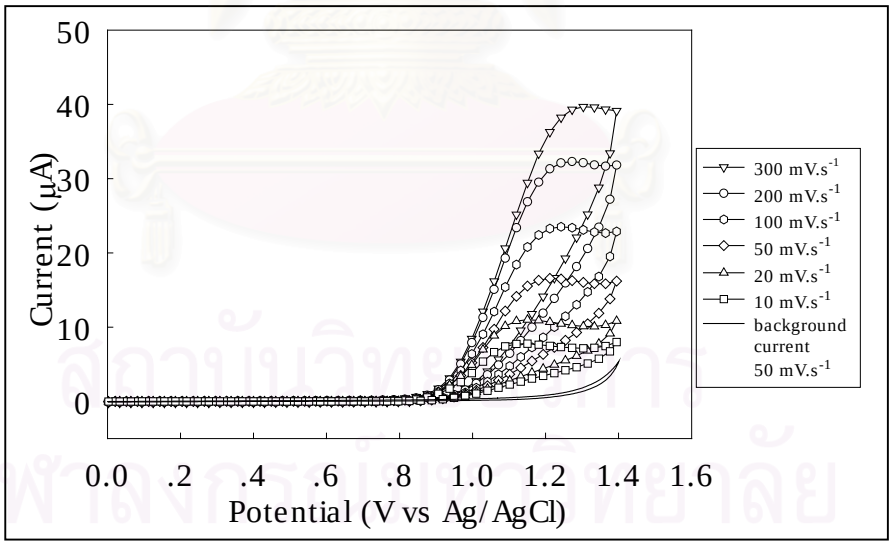

Figure B4 Cyclic voltammograms of 1 mM barbituric acid in 0.1 M phosphate buffer (pH 8) at the diamond electrode. The scan rate was varied from 10 -300 mV s^{-1}. Background cyclic voltammogram at 50 mV s^{-1} is also shown in this Figure (solid line).

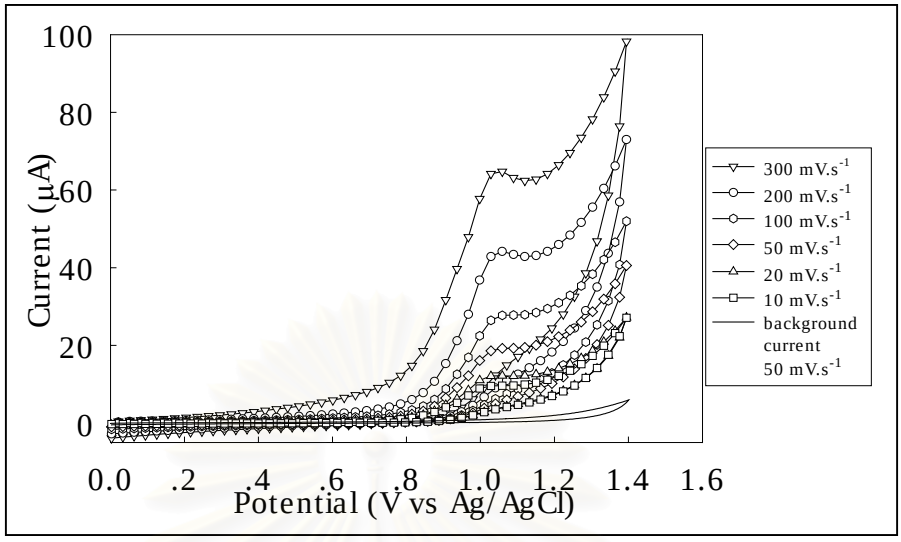

Figure B5 Cyclic voltammograms of 1 mM barbituric acid in 0.1 M phosphate buffer (pH 8) at glassy carbon electrode. The scan rate was varied from 10 -300 $mV.s^{-1}$. Background cyclic voltammogram at 50 $mV.s^{-1}$ is also shown in this Figure (solid line).

สถาบันวิทยบริการ
จุฬาลงกรณ์มหาวิทยาลัย

APPENDIX C

Cyclic voltammetric results (concentration dependence)

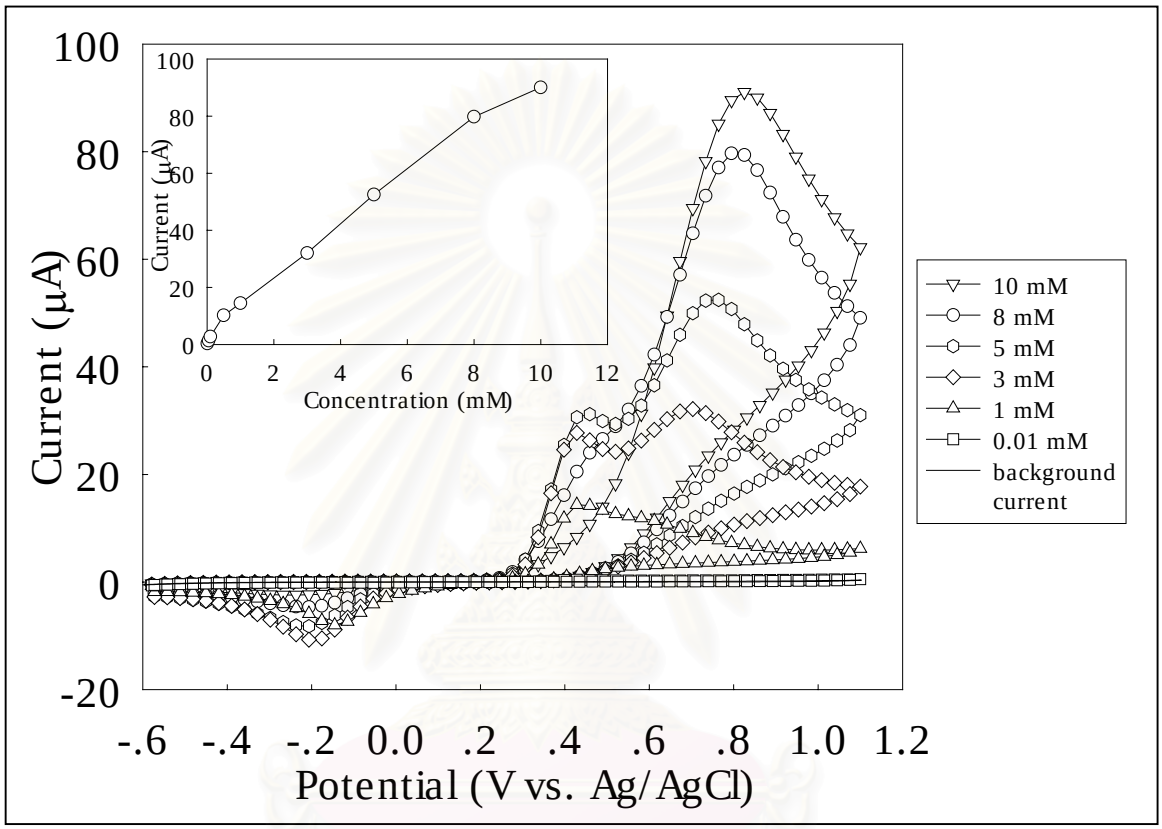

Figure C1 Cyclic voltammograms of acetaminophen (0.01 - 10 mM) in 0.1 M phosphate buffer (pH 8) at the diamond electrode. The scan rate was 20 mV s^{-1}. The corresponding calibration curve (inset Figure) and background cyclic voltammogram (solid line) are also shown.

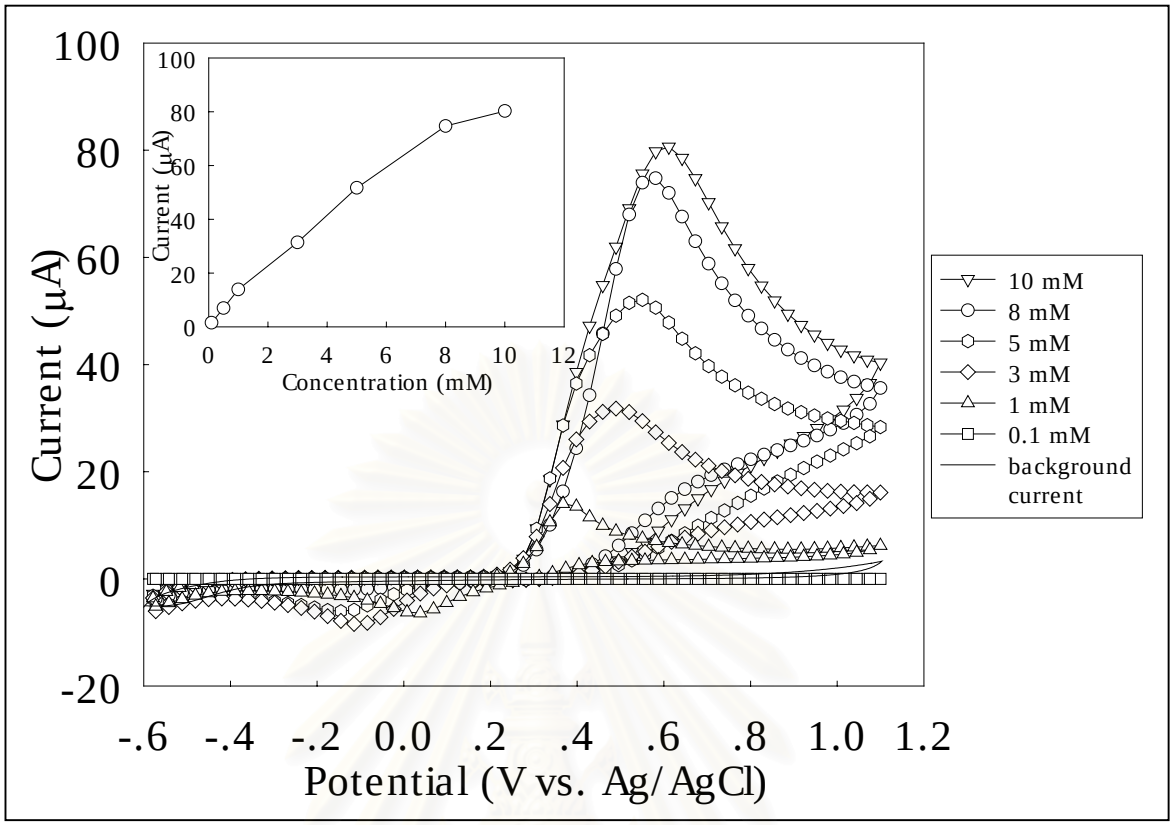

Figure C2 Cyclic voltammograms of acetaminophen (0.1 - 10 mM) in 0.1 M phosphate buffer (pH 8) at the glassy carbon electrode. The scan rate was 20 mV s^{-1}. The corresponding calibration curve (inset Figure) and background cyclic voltammogram (solid line) are also shown.

สถาบันวิทยบริการ
จุฬาลงกรณ์มหาวิทยาลัย

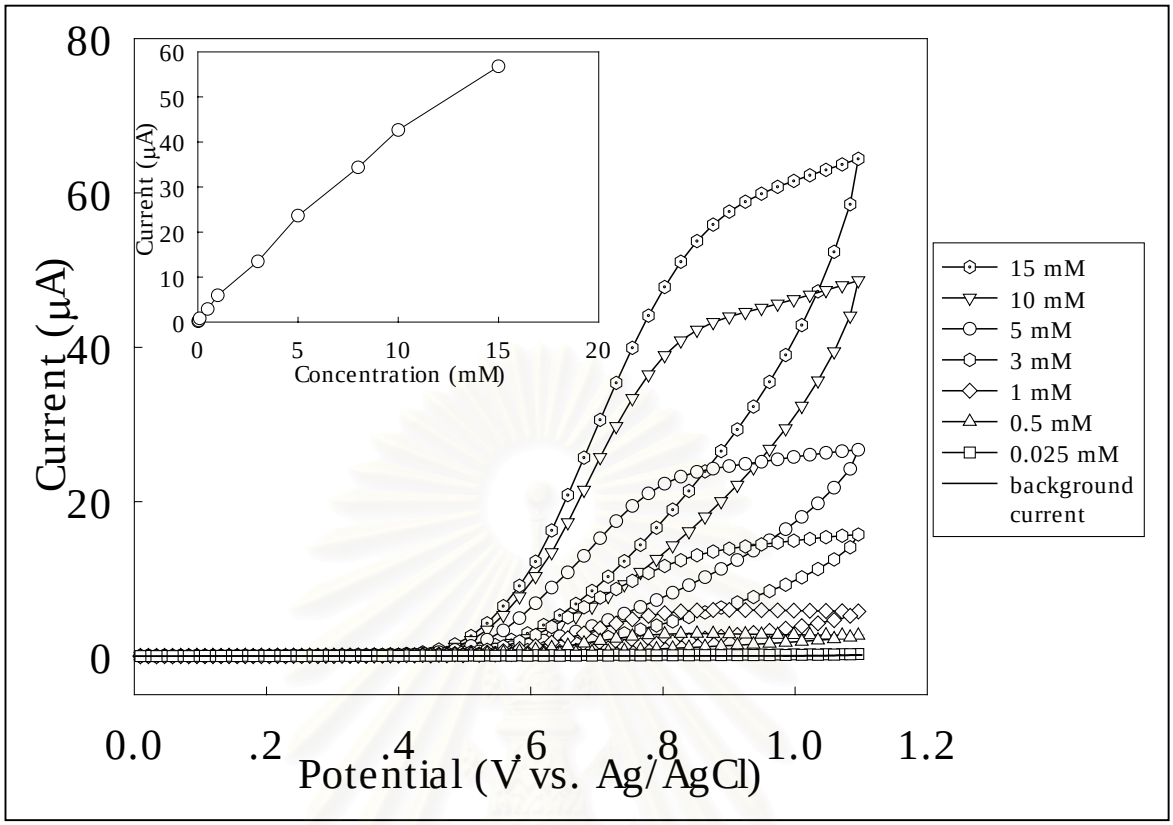

Figure C3 Cyclic voltammograms of D-penicillamine (0.025 - 15 mM) in 0.1 M phosphate buffer (pH 7) at the diamond electrode. The scan rate was 20 mV s^{-1}. The corresponding calibration curve (inset Figure) and background cyclic voltammogram (solid line) are also shown.

สถาบันวิทยบริการ
จุฬาลงกรณ์มหาวิทยาลัย

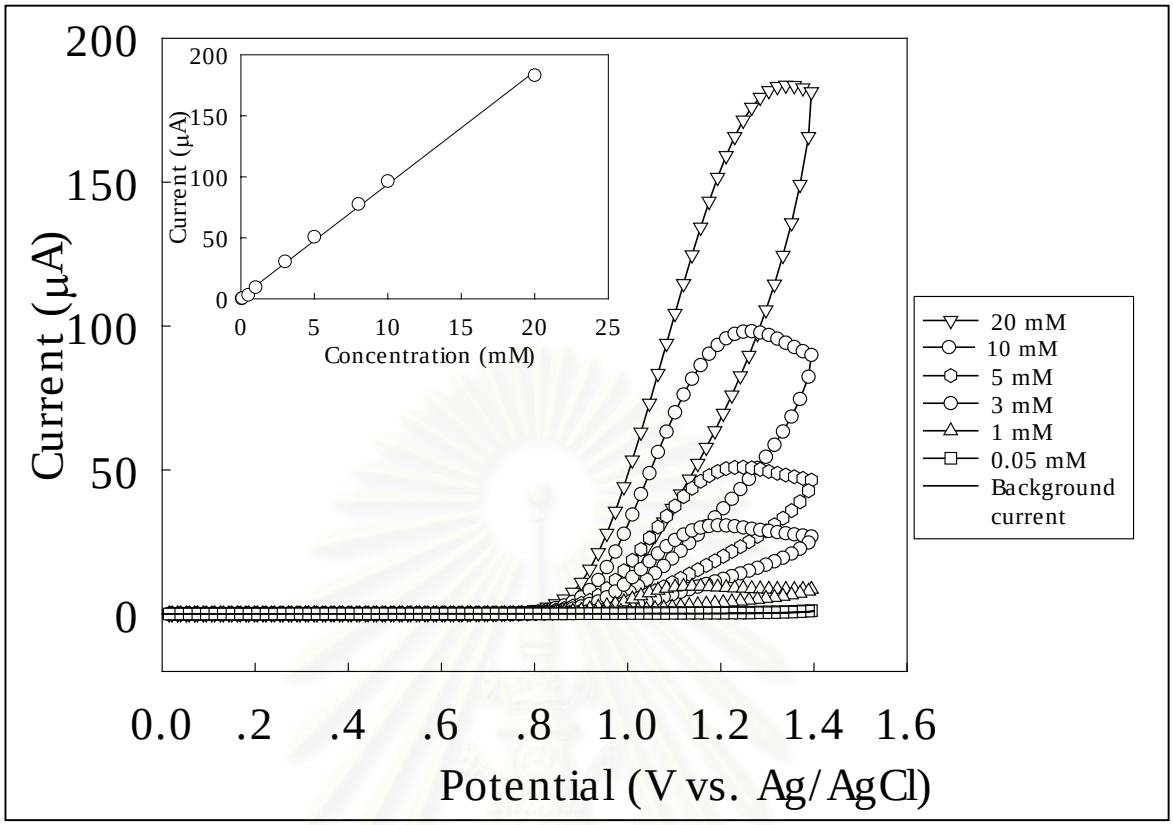

Figure C4 Cyclic voltammograms of barbituric acid (0.05 - 20 mM) in 0.1 M phosphate buffer (pH 8) at the diamond electrode. The scan rate was 20 mV s^{-1}. The corresponding calibration curve (inset Figure) and background cyclic voltammogram (solid line) are also shown.

สถาบันวิทยบริการ
จุฬาลงกรณ์มหาวิทยาลัย

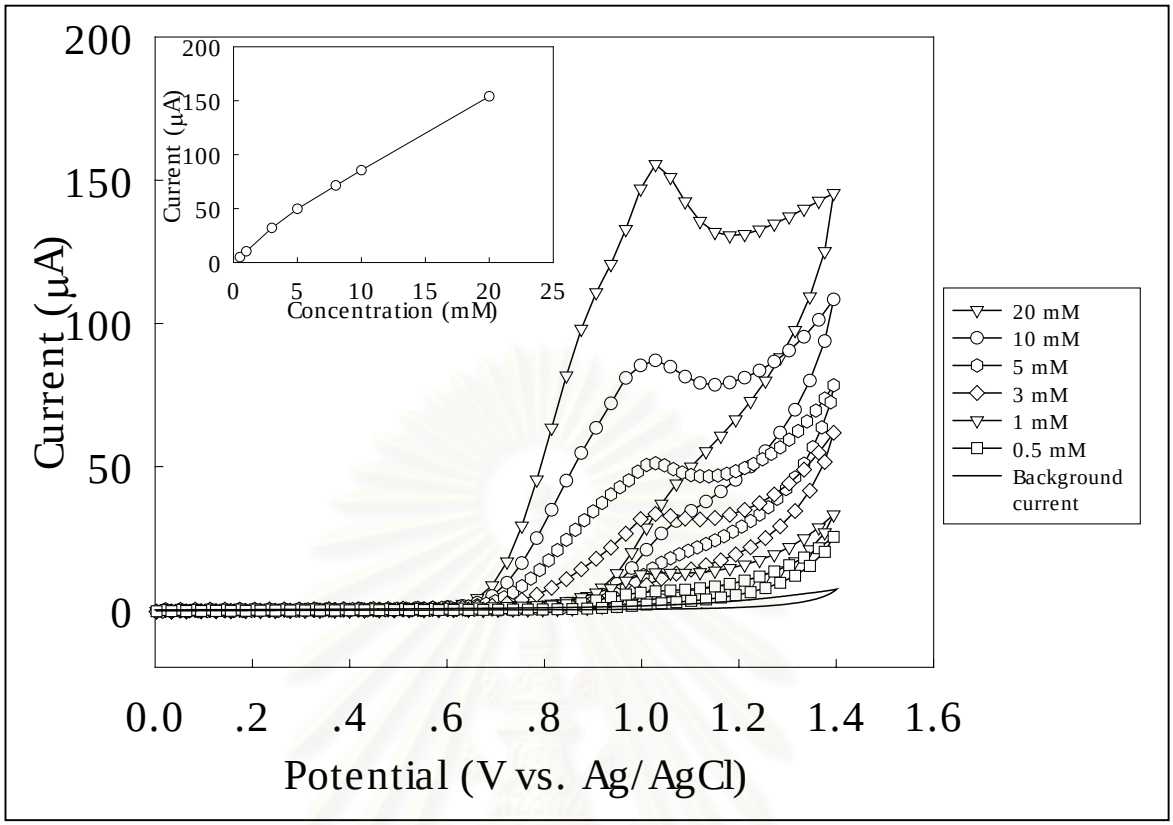

Figure C5 Cyclic voltammograms of barbituric acid (0.5 - 20 mM) in 0.1 M phosphate buffer (pH 8) at the glassy carbon electrode. The scan rate was 20 mV s^{-1}. The corresponding calibration curve (inset Figure) and background cyclic voltammogram (solid line) are also shown.

สถาบันวิทยบริการ
จุฬาลงกรณ์มหาวิทยาลัย

APPENDIX D

Flow injection with amperometric detection results and calibration curves

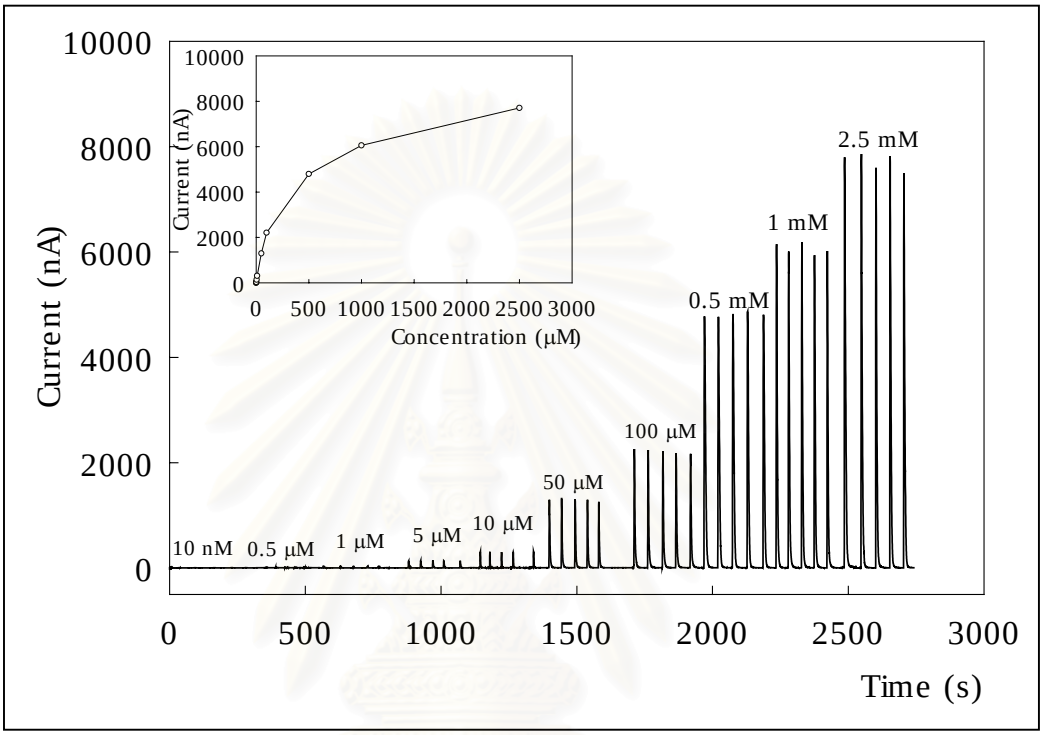

Figure D1 Flow injection with amperometric detection result of acetaminophen (10 nM – 2.5 mM) in 0.1 M phosphate buffer (pH 8) with 5 injections at the applied potential 0.55 V vs. Ag/AgCl. The flow rate was 1 ml min^{-1}. The corresponding calibration curve is also shown (inset Figure).

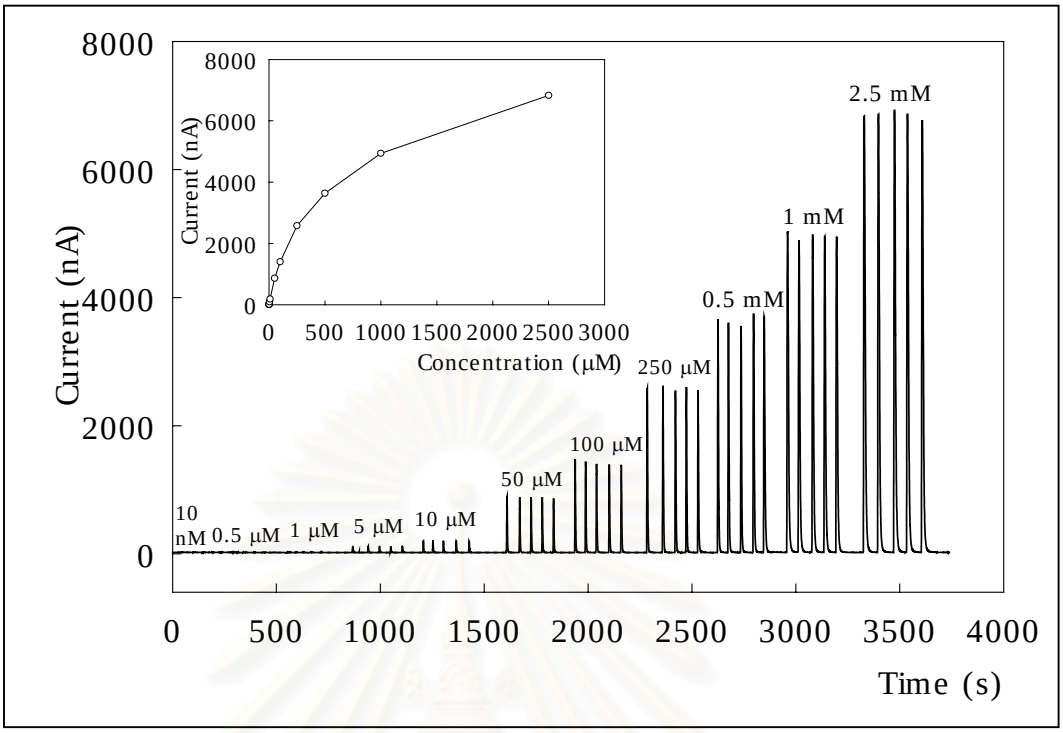

Figure D2 Flow injection with amperometric detection result of D-penicillamine (10 – 2.5 mM) in 0.1 M phosphate buffer (pH 7) with 5 injections at the applied potential 0.75 V vs. Ag/AgCl. The flow rate was 1 ml min^{-1}. The corresponding calibration curve is also shown (inset Figure).

สถาบันวิทยบริการ
จุฬาลงกรณ์มหาวิทยาลัย

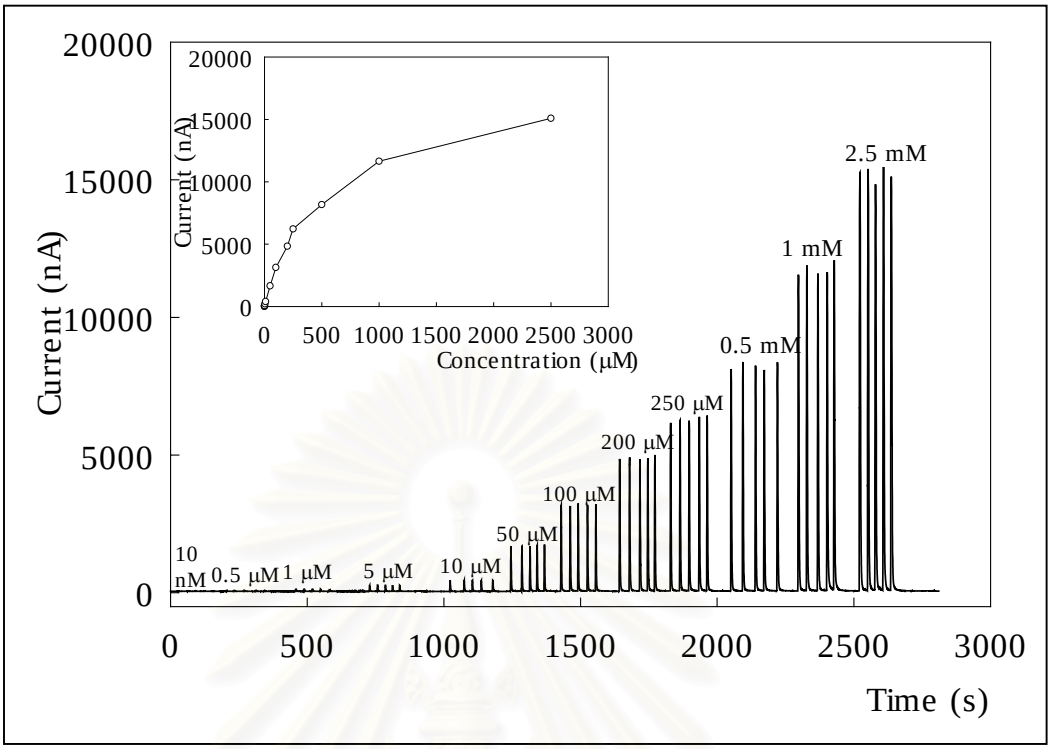

Figure D3 Flow injection with amperometric detection result of barbituric acid (10 nM – 2.5 mM) in 0.1 M phosphate buffer (pH 8) with 5 injections at the applied potential 1.075 V vs. Ag/AgCl. The flow rate was 1 ml min^{-1}. The corresponding calibration curve is also shown (inset Figure).

สถาบันวิทยบริการ
จุฬาลงกรณ์มหาวิทยาลัย

APPENDIX E

Flow injection with amperometric detection results of drug samples

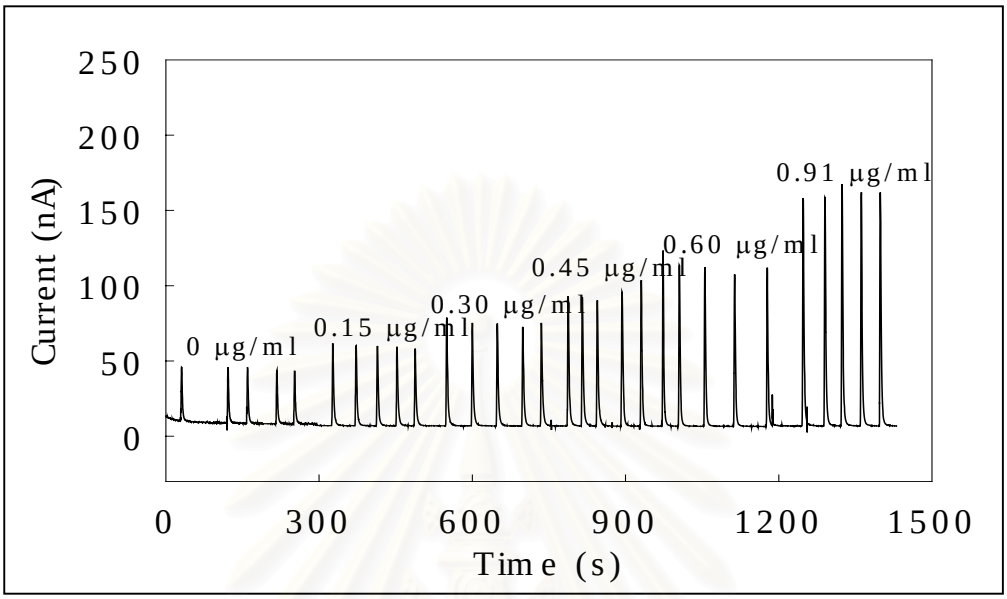

Figure E1 Flow injection with amperometric results of paracetamol syrup in 0.1 M phosphate buffer (pH 8) with 5 injections at the applied potential 0.55 V vs. Ag/AgCl. The flow rate was 1 ml min^{-1}.

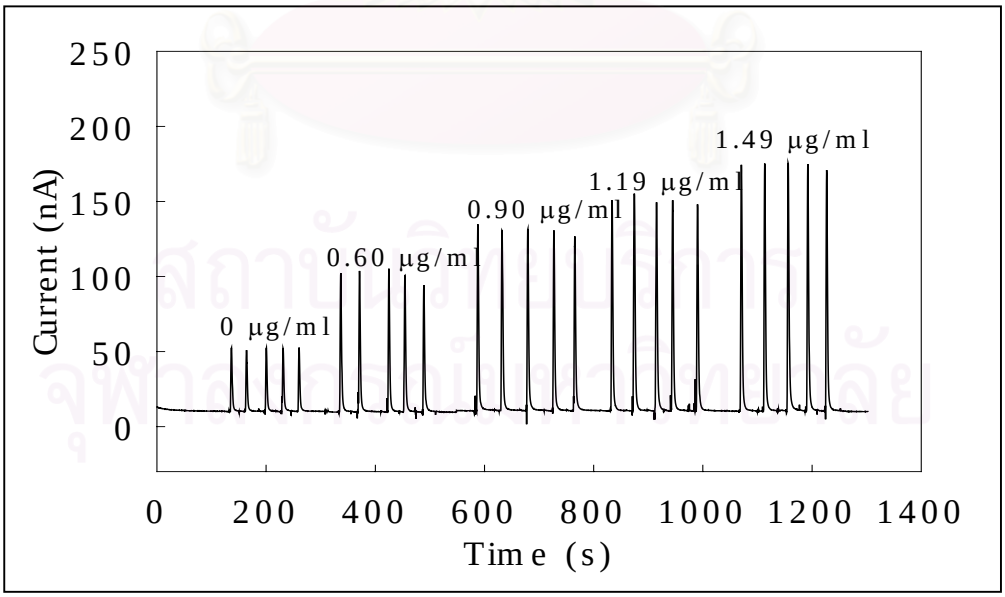

Figure E2 Flow injection with amperometric results of penicillamine capsule in 0.1 M phosphate buffer (pH 7) with five injections at the applied potential 0.75 V vs. Ag/AgCl. The flow rate was 1 ml min^{-1}.

APPENDIX F

Description of analytical performance characteristics

Accuracy

Accuracy refers to the closeness of agreement between the true value of the analyte concentration and the mean result that is obtained by applying the experiment procedure. There are various ways and units in which the accuracy can be expressed. Recovery is a term often used to describe accuracy, the equation for recovery is:

$$\%\text{Recovery} = \frac{\text{Measured value}}{\text{True value}} \text{x} 100$$

If the recovery were poor, it would be a good indication of a problem with the method. Standard addition is one technique that can be used to determine the recovery of spiked analyte. Relative error is the another term that can express the accuracy. The equation is shown below:

$$\%\text{error} = \frac{(\text{Measured value} - \text{True value})}{\text{True value}} \text{ x } 100$$

Precision

Precision is the measurement of several determinations of the same quantities. Repeatability is one method that is used to describe precision. It is done by multiple injections of a homogeneous sample and calculation of the relative standard deviation (%RSD). The equation for %RSD is shown below:

$$\%\text{RSD} = \frac{\text{standard deviation}}{\text{Mean}} \text{ x } 100$$

Linearity (Linear range)

A linearity is the range where the analyte response is linearly proportional to concentration. The working sample concentration and samples tested for accuracy should be in the linear range.

Sensitivity

Sensitivity is the change in the analytical response divided by the corresponding change in the concentration of a standard (calibration) curve, i.e. the slope of the analytical calibration.

Detection limit (LoD)

The detection limit of a method is the lowest analyte concentration that can be determined to be different from an analyte blank. There are numerous way that detection limit have been defined. An example is the lowest analyte concentration that is above the noise level of the system, typically, three time the noise level (S/N = 3). This term is used to describe low analyte concentrations (< 10 μM). For high analyte concentrations, the detection limit is defined as the lowest concentration that provides a signal to background ratio S/B of three. The equation of S/B ratio is shown below:

$$\text{S/B ratio} = \frac{(\text{total signal} - \text{blank signal})}{\text{blank signal}}$$

Selectivity

Selectivity gives an indication of how strongly the result is affected by other components (interferences) in the sample. Tolerance limit is the term that can be used to describe the specificity of the method. Tolerance limit is defined as the interference concentration that produces an error not exceeding ± 5% in the determination of analyte.

สถาบันวิทยบริการ
จุฬาลงกรณ์มหาวิทยาลัย

APPENDIX G

Determination of drug samples

The proposed method was applied to real samples e.g. penicillamine capsule using the standard addition method. The results are shown in Table G1.

Table G1 The results of penicillamine capsule determination by flow injection with amperometric detection at the diamond electrode.

Amount of added (μg/ml)	Current (nA)	
	1	2
0.00	36.51	41.828
0.60	83.03	90.588
0.90	106.82	119.82
1.19	126.8	140.24
1.49	147.38	164.62

The result obtained was used to plot the graphs, which was then extrapolated to meet the x-axis to get the value that can then be used to calculate for amount of penicillamine in the sample by the following equation:

$$A_0 = -A_{SA}V_{flask}/V_{unk}*D$$

where A_0 - amount of penicillamine in sample

A_{SA} - amount of penicillamine at the intercept point

V_t - total volume

V_{unk} - volume of unknown

D - dilution factor

The result was 256.62 and 253.90 mg in tablet. The label value was 250 mg. The relative errors of determination were 2.65 and 1.56%.

To check the accuracy of the method, recovery was also studied. The recovery was carried out by the standard addition method and the recovery could be calculated by using a regression equation of the standard addition graph. The regression equation is shown below in Table G2

Table G2 Regression equation of penicllamine capsule determination using standard addition method.

No	Regression equation
1	74.704x +37.653
2	82.813x+42.187

The results of recovery of the penicillamine sample are shown in Table G3

สถาบันวิทยบริการ
จุฬาลงกรณ์มหาวิทยาลัย

Table G3 Recovery study results of penicillamine capsule.

Amount of added (μg/ml)	Amount of found (μg/ml)		Percent of recovery (%)	
	1	2	1	2
0.60	0.58	0.59	97.75	99.60
0.90	0.94	0.93	104.69	103.39
1.19	1.18	1.19	99.23	100.00
1.49	1.48	1.47	99.17	98.51

The precision of the method was performed by injection, 10 times, of three concentrations of spiked standard solutions (0, 0.60 and 1.49 μg/ml). The results were then used to calculate %RSD. The results and % RSD at each concentration are shown in Table G4.

สถาบันวิทยบริการ
จุฬาลงกรณ์มหาวิทยาลัย

Table G4 The results of D-penicillamine of precision studied and %RSD.

No	Current (nA)		
	0	0.60	1.49
1	37.56	82.72	164.10
2	36.69	82.80	161.90
3	36.19	80.91	160.00
4	35.56	79.44	162.40
5	37.10	81.19	159.90
6	34.99	79.48	157.00
7	35.92	82.71	164.90
8	37.41	79.39	161.10
9	35.98	79.54	161.30
10	36.58	81.28	165.70
average	36.40	79.38	161.83
%RSD	2.1	1.7	1.5

Table G5 Influence of lactose on D-penicillamine determinaiton

[lactose]/[D-penicillamine]	%error
20:1	0.69
40:1	1.60
80:1	3.89
100:1	5.95

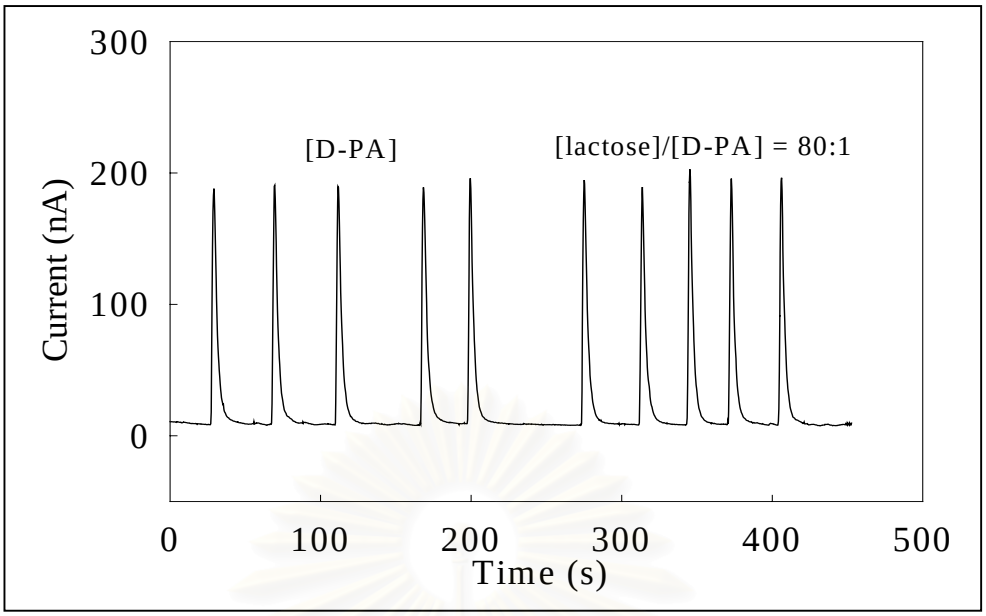

Figure G1 Flow injection with amperometric detection results for interference study. The first set of five injections belong to D-penicillamine 7.46 μg/ml (50 μM) in 0.1 phosphate buffer (pH 7). The second set of five injections obtained from the mixture of lactose and D-penicillamine with the concentration ratio 80:1.

The selectivity of the method was investigated by studying interferences from other species accompanying penicillamine in drug capsule. The possible interference of drug capsule was lactose, magnesium stearate and titanium dioxide but only lactose can dissolve in the solution. Therefore lactose was used in this study. The results obtained are shown in Table G5. The proposed method provided a tolerance limit at the [lactose] / [D-penicillamine] equal to 80:1 with % error equal to 3.89% (Figure G1). This concentration ratio is a tolerance limit of this method.

VITA

Miss Nattakarn Wangfuengkanagul was born on May, 13 1977, in Bangkok. She received her Bachelor Degree of Science in Industrial Chemistry (2^{nd} honor) from Faculty of Science, King Mongkut Institute of Technology Ladkrabang in 1999. In the same year, she continued her education in a Master degree in Analytical Chemistry at Chulalongkorn University.

สถาบันวิทยบริการ
จุฬาลงกรณ์มหาวิทยาลัย